6mer Seed Toxicity and Platinum Resistance in Ovarian Cancer

Monal Patel[1], Yinu Wang[2], Elizabeth T. Bartom[3,4], Rohin Dhir[5],
Kenneth P. Nephew[6], Daniela Matei[2,7],
Andrea E. Murmann[1], Ernst Lengyel[5], and Marcus E. Peter[1,3,7,*]

[1]Department of Medicine/Division Hematology/Oncology, [2]Department of Obstetrics and Gynecology, [3]Department of Biochemistry and Molecular Genetics, [4]Department of Preventive Medicine, Feinberg School of Medicine, Northwestern University, Chicago, IL, [5]Department of Obstetrics and Gynecology/Section of Gynecologic Oncology, University of Chicago, Chicago, IL, [6]Medical Sciences, Indiana University School of Medicine, Bloomington, IN, and [7]Robert H. Lurie Comprehensive Cancer Center, Chicago, IL

Running title: 6mer Seed Toxicity and Ovarian Cancer

Keywords:
Cancer, RNAi, platinum, RISC, miRNAs, ovarian cancer

Financial support:
This work was funded by grant R35CA197450 to M.E.P., R50CA221848 to E.T.B., and Ovarian Cancer Research Alliance grant number 458788 to K.P.N, D.M. and M.E.P.

Corresponding author: Marcus Peter, E-mail: m-peter@northwestern.edu, phone: 312-503-1291; FAX: 312-503-0189.

ABSTRACT

Development of platinum (Pt) resistance is a major barrier to curing ovarian cancer (OC). 6mer seed toxicity is a novel cancer killing mechanism mediated by tumor suppressive miRNAs with a toxic 6mer seed sequence (positions 2-7) through the RNA-induced silencing complex (RISC). The most toxic 6mer seeds are G-rich and kill cells by targeting the 3' untranslated region of genes critical for cell survival. We now show that treatment of OC cells with Pt leads to an increase in RISC-bound miRNAs carrying toxic 6mer seeds and a decrease in miRNAs with nontoxic seeds. Pt-resistant cells did not exhibit this Pt induced toxicity shift but retained sensitivity to death mediated by siRNAs carrying toxic 6mer seeds. Analysis of RISC-bound miRNAs in OC patients revealed that miRNA 6mer seed toxicity ratios were predictive of treatment outcomes. Our results suggest that 6mer seed toxicity can be exploited to treat patients with Pt-resistant OC.

INTRODUCTION

Micro (mi)RNAs are short 19-22 nt long double-stranded noncoding RNAs negatively regulating gene expression. The human genome is estimated to code for ~8300 miRNAs (1). They are important regulators of differentiation and development and are deregulated in virtually all human cancers where they can function as tumor suppressors or oncogenes (2-4). Their activity involves only a very short region of complete complementarity, the 'seed', at positions 2-7/8 of the guide strand of the miRNA (5, 6) with 'seed matches' predominantly located in the 3' untranslated region (3' UTR) of targeted mRNAs (7, 8) resulting in gene silencing (9). miRNA biogenesis begins in the nucleus with the transcription of a primary miRNA precursor (10). The Drosha/DGCR8 microprocessor complex first processes them into pre-miRNAs (11), which are then exported by exportin 5 from the nucleus to the cytoplasm (12). Once in the cytoplasm, Dicer/TRBP processes them further (13, 14), and these mature double stranded (ds)RNA duplexes are then loaded onto Argonaute (Ago) proteins forming the RNA-induced silencing complex (RISC) (15). The active miRNA guide strand, incorporates into the RISC (15), while the inactive passenger strand is degraded (16).

Epithelial ovarian cancer (OC) is one of the deadliest gynecological malignancies (17). Despite recent advances in understanding its biology (18) and developing new treatments (19), the vast majority of women with advanced stage OC develop incurable disease recurrence and acquire resistance to platinum (Pt), which is part of the standard of care for first line treatment of OC (20). A large body of literature supports the role of aberrantly expressed miRNAs in different aspects of OC biology, such as sensitivity to treatment and long-term treatment outcome. At least 87 miRNAs were reported to either confer acquired therapy resistance, resensitize OC cells to treatment, or to correlate with or predict OC treatment outcome (Supplementary Table S1 and S2). However, there is very little agreement or overlap in reported miRNAs, raising the question of how this bewildering array of different miRNAs can be linked to therapy resistance in OC.

We previously discovered that a large number of si- and shRNAs were toxic to all cancer cells independent of their intended target (21). Cells died of simultaneous activation of multiple cell death pathways (21) and could not become resistant to treatment (22). Subsequently, we found that Ago2, a critical component of the RISC, was required for cells to die and that the toxic si/shRNAs acted like miRNAs by targeting the 3' UTRs of essential survival genes (23, 24). A 6mer seed present in the guide/antisense strand of the si/shRNA duplex (23) is sufficient for Death Induced by Survival gene Elimination (DISE) (23, 25).

In an arrayed screen of all possible 4096 6mer seeds in a neutral backbone 19mer siRNA, we determined that the most toxic 6mer seeds were universally high in G nucleotides at the 5' end of the seed, largely independent of tissue origin and species ((26) and 6merdb.org). For human cells, we recently identified the seed consensus GGGGGC (targeting the seed match GCCCCC in a miRNA like fashion) as the most toxic seed sequence (24). Toxic 6mer seeds are found in tumor-suppressive miRNAs, including the prototypical tumor suppressive miRNA families, miR-34/449-5p and miR-15/16-5p (26, 27), suggesting that 6mer seed toxicity (6mer Seed Tox) is an anticancer mechanism. When we treated xenografted OC with siRNAs containing toxic seeds, normal tissues were unaffected (22). Various cancer cell lines became more sensitive to 6mer Seed Tox after induction of EMT or by increasing their cancer stemness (28), both well-documented mechanisms of chemotherapy resistance (29).

By analyzing miRNAs merely based on the toxicity of their 6mer seed we now report that in OC patients the balance of miRNAs containing toxic *versus* nontoxic seeds strongly associates with the outcome of Pt-based chemotherapy. Treatment of OC cells with Pt results in an increase of RISC bound miRNAs with toxic seed-bearing miRNAs. In contrast, Pt-R cancer cells have fewer toxic seed containing miRNAs in their RISC, however, they are more sensitive to toxic seed containing siRNAs than Pt-S cells by taking up these siRNAs more readily than nontoxic siRNAs. Analyzing the 6mer seed composition of RISC bound miRNAs may predict which patients are Pt resistant at the time of initial diagnostic surgery or may acquire Pt-resistance and points at 6mer Seed Tox as a potential treatment for Pt resistant OC.

RESULTS

Both Toxic siRNAs and Carboplatin Exert Toxicity Through RNAi.
We decided to use the two highly toxic seeds GGCAGU (found in miR-34a-5p) and GGGGGC (found in miR-1237-5p) embedded in an siRNA to probe cells. Both siGGCAGU and siGGGGGC were more toxic to Dicer deficient 293T than wt cells (Supplementary Fig. S1A-S1C) and killed cells through RNAi as both of them showed severely reduced toxicity to Ago2 k.o. HeLa cells, yet they were highly toxic to wt HeLa cells (Supplementary Fig. S1D). Similarly, these two siRNAs were also more toxic to wt than to Ago2 k.o. 293T cells (Supplementary Fig. S1E). We previously reported that HCT116 cells deficient for either Drosha or Dicer which are devoid of canonical miRNAs were hypersensitive to 6mer Seed Tox and cisplatin (Cis) (23). We now show that Dicer k.o. 293T cells are also much more sensitive to the toxic effects of the clinically used carboplatin (Carbo) (Supplementary Fig. S1F) while isogenic Ago2 k.o. 293T cells showed a reduced susceptibility to the toxicity of Carbo (Supplementary Fig. S1G). These data suggest that the composition of RISC bound miRNAs and RNAi determines not only the activity of toxic siRNAs but at least in part also the sensitivity of cells to Pt.

Platinum-Tolerant OC Cells Are Sensitive to 6mer Seed Tox.
To determine whether 6mer Seed Tox contributes to the response of OC cells to Pt, we first tested two cell line pairs representing a Pt sensitive (Pt-S) and resistant (Pt-R) phenotype, respectively. A2780R cells were made resistant by culturing A2780 cells for 5 cycles with increasing concentrations of Cis (30). PEO1 and PEO4 cells were derived from the same patient at different times after combination chemotherapy with Cis, chlorambucil and 5-fluorouracil (31) with PEO4 being a later isolate from the patient after second relapse and hence more resistant to Pt drugs. Treatment of the A2780 cell pair with Cis confirmed that the A2780R cells were more resistant to Cis than the parental cells (Fig. 1A and B). Interestingly, A2780R cells were more sensitive to both siGGCAGU and siGGGGGC than the parental cells (Fig. 1C and D). A similar phenomenon was observed for the PEO1/4 cell pair when treated with Carbo or toxic siRNAs (Fig. 1E-H). Finally, this observation was confirmed by testing another recently described Pt-S/Pt-R OC cell line pair, OV81/OV81 CP40, derived from a PDX mouse model of high grade serous OC (Supplementary Fig. S2) (32). In this case, the Pt-R cells were similarly sensitive to 6mer Seed Tox as the parental Pt-S cells, particularly when treated with siGGGGGC. These data suggest that 6mer Seed Tox could be a viable way to kill therapy resistant OC cells. It does not seem to be affected by cross resistance to various therapies often observed in therapy resistant cancers (33).

Presenting The miRNA Space as a Function of Seed Toxicity - The Seed Tox Plot.
We noticed that many seemingly unrelated miRNAs share seeds of similar toxicity and have now developed a way to represent all miRNAs at their actual expression levels in cells or tissues in a simple graph by plotting the miRNAs according to their seed toxicities (the Seed Tox plot). When comparing miRNA expression in different human tissues, we found that most tissues express predominantly nontoxic seed-containing miRNAs (Supplementary Fig. S3, pie charts, green slices, viability >50%) with only a small fraction of miRNAs having a predicted seed with high toxicity (red slices, viability <20%). A few abundant miRNAs are expressed across all tissues (Supplementary Fig. S3). These include the highly toxic miRNAs 22-3p and 24-3p (red), the intermediately toxic miRNAs miR-126-3p, miR-23b-3p, miR-29a-3p (blue), and the nontoxic miRNA members of the let-7 family, miR-125b-5p and miR-21-5p (green). Based on our *in vivo* treatment data (22), we postulate that it is the large amount of nontoxic miRNAs that protects normal tissues from 6mer Seed Tox.

Enrichment of miRNAs in The RISC in OC Cells.
miRNAs in cancer are almost always studied by quantifying them in the total RNA fraction. However, previous reports demonstrated that the majority of mature miRNAs are not Ago associated (34) and that endogenous miRNAs vary widely in their level of RISC association (35, 36). To assess the 6mer Seed Tox of biologically relevant miRNAs, we pulled down all Ago proteins and their associated miRNAs (23) from two OC cell lines allowing us to determine the exact positions 2-7 of RISC-bound guide strands. The results were compared to the standard analysis of total small RNAs in a Seed Tox plot with the x-axis showing the seed toxicity (Supplementary Fig. S4A and S4B). A number of miRNAs were highly enriched in the RISC-bound fraction of both cell lines. These include the toxic miRNAs 22-3p and 24-3p and the nontoxic miRNA miR-125b-5p (Supplementary Fig. S4). In addition, members of the toxic miRNA family miR-15/16, miR-15a/b-5p and miR-424-5p were also highly enriched (Supplementary Fig. S4C). Other miRNAs, most notably the highly abundant members of the let-7-5p family were reduced in the RISC (Supplementary Fig. S4C). Many of these miRNAs

with widely different presences in the RISC versus total were also recently reported for 293T and A549 cells (asterisks in Supplementary Fig. S4C, (35)). This analysis demonstrates that analyzing RISC bound miRNAs will allow to more accurately assess functionally relevant miRNAs (critical for analysis of 6mer Seed Tox) compared to the commonly used quantification of total miRNA levels and was therefore used in the following.

Changes in RISC Composition Related to Short and Long-Term Treatment with Platinum.
Next, we determined the toxicity of RISC bound miRNAs in Pt-S OC cells short-term treated with Pt-based chemotherapy or in Pt-R (long-term treated) cells (Fig. 2). The RISC of A2780 (Pt-S) and A2780R (Pt-R) cells untreated or treated with Cis for 72 hrs (a time point before the onset of cell death) was pulled down and the toxicity of all detected miRNAs plotted (Fig. 2A). In short-term Cis treated A2780 cells, highly toxic RISC-bound miRNAs (viability <20%) including miR-22/24-3p were significantly upregulated, while miRNAs with nontoxic seeds (viability >80%) were down (Fig. 2D). The Cis induced increase in toxic miRNAs was no longer significant in the Cis resistant A2780R cells (Fig. 2B). We then compared the RISC content between Pt-S and Pt-R cells (Fig. 2C). The A2780R cells contained fewer toxic miRNAs and more nontoxic miRNAs in the RISC compared to the Pt-S cells (Fig. 2D). A striking difference between the Pt-S and Pt-R cells was the increase in miR-21-5p in the RISC of the Pt-R cells (Fig. 2C and Supplementary Fig. S5A). Inhibiting miR-21-5p (Supplementary Fig. S5B) rendered Pt-R cells more sensitive to Cis (Supplementary Fig. S5C). The difference in expression of the toxic miRNAs 22-3p and 24-5p or the overexpression of miR-21-5p in the A2780R cells was not apparent when the toxicity of total miRNAs was analyzed (Supplementary Fig. S6). Similar to A2780 cells Pt treatment of PEO1 cells resulted in a significant increase of RISC bound toxic miRNAs including 22/24-3p (Fig. 2E) but not in the Pt-R PEO4 cells (Fig. 2F). Again the toxic miRNAs were significantly underrepresented in the RISC of the Pt-R PEO4 cells when compared to PEO1 cells (Fig. 2G). Similar changes in the balance between toxic and nontoxic RISC bound miRNAs were therefore found in both OC cell line pairs (Fig. 2D, H). However, nontoxic miRNAs other than miR-21-5p were upregulated in the resistant PEO4 cells (green arrows in Fig. 2G). Our data suggest that Pt treatment of Pt-S OC cells leads to an incorporation of miRNAs with highly toxic seeds into the RISC and the opposite effect is seen in Pt-R cells which have fewer toxic miRNAs and an increase in nontoxic miRNAs in their RISC. We propose that this "RISC priming" with miRNAs carrying toxic 6mer seeds versus miRNAs with nontoxic seeds determines whether OC cells respond to Pt based therapy or not.

To determine whether the changes detected in cell lines treated in vitro can be found in the RISC of OC xenografts grown in mice and treated with Pt, we injected OVCAR5 tumors orthotopically into nude mice and treated them repeatedly with either PBS or Carbo (Supplementary Fig. S7A). Tumors treated with Carbo were in general smaller compared to PBS injected control animals (insert a in Supplementary Fig. S7B). Consistent with the cell line models of acquired Pt resistance, *in vivo* Pt treated OVCAR5 tumors showed a reduction of toxic RISC-bound miRNAs with an increase in nontoxic miRNAs (Supplementary Fig. S7C). The clearest increase of nontoxic miRNAs was miR-194-5p, a miRNA recently reported to confer Pt resistance in OC (37) (Supplementary Fig. S7B, S7C). This increase correlated with the degree of Pt resistance of the tumors isolated from the Carbo treated mice after an *in vitro* culture for 5 days (insert b in Supplementary Fig. S7B) and underscores our hypothesis that OC cells may have different ways to acquire therapy resistance by upregulating various miRNAs with nontoxic 6mer seeds.

Preferred Uptake of Toxic siRNAs into the RISC of Platinum Tolerant Cells.
To determine why some Pt resistant cells were more sensitive to toxic 6mer seed containing siRNAs, we transfected the A2780/A2780R cell pair with a low amount (1 nM) of either the nontoxic siUAGUCG (siNT1), the highly toxic siGGCAGU, or siGGGGGC. At this concentration, the latter two siRNAs were not toxic to the parental cells but significantly reduced cell growth of the Pt-R cells (Supplementary Fig. S8A). In all transfected cells analyzed 24 hrs post transfection, large numbers of RISC-bound and total reads derived from the guide strand of the transfected siRNAs (Supplementary Fig. S8B) were detected across all samples with negligible numbers of reads derived from the blocked passenger strand (Supplementary Fig. S8C). We noticed an equal uptake of the nontoxic siRNA into Pt-S and Pt-R cells and their RISC, with a much higher uptake of the two toxic siRNAs in A2780R cells (Fig. 3A-D, Supplementary Fig. S8D-S8F). The 5 most abundant exogenous siRNA sequences that were detected in cells and incorporated into the RISC had the AA 3' overhang in the guide of the siRNA duplex removed and a number of species showed evidence of 3' uridylation (Fig. 3E). Trimming and tailing (addition of 2-3 nts) of miRNAs has been described to be part of a common mechanism of miRNA turnover (38). While tailing does not allow to predict RISC association (39), the two toxic guides

showed a higher percentage of the double UU tailing event and most strikingly, the double uridylated species was the one most highly enriched in the Pt-R cells pointing at a difference in the way toxic small RNA may be processed by Pt-S and Pt-R cells.

Based on these results, we were able to assess the ratio of toxic siRNA to RISC bound miRNA required to negatively affect a cell. Because Ago k.o. cells are resistant to the effects of toxic siRNAs we know that the toxicity is dependent on Ago2 being part of the RISC. The nontoxic siUAGUCG replaced about the same amount of miRNAs from the RISC in Pt-S and Pt-R cells, while the two toxic siRNAs were less efficient in replacing miRNAs in the Pt-S cells (Fig. 3D). The overall seed toxicity of all RISC bound reads in cells transfected with the two toxic siRNA significantly dropped in A2780R cells, resulting in a relatively small change in overall 6mer seed composition of RISC bound sRNAs between the A2780 and A2780R cells (Supplementary Fig. S8G). These data suggest that a moderate shift of seed toxicity of about 10% or less is sufficient to reduce cell growth and/or cause cell death.

Changes in Tumors of OC patients Caused by Platinum Based Therapy.

To determine whether changes in toxic and nontoxic 6mer seed containing miRNAs are associated with Pt resistance in OC patients, we studied a well characterized group of Pt sensitive and Pt resistant patients with FIGO stage III/IV high grade serous OC who underwent primary debulking surgery followed by adjuvant chemotherapy with Carbo and Paclitaxel (Supplementary Table S3). Fresh frozen primary OC tissue specimens were subjected to an Ago pull down/smRNA Seq analysis. Two cohorts of patients were compared: Group I: 9 patients were Pt refractory or resistant (recurrence <180 days after the end of chemo = Pt-R patients), Group II was platinum sensitive, experiencing a late recurrence (>180 days) or no recurrence (= Pt-S patients) (Fig. 4A). Because the RISC composition could be affected by the age of the patients both groups were age matched (Supplementary Fig. S9A). miRNA enrichment in the pulled down RISC was highly efficient. Across all 21 samples, between 97.4% and 98.1% of all Ago bound reads were miRNAs. When ranking all highly abundant reads derived from miRNAs (sum >10,000 across all samples) according to the fold change in the Pt-S patients, we found that tumors in Pt-S patients had an enrichment of miRNAs with more toxic seeds while Pt-R tumors were enriched in miRNAs with *non*toxic seeds (Fig. 4B). This correlation was also apparent when all ~38,000 reads were ranked according to the predicted 6mer Seed Tox of each read (Supplementary Fig. S9B). When we reanalyzed the data in Fig. 4B using the time to relapse after the end of treatment as a continuous variable and ranked the abundant reads according to the highest Pearson correlation with seed toxicity, rather than comparing the two groups (Pt-S vs. Pt-R), the correlation was similar (Supplementary Fig. S9C). A shorter time to relapse correlated with higher amounts of non-toxic RISC-bound miRNAs.

Comparing the significant differences in RISC-bound miRNAs between the two groups ($p<0.05$, >1.5x fold) in a Seed Tox plot identified miR-449 and miR-195-5p as depleted and miR-125a-5p, miR-125b-5b, miR-199a-5p, miR-99a/b-5p, miR-100-5p, miR-376c-3p, miR-451a, miR-214-3p, miR-194-5p, miR-144-3p and miR-199a/b-3p as enriched in Pt-R tumors (Fig. 4C). That RISC-bound miRNAs enriched in the Pt-R tumors had a significantly higher seed viability than in the Pt-S tumors, was also reflected in the change in seed composition (insert in Fig. 4C). These data suggest that it is not an individual miRNA but a combination of nontoxic miRNAs that confers Pt resistance to human OC.

The average seed composition of total RISC-bound miRNAs in the tumors was different (Supplementary Fig. S10A). An unsupervised hierarchical cluster analysis of the reads with the ten most frequent 6mer seeds separated patient tumors into two types (Supplementary Fig. S10B). One type contained seeds present in miR-200 family members, and the other type contained seeds found in miR-21-5p and members of the let-7-5p family. However, both types contained Pt-S and Pt-R patients and therefore do not correlate with outcome.

When focusing on only the most highly expressed miRNAs in Pt-R patient tumors, we found six miRNAs to correlate with Pt resistance in OC patients: miR-125a-5p, miR-125b-5p, miR-214-3p, miR-100-5p, miR-199-5p, and miR-199a/b-3p (Supplementary Table S4). Grouping patients with the 50% highest and lowest combined reads of these six miRNAs separated Pt-S from Pt-R patients (Fig. 4D). These six highly abundant miRNAs also correlated individually with the Pt sensitive days (Fig. 4E). Individual Kaplan-Meier analyses with these six miRNAs showed that the separation is largely driven by four miRNAs (miR-125a-5p, miR-125b-5p, miR-100-5p, and miR-199-5p) using the combination of these miRNAs allowed for the best distinction of Pt-S and Pt-R patients (Supplementary Fig. S11).

Analysis of Primary Tumors and Recurrences in Patients with Very Long Overall Survival.

A comparison of matched primary tumors with recurrences is often not feasible in OC as patients are usually only operated on once. However, we recently described a subgroup of patients that for unknown reasons maintain Pt sensitivity and/or have oligometastatic recurrences (40, 41). Because some of these patients undergo a secondary surgery, we were able to compare 6mer Seed Tox between the initial tumor and the recurrence (Fig. 5A and Supplementary Table S3). Two patients (#290 and #200) overlapped with the above analysis (Fig. 4), however, we analyzed a different tumor site, allowing us to test both the similarities between these tumors and the reproducibility of the Ago pull down/smRNA Seq analysis (Supplementary Fig. S12). The independent analyses of the two tumors from the same patients were more similar when compared to the average of the other primary tumors in the second set.

Overall Seed Tox was higher in the recurrent tumors based on a comparison of the most abundant reads in the matched primary tumors (Fig. 5B). Integrating all reads of the primary tumors and the recurrences revealed that some miRNAs with toxic seeds were up (e.g. miR-22-3p and the miR-15/16-5p family), while miRNAs with nontoxic seeds (miR-26a/b-5p, let-7-5p family, miR-143-5p, miR-125a/b-5p, miR-30-5p family) were downregulated in the recurrent tumors (Supplementary Fig. S13A). While the recurrences and primary tumors were from the same patients, we could not exclude that the difference in Seed Tox of RISC bound miRNAs was due to differences in the tumor microenvironment or the distinct anatomic locations of the 1st and 2nd surgery. An unsupervised hierarchical cluster analysis based on RISC-bound miRNAs showed that the primary and recurrent tumors from four patients were highly related regardless of anatomic location, suggesting that the detected miRNAs were tumor specific (Supplementary Fig. S13B). A Seed Tox plot was generated of the samples of these four tumor pairs (Fig. 5C). A few miRNAs with toxic seeds were upregulated in the recurrences, while several miRNAs (e.g. miR-125b-5p) with nontoxic seeds were downregulated (paired analysis, $p<0.05$, >1.5x change). This resulted in a significant drop in average toxicity of all miRNAs enriched in recurrences (Fig. 5D). To identify the miRNAs driving these changes, we plotted all miRNAs that were significantly deregulated in the same direction in this subgroup of patients (Fig. 5E). In this analysis in which we applied a paired Student's T test in three out of 4 patients, the most abundant upregulated miRNA was miR-15b-5p which can kill cancer cells in part through 6mer Seed Tox (27), and the most abundant downregulated nontoxic miRNA was again miR-125b-5p. Analysis of all patient tumor pairs suggests that the differences seen between primary tumors and matched recurrences in this rare patient population are due to intrinsic changes in the tumor cells. Tumors of “multiple Pt responders" (42), do not acquire Pt resistance through upregulation of nontoxic/protective miRNAs. Based on our data we predict that the recurrences in these patients are as Pt sensitive as the initial tumors.

DISCUSSION

We have advanced a novel concept to explain how miRNA families target gene networks regulating cell fate. This concept is not based on the activity of any individual miRNA or its targets but on the assumption that it is the entirety of all miRNAs that determines through 6mer Seed Tox whether genes critical for cell survival are being silenced. We are now proposing that miRNAs with highly toxic seeds can be countered by large quantities of miRNAs that carry nontoxic seeds. Testing this concept required assessing position 2-7 of RISC bound miRNA guides. To obtain this information, we combined the method of Ago pull down/smRNA Seq with a specific bioinformatics pipeline to analyze 6mer seeds in short reads. The method does not require crosslinking of the miRNAs with their target mRNAs as the primary goal of our study was not to identity miRNA targets, but to determine the seed content of the RISC in cancer cells and tumor tissue. Recent data suggest that many miRNAs detected in total RNA are part of a low-molecular-weight RISC that is not associated with either GW182 or mRNAs (36). By using a GW182 peptide to pull down Ago proteins we may have preferentially isolated active RISC complexes as only those active (high-molecular-weight) complexes comprise of miRNA, Ago, mRNAs and GW182 (36). This is supported by our recent observation that the GW182 peptide could not efficiently pull down Ago in Drosha k.o. cells devoid of most miRNAs (26) despite Ago expression levels being unchanged (23) and provides an explanation for the large variation we found between total and RISC-bound miRNAs for a number of miRNAs.

We also developed a way to visualize all significantly expressed miRNAs in one simple plot. The 6mer Seed Tox plot relies only on the predicted toxicity of every miRNA based on our screen of all 6mer seeds. miRNAs that are part of different families with entirely different biological functions may have similar seed toxicities and will be found in the same peaks. Using these analyses, we provide evidence that it is the balance between toxic and nontoxic 6mers embedded in miRNAs that determines whether cancer cells die or resist Pt-based chemotherapy. We provide the first evidence that efficient Pt induced cell death is dependent on a functional RNAi system and that cells devoid of miRNAs (most of which contain nontoxic seeds) are highly sensitive to Pt induced cell death. The immediate reaction of OC cells to Pt is downregulation of miRNAs with nontoxic seeds and upregulation of miRNAs containing highly toxic 6mer seeds such as miR-22-3p and miR-24-3p. Both of these miRNAs are upregulated in human embryonic stem cells lines upon differentiation (43) and both have been shown to induce cell death when transfected into HCT116 cells (44). In contrast, OC cells that have acquired resistance after long-term Pt exposure show the opposite pattern: These Pt-R cells contain fewer toxic miRNAs and more nontoxic RISC-associated miRNAs. Consistent with the *in vitro* data tumors from patients with Pt resistance had more miRNAs with nontoxic seeds, while Pt sensitive patients had more miRNAs with toxic seeds. Confirming the proposed concept, recurrent tumors from patients that remain Pt sensitive had higher concentrations of toxic miRNAs in their RISC compared to the original primary tumor. In both analyses of patient tumors the nontoxic miRNA most relevant to primary OC tumors was the abundant miRNA miR-125b-5p.

While our study is based on a relatively small number of patients, this is the first analysis of primary human tumors based exclusively on RISC-bound miRNAs. Traditionally, analysis of miRNAs in human cancers is done using total RNA. It is based on the assumption that quantification of total miRNA amounts in cells or tissue allows to assess the functional relevance of expressed miRNAs. Yet, a recent study has shown that the level of Ago-bound miRNAs is a better indicator of miRNA activity than the total level of miRNA expression. The differential binding of miRNAs to the RISC was found to be cell type specific (35), and to be independent of GC content of miRNAs. However, it was strongly dependent on the abundance of complementary mRNA targets. Our data now suggest this to be true for ovarian tumors and identify a number of miRNAs to be preferentially associated with Ago proteins, some of which we then found to be associated with the response of OC cells to Pt-based chemotherapy.

Our published data on reducing tumor growth in xenografted OC bearing mice by delivering toxic siRNAs without affecting normal tissues (22, 45) is consistent with a model in which high amounts of nontoxic miRNAs protect cells from 6mer Seed Tox. This, however, raises the question of why Pt-resistant cells, which apparently also express a higher amount of nontoxic miRNAs, are still susceptible to 6mer Seed Tox. One explanation could be a different way cancer cells use nontoxic seed containing miRNAs or load toxic siRNAs into the RISC when compared to normal tissues. It is known that in normal tissues Ago proteins are unstable when not bound to miRNAs. Both mouse embryonic fibroblasts lacking Dicer expression (46), or mouse embryonic stem cells with knocked out Dicer or DGCR8 (47) contained less Ago proteins. In contrast, in cancer cells, we did not find a reduction in AGO1 or AGO2 expression in cells deficient in either Dicer or Drosha in

HCT116 and 293T cells (23) suggesting a fundamental difference in the way Ago proteins act in certain normal and in cancer cells.

It is not only the binding of miRNAs to Ago proteins that stabilizes them, but also the amount of mRNAs with targeted seed matches that bind to these miRNAs (35). Our finding that the two toxic siRNAs siGGCAGU and siGGGGGC are present in higher numbers and loaded into the RISC more efficiently than the nontoxic siUAGUCG when transfected into Pt-R cells could be due to the two toxic siRNAs targeting survival/housekeeping genes (26). We propose two possible models of why Pt-R cells preferentially take up toxic siRNAs: Either Pt-R cells process such siRNAs in a different way supported by our finding that Pt-R cells seem to prefer 3' diuridylated siRNAs in the RISC or Pt-R cells express more targeted mRNAs after upregulating survival genes.

Our data suggest that focusing on single miRNAs or even miRNA families may not result in a reliable marker for Pt resistant OC. We hypothesize that OC cells can acquire Pt resistance by upregulating any miRNA that carries a nontoxic 6mer seed consistent with countless reports providing evidence for the involvement of single miRNAs in Pt resistance in OC cell lines (37, 48-55) (Supplementary Table S1 and S2). Pt resistance in different OC cell line models and in OC patients may be driven by a variety of nontoxic miRNAs. This is supported by our RNAseq data derived from different models (Table 1). We conclude that Pt resistance in each of the three models and in human patients may be driven by different nontoxic miRNAs reported to render OC cells Pt tolerant. Our Cis resistant A2780R utilize miR-21-5p, PEO4 cells are more tolerant to Carbo in part due to upregulation of miR-130a-3p and OVCAR5 cells exposed to prolonged treatment with Carbo *in vivo* upregulate mostly miR-194-5p. Finally, in tumors from Pt-R patients we found evidence for an upregulation of RISC-bound miR-214-3p and most prominently miR-125b-5p in the most Pt resistant patients. While any of these miRNAs could serve as both a target for therapy and as biomarkers, it is entirely possible that different miRNAs will be identified to confer therapy resistance in other cell lines and patient analyses. What they may all share is the presence of a nontoxic seed. Using artificial toxic 6mer seed containing miRNAs or siRNAs could therefore be used to eliminate OC and other cancers and our data suggest that Pt resistant tumors may be at least as sensitive to these toxic siRNAs as chemotherapy sensitive tumors.

METHODS

Reagents and Antibodies

Carboplatin (Carbo) (#C2538) was purchased from Sigma-Aldrich, Cisplatin (Cis) (#1134357) was from Millipore Sigma, Lipofectamine RNAimax (#13778150) from Thermofisher Scientific. Primary antibodies for western blot: Anti-Argonaute-2 antibody (#ab32381) was purchased from Abcam; anti-Dicer (D38E7) antibody (#5362) from Cell Signaling; anti-β-actin antibody (#sc-47778) was purchased from Santa Cruz. The secondary antibody was a goat anti-rabbit IgG-HRP (#4030-05) from Southern Biotech.

Cell Lines

Human OC cell lines HeyA8, OVCAR5 were cultured in RPMI 1640 medium (Cell gro #10-040 CM) supplemented with 10% heat-inactivated fetal bovine serum (FBS) (Sigma-Aldrich # 14009C), 1% L-glutamine (Mediatech Inc), and 1% penicillin/streptomycin (Mediatech Inc); PEO1 and PEO4 cells were cultured in the above medium and supplemented with 2 mM sodium pyruvate (Mediatech Inc). 293T WT, 293T Dicer k.o. cells [Clone #2-20; (56)], HeLa control and HeLa Ago2 k.o. were a kind gift from Dr. Sarah Gallois-Montbrun (57), 293T Ago2 k.o. cells were provided from Dr. Klaas Mulder (58) and OC cell lines A2780 and A2780R (29) and OV81.2 and OV81 CP40 (32) were all grown in DMEM medium (Gibco #12430054) supplemented with 10% FBS, 1% L-glutamine and 1% penicillin/streptomycin. All cell lines were authenticated by STR profiling and tested for mycoplasma using PlasmoTest (Invitrogen).

Western Blot Analysis

Cells were lysed using Killer RIPA lysis buffer (150mM NaCl, 10 mM Tris HCl pH7.2, 1% sodium dodecyl sulfate (SDS), 1% TritonX-100, 1% Deoxycholate, 5 mM EDTA) and freshly added PMSF (1 mM) and Protease Inhibitor Cocktail (Roche #11836170001). Equal amounts of protein (30 μg) were resolved on a 10% SDS-PAGE gel and Western blot was performed as previously described (23). Visualization of protein bands was performed using the SuperSignal™ West Dura Extended Duration Substrate (Thermo Fisher Scientific #34076). Antibodies diluted in 5% dry milk powder in 0.1% Tween-20/TBS (TBST): anti-Argonaute-2 (1:1000), anti-β-actin (1:5000), anti-rabbit IgG HRP (1:5000). Anti-Dicer antibody was diluted (1:1000) in 5% BSA in TBST.

Assessing Cell Growth and Viability Assay

For transfection in 96-well plates to monitor cell growth using IncuCyte Zoom (Essen Bioscience), 50 μl Optimem (Fisher Scientific #331985088) mix containing RNAimax and 10 nM siRNA (siNT1, siGGCAGU or siGGGGGC) was used. RNAimax amounts per 96-well were optimized for each cell line used: A2780 (0.2 μl), PEO1/4 (0.3 μl), 293T (0.1 or 0.2 μl), OV81.2 (0.2 μl). Seeding densities for reverse transfection with siRNAs or Pt treatment in 96-well plates were also optimized for each cell line used: A2780/A2780R and OV81.2/OV81 CP40 (1500 cells), PEO1/PEO4 and 293T (1500 cells). The following siRNA oligonucleotides were obtained from Integrated DNA Technology and annealed per the manufacturer's instructions:
siUAGUCG (siNT1) sense: mUmGrGrUrUrUrArCrArUrGrUrCrGrArCrUrArATT
siUAGUCG (siNT1) antisense: rUrUrArGrUrCrGrArCrArUrGrUrArArArCrCrAAA
siGGCAGU (si34a-5p^{Seed}) sense: mUmGrGrUrUrUrArCrArUrGrUrArCrUrGrCrCrATT
siGGCAGU (si34a-5p^{Seed}) antisense: rUrGrGrCrArGrUrArCrArUrGrUrArArArCrCrAAA
siGGGGGC sense: mUmGrGrUrUrUrArCrArUrGrUrGrCrCrCrCrCrATT
siGGGGGC antisense: rUrGrGrGrGrGrCrArCrArUrGrUrArArArCrCrAAA
For treatment with Cis or Carbo, cells were seeded in triplicates in 96-well plates and treated with the indicated drug concentrations. Cell growth was monitored using IncuCyte Zoom live-cell imaging system (Essen Bioscience) with a 10x objective. The confluency curves were generated using the IncuCyte Zoom software (version 2015A). A viability assay that measures the level of ATP within cells was done in 96-well plates. Briefly, 72 hrs post-treatment with drugs or 96 hrs post reverse transfection with siRNAs, media in each well was replaced with 70 μl fresh medium and added 70 μl of Cell Titer-Glo reagent (Promega #G7570). The plates were covered with aluminum foil and shaken for 5min and then incubated for 10 min at room temperature before reading the luminescence on a BioTek Cytation 5. IC_{50} values for cisplatin or carboplatin in viability assay comparing Pt sensitive with Pt tolerant cells were determined using GraphPad Prism 6 software by logarithm normalized sigmoidal dose curve fitting.

miR-21-5p Inhibition and Real-time PCR

Real-time PCR was performed for miR-21-5p in A2780R cells infected with lentivirus from Zip control (pLenti-III-mir-GFP control vector from Applied Biological Materials #m001) or Zip-21 (LentimiRa-GFP-has-miR-21-5p vector, Applied Biological Materials #mh10276). Briefly, 25 ng total RNA was used to make cDNA using the High-Capacity cDNA Reverse Transcription Kit (Applied Biosystems #4368814). The qPCR was then done using the Taqman Gene Expression Master Mix (ThermoFisher Scientific #4369016) as previously described (59) using the following primers: hsa-miR-21 (Thermofisher #0003970) and Z30 (Thermofisher #001092). The relative expression of miR-21-5p was normalized to the level of Z30. Statistical analysis was performed using Student's T-test.

In Vivo Treatment of OVCAR5 Cells with Carbo.

Female (6-8 weeks old) athymic nude mice (*Foxn1*^{nu}, Envigo) were injected intraperitoneally (i.p.) with 2 million OVCAR5 OC cells to induce tumors. After 2 weeks inoculation (60), mice were treated i.p. with PBS (control, mice ID: 791, 792, 793, 794, n=4), or 25 mg/kg carboplatin (n = 5) as following treatment regimens: once-a-week for 3 weeks (stage 1, n=2, mice ID: 795, 797); 3-week Carbo followed by two-week no drug recovery (Stage 2, n = 1, mice ID: 796); additional two weeks (5 weeks Carbo in total) Carbo after recovery (Stage 3, n = 2, mice ID: = 798, 800). Xenograft tumors were collected 1 week after carboplatin treatment and processed for cancer cell isolation and RNA extraction. Tumors were mechanically and enzymatically dissociated in Dulbecco's modified Eagle's medium/F12 (Thermo Fisher Scientific, Ref# 11320) containing collagenase (300 IU/ml, Sigma-Aldrich, Cat# C7657) and hyaluronidase (300 IU/ml, Sigma-Aldrich, Cat# H3506) for 2 hours at 37°C. Red blood cell lysis used RBC lysis buffer (BioLegend, Cat# 420301), followed by DNase (1 mg/ml, Sigma Aldrich, Cat# DN25) treatment and filtering through a 40 µm cell strainer (Fisher Scientific, Cat#NC0147038) to produce single cell suspension. EasySep^{TM} Human Epcam positive selection kit (Stemcell Technologies, Cat# 17846) was used on the single cell suspension for Epcam positive OC epithelial cell selection followed by manufacturer instructions.

Small Total RNA Seq

For small RNA-seq experiments, cells were lysed using Qiazol. For all RNA-Seq samples, a DNAse digestion step was included using the RNAse-free DNAse set (Qiagen #79254). Total RNA was isolated using the miRNeasy Mini Kit (Qiagen # 74004). The quality of RNA was determined using an Agilent Bioanalyzer. The RNA library preparation and subsequent sequencing on Illumina HiSEQ4000 was then done by the NU-Seq Core at Northwestern University.

Raw read sequences were trimmed with trim_galore to remove all standard Illumina adapters, leaving reads at least 6 bp in length. In addition, any reads containing the substring GTCCGACGATC followed by 3 to 5 nucleotides were discarded. This removed any remaining 5' adapter sequences and ensured that only RISC bound sRNAs were analyzed which was critical to determine position 2-7 of each read. Trimmed reads were then sorted, uniq'd, counted. A six nucleotide Unique Molecular Identifier (UMI) was removed from each read, and the numbers of reads associated with the same core read sequence and any UMI were summed to generate the raw read count for a particular sample. Counts were tabulated for each read and sample and normalized per million reads in the column (sample) sum. Reads were blasted (blastn-short) against custom blast databases created from all processed human miRNAs (miRbase 22.1) and from the most recent RNA world database (human_and_virus_vbrc_all_cali_annoDB_sep2015) obtained from the Tuschl lab at Rockefeller University. Processed miRNA hits were filtered for 100% identity, and a match length of at least 18 bases. RNAworld hits were filtered for at least 95% identity, with the match starting within the first 9 bp of the sequencing reads. These filtered blast results were used to annotate reads with their likely source, and when no blast hit passed these filters, the read was annotated "noMatch". Reads were also associated with their 6mer seed (positions 2-7) and with the previously identified seed toxicity determined in human OC cells HeyA8 (26) (6merdb.org). For tractability, only reads with a total count of at least 6 CPM summed across all samples were retained for further analyses. To identify reads enriched in a particular group of samples, we used the R package EdgeR with the un-normalized read counts, annotating the resulting reads with seed toxicity and blast-based annotation as described above.

Ago Pull-Down and Subsequent Small RNA-Seq

For Ago pull-down experiments, transfections or treatments described above for 96-well plates, were scaled up for 150 mm dishes. At the required time point for pull-down, cells were washed with PBS and 10 million cell

pellets were frozen at -80 °C until ready to be lysed using 1 ml NP40 lysis buffer [50 mM Tris pH 7.5, 150 mM NaCl, 5 mM EDTA, 0.5% NP-40, 10% (v/v) glycerol, 1 mM NaF; supplemented with 1:200 EDTA-free protease inhibitors (Millipore #539134) and 1:1000 RNaisin Plus (Promega #N2615) before use]. Mouse or patient tumor lysates were prepared by first chopping 250 mg tissue with a clean razor blade and then using a Dounce homogenizer containing 1 ml NP40 lysis buffer. In patient tumors for which 250 mg tissue was not available, at least 100 mg tissue was used for pull down. The tissue was homogenized by passing the pestle up and down the cylinder several times while keeping the homogenizer cool on ice. Cell or tissue lysates were then incubated on ice for 15 min, vortexed, and then centrifuged at 20,000 g for 20 min. The lysates were then transferred to siliconized microcentrifuge tubes (low-binding, Eppendorf #022431021), and Ago1-4 were pulled down using 500 μg of Flag-GST-T6B peptide (61) and with 80 μl anti-Flag M2 Magnetic beads (Sigma #M8823) for 3 hrs on a rotor at 4°C. The precipitate was washed three times in NP40 lysis buffer and during the last wash, 10% of the beads were removed and incubated at 95°C for 5 min in 2x SDS-PAGE sample buffer. The efficiency of the pull down was determined by running these samples on a 10% SDS-PAGE gel, transferring to nitrocellulose membrane and immunoblotting against Ago2 (Abcam #32381). 500 μl TRIzol reagent was added to the remaining beads and RNA was extracted using the manufacturer's instructions. The RNA pellet was dissolved in 20 μl water. Half of the RNA sample was dephosphorylated with 0.5 U/μl of CIP alkaline phosphatase at 37°C for 15 min and then radiolabeled with 0.5μCi γ-^{32}P-ATP and 1 U/μl T4 PNK kinase for 20 min at 37°C. The RNAs interacting with Ago1-4 were visualized on a 15% Urea-PAGE. The other half of the RNA sample was used for a small RNA library preparation, as previously described (62). Concisely, RNA was ligated with 3'-adenylated adapters and separated on a 15% denaturing Urea-PAGE. The RNA corresponding to insert size of 19-35 nt was eluted from the gel, ethanol precipitated and then ligated with the 5' adapter. The RNA samples were then separated on a 12% Urea-PAGE, extracted from the gel and reverse transcribed using Superscript III reverse transcriptase (Invitrogen #18080-044) and the cDNA was amplified by PCR. The cDNA was sequenced on Illumina Hi-Seq 4000. 19nt RNA size marker: rCrGrUrArCrGrCrGrGrGrUrUrUrArArArCrGrA
35nt RNA size marker: rCrUrCrArUrCrUrUrGrGrUrCrGrUrArCrGrCrGrGrArArUrArGrUrUrUrArArArCrUrGrU
The following set of eight 3' adenylated adapters was used, each containing a unique 6mer barcode sequence at the 5' end (underlined). These barcodes were used to separate the reads into individual pull-down samples before proceeding with the small RNA pipeline as described above. For ease of use, the sequence files uploaded to GEO have already been split into reads from individual experiments:
Adapter 1-rAppNN<u>CTGACA</u>TGGAATTCTCGGGTGCCAAGG-L
Adapter 2-rAppNN<u>ACTAGC</u>TGGAATTCTCGGGTGCCAAGG-L
Adapter 3-rAppNN<u>GTACGT</u>TGGAATTCTCGGGTGCCAAGG-L
Adapter 4-rAppNN<u>TGTACG</u>TGGAATTCTCGGGTGCCAAGG-L
Adapter 5-rAppNN<u>CAGCAT</u>TGGAATTCTCGGGTGCCAAGG-L
Adapter 6-rAppNN<u>TCATAG</u>TGGAATTCTCGGGTGCCAAGG-L
Adapter 7-rAppNN<u>ATAGTA</u>TGGAATTCTCGGGTGCCAAGG-L
Adapter 8-rAppNN<u>GATGCT</u>TGGAATTCTCGGGTGCCAAGG-L
5' adapter with unique molecular identifiers (UMI): GTTCAGAGTTCTACAGTCCGrArCrGrArUrCrNrNrNrN
5' adapter without UMI: rGrUrUrCrArGrArGrUrUrCrUrArCrArGrUrCrCrGrArCrGrArUrC (used only in the experiment shown in Fig. 2).
RT primer sequence: GCCTTGGCACCCGAGAATTCCA
Four 3' PCR primers were used each containing a unique index (underlined) recognized by Illumina:
Primer1:CAAGCAGAAGACGGCATACGAGAT<u>CGTGAT</u>GTGACTGGAGTTCCTTGGCACCCGAGAATTCCA
Primer2:CAAGCAGAAGACGGCATACGAGAT<u>ACATCG</u>GTGACTGGAGTTCCTTGGCACCCGAGAATTCCA
Primer3:CAAGCAGAAGACGGCATACGAGAT<u>GCCTAA</u>GTGACTGGAGTTCCTTGGCACCCGAGAATTCCA
Primer4:CAAGCAGAAGACGGCATACGAGAT<u>TGGTCA</u>GTGACTGGAGTTCCTTGGCACCCGAGAATTCCA
5'PCR primer:
AATGATACGGCGACCACCGAGATCTACACGTTCAGAGTTCTACAGTCCGA

The Seed Tox Plot

Reads were aggregated (read numbers collapsed) first by the seed sequence (position 2-7 of each read) and then by the miRNA and RNA World RNA that the read aligned to (Blast search see above). Each seed sequence had an assigned percent cell viability from the 4096 siRNA screen in the OC cell line HeyA8 ((26) and 6merdb.org), the aggregated read numbers were further binned in RStudio based on the HeyA8 cell

viability in 1% increments. Seed tox plots (number of reads on Y axis and See viability on X axis) were then generated using Excel with smoothing enabled. The file with the collapsed data was used to identify the most abundant miRNAs that make up each peak in the 6mer Seed Tox plot and when a peak consisted of more than one abundant miRNA (>5000 or >1000 reads) miRNAs were listed in the order of abundance.

Analysis of smRNAs in Normal Tissues.
Data of total smRNA were retrieved (accession #GSE11879) and analyzed from 9 human tissues. To compare different tissues and consistently identify and label the most abundant miRNAs all 9 data sets were normalized to 1,000,000 reads. For each tissue, miRNAs were labeled in Seed Tox plots with >5000 norm average reads. When a peak contained more than one miRNA they are shown in the order from highest to lowest abundance.

Seed and Tox Analysis
To determine the average Seed Tox of all reads in a data set or to determine the average 6mer seed composition of reads in a data set, numbers for all individual reads were divided by a factor that reduced the number of the most abundant read to less than 1000. In a comparison analysis significantly up- or downregulated reads were processed separately. Associated toxicity and 6mer seed sequences for each read were then multiplied by this factor using a Perl script. The resulting read numbers were plotted as a box plot using the chart function of StatPlus:Mmac Pro v.7.3.3. using default settings and p values of deregulated seed toxicities were determined using a Wilcoxon rank test. Expanded seed sequences were plotted using Weblogo (http://weblogo.berkeley.edu) as a custom frequency plot.

Comparison of Total and RISC Bound sRNAs.
RNA Seq data sets were used for either total smRNA (DISE26 for A2780 and GSM3029765/GSM3029766 for HeyA8) or Ago bound smRNAs (DISE18 for A2780 and GSM3029217/GSM3029218 for HeyA8). To compare the amount of total versus RISC bound miRNAs all four data sets (with two duplicates each) were combined into one file using R. Each read column was renormalized to 1,000,000 reads. All reads were isolated with a length of 19-25 nt before generating Seed Tox plots.

Patient Samples and Analysis
All patient samples (described in Supplementary Table S3) were collected at the University of Chicago Medical Center following approval from the Institutional Review Board, and after obtaining written informed consent from the patients. All patients included in the study underwent primary debulking surgery for advanced stage (no patients undergoing neo-adjuvant treatment were included), metastatic high grade serous OC by a Gynecologic Oncologist. The tissue was snap frozen at the time of surgery and stored at -80C until further use. Clinico-pathologic data was collected prospectively and updated every three months based on clinical exam, CA-125, or imaging.

Analysis of Correlation Between Patient Groups and Seed Tox.
Total norm count data were used. Reads were aggregated according to reads and blasted miRNAs. Patients were either separated into the two groups (Pt-R and Pt-S) compared or read associated toxicity was correlated using Pearson correlation (including p values) with Pt sensitive days as given in Supplementary Table S3.

Identification of The Most Abundant miRNAs Enriched in Pt-R Patients.
Total norm count data after adapter removal were used. Reads were aggregated according to reads and blasted miRNAs. All reads with an average read number of 1000 or more across all samples used for this analysis. Student's t-test ($p<0.05$) was used to identify all miRNAs that were enriched in the Pt-R patients (>1.5x).

Unsupervised Hierarchical Cluster Analysis and Heat Maps.
Either the collapsed reads of the ten most abundant miRNAs (carrying the same 6mer seed) (Supplementary Fig. S10B) or the most abundant miRNAs (>10,000 ave reads across all samples) (Supplementary Fig. S13B) were hierarchically clustered and plotted in R according to pairwise Pearson correlation.

Kaplan-Meier Analysis

Samples were divided into two groups according to expression of particular seeds/miRNAs, and survfit/ggsurvplot was used in R to create Kaplan-Meier curves contrasting the time to recurrence between the two groups.

Statistical Analyses

IncuCyte experiments were performed in triplicates, and the data expressed as mean ± standard error. Continuous data were compared using t-tests for two independent groups. For evaluating continuous outcomes over time, two-way ANOVA was performed using the Stata1C software, where the treatment condition was used as component of primary interest and time as a categorical variable. When controls were very different between different treated cells, a binomial test was used for comparisons of single proportions to hypothesized null values (26).

Data Availability

smRNA Seq data were deposited at GEO under the GSE series GSE165148. Data can be accessed using reviewer access token ojsdemaabzytdgx.

Authors' Disclosures

The authors declare no potential conflicts of interest.

Author Contributions

M. Patel: Performed experiments, wrote the manuscript. **Y. Wang**: Performed experiments. **A.E. Murmann:** Performed experiments. **E.T. Bartom:** Performed bioinformatics analyses. **R. Dhir:** Provided OC patient material. **K. Nephew:** Contributed a cell line and expertise. **D. Matei:** Provided cell lines, expertise and supervised the animal experiment. **E. Lengyel:** Provided OC patient material, wrote the manuscript. **M.E. Peter:** Conceived the project, supervised research, and wrote the manuscript.

Acknowledgments

We are grateful to Drs. Gallois-Montbrun and Mulder for providing Ago2 k.o. cell lines.

Figure legends

Figure 1. Platinum tolerant Pt-R OC cells are at least as sensitive to toxic 6mer seeds as Pt-S cells**. A,** Change of confluency of A2780 and A2780R cells over time treated with 5 μM Cis. **B,** Dose response curves (96 hrs ATP viability assay) of cells in A. **C,** Change of confluency of A2780 and A2780R cells over time treated with either 10 nM siNT1, siGGCAGU, or siGGGGGC. **D,** Viability of the cells in C after transfection with 10 nM of the siRNAs. **E,** Change of confluency of PEO1 and PEO4 cells over time treated with 1 μg/ml Carbo. **F,** Dose response curves (96 hrs ATP viability assay) of cells in E. **G,** Change of confluency of PEO1 and PEO4 cells over time treated with either 10 nM siGGCAGU or siGGGGGC. **H,** Viability of the cells in G after transfection with 10 nM of the siRNAs. Each data point (A, B, C, E, F & G) represents mean ± SE of three replicates. Each bar (D, H) represents ± SD of three replicates. P-values were calculated using ANOVA (A, C, E, G), or student's t-test (D, H). ** $p<0.0001$, * $p<0.05$.

Figure 2. Change in seed toxicity of RISC bound miRNAs in OC cells exposed to platinum. **A** and **B,** RISC-bound sRNA Seed Tox plots of A2780 (A) or A2780R (B) cells treated with 5 μM Cis or PBS for 72 hrs. Green arrows, net increase, and red arrows, net decrease of >1000 reads in peak in Cis treated cells, respectively. **C,** RISC-bound sRNA Seed Tox plots of PBS treated A2780 and A2780R cells. Green arrows, net increase, and red arrows, decrease of >1000 reads in peak in A2780R cells, respectively. **D,** RISC composition of A2780 cells or cells made resistant with long-term treatment with cisplatin (A2780R). Shown are pie-charts of short-term (S-Cis) or long-term (L-Cis) treated cells. Reads with a predicted 6mer seed viability of <20% are shown in red, >80% in green, and in between in grey. **E,** RISC-bound sRNA Seed Tox plots of PEO1 cells treated with 1 μg/ml Carbo or water for 72 hrs. Green arrows, net increase, and red arrows, net decrease of >1000 reads in peak in Carbo treated cells, respectively. **F,** RISC-bound sRNA Seed Tox plots of PEO4 cells treated with 1 μg/ml Carbo or water for 72 hrs. **G,** RISC-bound sRNA Seed Tox plots of water treated PEO1 and PEO4 cells. Green arrows, net increase, and red arrows, decrease of >1000 reads in peak in PEO4 cells, respectively. **H,** RISC composition of PEO1 or PEO4 cells. Shown are pie-charts of short-term (S-Carb) or long-term (RX) treated cells isolated from patients. Reads with a predicted 6mer seed viability of <20% are shown in red, >80% in green, and in between in grey. P values were calculated using pairwise comparisons of all reads in the two different treatments in two groups: reads with predicted viability >80% and <20% (blue stippled lines). In these areas, the most significantly changed miRNAs are labeled. The average miRNA content of RISC bound sRNAs across all A2780/PEO samples was 97.6%/97.8%, respectively. Length of green and red arrows corresponds to number of reads (inserts in A and E).

Figure 3. Platinum resistant, A2780R cells have more toxic miRNAs in their RISC than sensitive A2780 cells. **A-C,** Seed Tox plot of RISC bound miRNAs and exogenous siRNAs in A2780/A2780R cells 24 hrs after transfection with either the nontoxic siUAGUCG (siNT1), or the highly toxic siGGCAGU, or siGGGGGC. **D,** Percent miRNAs and exogenous siRNAs in the RISC of the siRNA transfected cells. Student's test p-values are shown. **E,** siRNA read species (detected as DNA) derived from the transfected three siRNAs in the total RNA and associated with the RISC. *Left:* The top 5 most abundant species. *Right:* The same four species were the most abundant species in all samples (total or RISC bound).

Figure 4. Lower Seed Tox of RISC-bound sRNAs in OC tumors is associated with increased resistance to chemotherapy. **A,** Pt sensitive days (days between the end of the last cycle of Pt-based chemotherapy and first relapse) in two groups of OC patients: Pt resistant (Pt-R) and Pt sensitive (Pt-S). Orange dots indicate two patients with intermediate (180 – 365 days since last treatment) Pt sensitivity. **B,** Pearson correlation between the fold change in Pt-S versus Pt-R patients and the 6mer Seed Tox (% viability in HeyA8 cells). Shown are miRNAs with a sum of >10,000 across all samples (representing 85.4% of all reads). miRNA content of this pull down was 97.4-98.1%. **C,** Seed Tox plot of RISC-bound miRNAs differentially expressed ($p<0.05$, >1.5x fold change) in Pt-S versus Pt-R patients. Green arrows, net increase, and red arrows, net decrease of >1000 reads in peak in Pt-R tumors, respectively. Inserts: *Left:* Average Seed Tox of all sRNAs enriched in either Pt-R or Pt-S patients. *Right:* matching seed compositions. **D,** Kaplan-Meier analysis of patients with the top and bottom highest RISC content of the average of the six miRNAs shown (including their 6mer seeds). Noncanonical seeds are in blue. **E,** Regression analysis of the six miRNAs in D plotted against the number of Pt sensitive days.

Figure 5. The RISC in recurrent OC tumors in a group of long-term survivors is enriched in miRNAs with toxic 6mer seeds compared to the primary cancer. **A,** List of 10 long-term survivor OC patients with sites of recurrences given. Patients pairs of a subgroup of four highly related primary and recurrent tumor pairs are shown in red (see Supplementary Fig. S13B). Survival days are as of 12/22/2020. **B,** Pearson correlation between the fold change in recurrences versus primary tumors and the 6mer Seed Tox (% viability in HeyA8 cells). Shown are miRNAs with a sum of >10000 across all samples (representing 81.4% of all reads). miRNA content of this pull down was 97.2-98.4%. **C,** Seed Tox plot of RISC-bound miRNAs differentially expressed (paired analysis, $p<0.05$, >1.5x fold change) in recurrences versus matched primary tumors in the subgroup of four patients. Note, miR-15b-5p was not detected in this analysis which used the EdgeR software package for to obtain paired p-values and it had a p-value of 0.057. Green arrows, net increase, and red arrows, net decrease of >1000 reads in peak in recurrent tumors, respectively. **D,** *Top:* Average Seed Tox of all sRNAs enriched in either primary tumor (P) or recurrences (R). *Bottom:* Matching seed compositions. **E,** Changes in RISC bound miRNA read numbers in recurrences versus primary tumors in the subgroup of patients. Shown are all miRNAs that are significantly up (top) or downregulated (bottom) (paired Student's t-test $p<0.05$, >1.5x fold) in all four patients in the same direction.

REFERENCES

1.Alles J, Fehlmann T, Fischer U, Backes C, Galata V, Minet M, Hart M, Abu-Halima M, Grasser FA, Lenhof HP, Keller A, Meese E. (2019). An estimate of the total number of true human miRNAs. Nucleic Acids Res. 47:3353-64.

2.Yan M, Yang X, Shen R, Wu C, Wang H, Ye Q, Yang P, Zhang L, Chen M, Wan B, Zhang Q, Xia S, Lu X, Shao G, Zhou X, Yu J, Shao Q. (2018). miR-146b promotes cell proliferation and increases chemosensitivity, but attenuates cell migration and invasion via FBXL10 in ovarian cancer. Cell Death Dis. 9:1123.

3.Svoronos AA, Engelman DM, Slack FJ. (2016). OncomiR or Tumor Suppressor? The Duplicity of MicroRNAs in Cancer. Cancer Res. 76:3666-70.

4.Chan JK, Blansit K, Kiet T, Sherman A, Wong G, Earle C, Bourguignon LY. (2014). The inhibition of miR-21 promotes apoptosis and chemosensitivity in ovarian cancer. Gynecol Oncol. 132:739-44.

5.Lewis BP, Shih IH, Jones-Rhoades MW, Bartel DP, Burge CB. (2003). Prediction of mammalian microRNA targets. Cell. 115:787-98.

6.Lai EC. (2002). Micro RNAs are complementary to 3' UTR sequence motifs that mediate negative post-transcriptional regulation. Nat Genet. 30:363-4.

7.Selbach M, Schwanhausser B, Thierfelder N, Fang Z, Khanin R, Rajewsky N. (2008). Widespread changes in protein synthesis induced by microRNAs. Nature. 455:58-63.

8.Baek D, Villen J, Shin C, Camargo FD, Gygi SP, Bartel DP. (2008). The impact of microRNAs on protein output. Nature. 455:64-71.

9.Eulalio A, Huntzinger E, Izaurralde E. (2008). GW182 interaction with Argonaute is essential for miRNA-mediated translational repression and mRNA decay. Nat Struct Mol Biol. 15:346-53.

10.Lee Y, Kim M, Han J, Yeom KH, Lee S, Baek SH, Kim VN. (2004). MicroRNA genes are transcribed by RNA polymerase II. EMBO J. 23:4051-60.

11.Han J, Lee Y, Yeom KH, Kim YK, Jin H, Kim VN. (2004). The Drosha-DGCR8 complex in primary microRNA processing. Genes Dev. 18:3016-27.

12.Yi R, Qin Y, Macara IG, Cullen BR. (2003). Exportin-5 mediates the nuclear export of pre-microRNAs and short hairpin RNAs. Genes Dev. 17:3011-6.

13.Bernstein E, Caudy AA, Hammond SM, Hannon GJ. (2001). Role for a bidentate ribonuclease in the initiation step of RNA interference. Nature. 409:363-6.

14.Hutvagner G, McLachlan J, Pasquinelli AE, Balint E, Tuschl T, Zamore PD. (2001). A cellular function for the RNA-interference enzyme Dicer in the maturation of the let-7 small temporal RNA. Science. 293:834-8.

15.Wang Y, Sheng G, Juranek S, Tuschl T, Patel DJ. (2008). Structure of the guide-strand-containing argonaute silencing complex. Nature. 456:209-13.

16.Leuschner PJ, Ameres SL, Kueng S, Martinez J. (2006). Cleavage of the siRNA passenger strand during RISC assembly in human cells. EMBO Rep. 7:314-20.

17.Bast RC, Jr., Matulonis UA, Sood AK, Ahmed AA, Amobi AE, Balkwill FR, Wielgos-Bonvallet M, Bowtell DDL, Brenton JD, Brugge JS, Coleman RL, Draetta GF, Doberstein K, Drapkin RI, Eckert MA, Edwards RP, Elias KM, Ennis D, Futreal A, Gershenson DM, Greenberg RA, Huntsman DG, Ji JXY, Kohn EC, Iavarone C, Lengyel ER, Levine DA, Lord CJ, Lu Z, Mills GB, Modugno F, Nelson BH, Odunsi K, Pilsworth JA, Rottapel RK, Powell DJ, Jr., Shen L, Shih I-M, Spriggs DR, Walton J, Zhang K, Zhang R, Zou L. (2019). Critical questions in ovarian cancer research and treatment: Report of an American Association for Cancer Research Special Conference. Cancer. 125:1963-72.

18.(2011). Integrated genomic analyses of ovarian carcinoma. Nature. 474:609-15.

19.Kurnit KC, Fleming GF, Lengyel E. (2020). Updates and New Options in Advanced Epithelial Ovarian Cancer Treatment. Obstet Gynecol.

20.Agarwal R, Kaye SB. (2003). Ovarian cancer: strategies for overcoming resistance to chemotherapy. Nat Rev Cancer. 3:502-16.

21.Hadji A, Ceppi P, Murmann AE, Brockway S, Pattanayak A, Bhinder B, Hau A, De Chant S, Parimi V, Kolesza P, Richards JS, Chandel N, Djaballah H, Peter ME. (2014). Death induced by CD95 or CD95 ligand elimination. Cell Reports. 10:208-22.

22.Murmann AE, McMahon KM, Halluck-Kangas A, Ravindran N, Patel M, Law C, Brockway S, Wei JJ, Thaxton CS, Peter ME. (2017). Induction of DISE in ovarian cancer cells in vivo. Oncotarget. 8:84643-58.

23.Putzbach W, Gao QQ, Patel M, van Dongen S, Haluck-Kangas A, Sarshad AA, Bartom E, Kim KY, Scholtens DM, Hafner M, Zhao JC, Murmann AE, Peter ME. (2017). Many si/shRNAs can kill cancer cells by targeting multiple survival genes through an off-target mechanism. eLife. 6: e29702.
24.Patel M, Bartom ET, Murmann AE, Peter ME. (2020). Identification of the toxic 6mer seed consensus in human cancer cells. BioRxive. https://doi.org/10.1101/2020.12.22.424040.
25.Corbin JM, Geordescu C, wren JD, Xu C, Asch AS, Ruiz-Echevarria MJ. (2020). Seed-mediated RNA interference of androgen signaling and survival networks induces cell death in prostate cancer cells. BioRxive. https://doi.org/10.1101/2020.07.17.209379.
26.Gao QQ, Putzbach W, Murmann AE, Chen S, Ambrosini G, Peter JM, Bartom E, Peter ME. (2018). 6mer seed toxicity in tumor suppressive miRNAs. Nature Comm. 9:4504.
27.Murmann AE, Bartom ET, Schipma MJ, Vilker J, Chen S, Peter ME. (2019). 6mer seed toxicity in viral microRNAs. iScience. 23: 100737.
28.Ceppi P, Hadji A, Kohlhapp F, Pattanayak A, Hau A, Xia L, Liu H, Murmann AE, Peter ME. (2014). CD95 and CD95L promote and protect cancer stem cells. Nature Commun. 5:5238.
29.Wang Y, Zong X, Mitra S, Mitra AK, Matei D, Nephew KP. (2018). IL-6 mediates platinum-induced enrichment of ovarian cancer stem cells. JCI insight. 3:e122360.
30.Li M, Balch C, Montgomery JS, Jeong M, Chung JH, Yan P, Huang TH, Kim S, Nephew KP. (2009). Integrated analysis of DNA methylation and gene expression reveals specific signaling pathways associated with platinum resistance in ovarian cancer. BMC Med Genomics. 2:34.
31.Wolf CR, Hayward IP, Lawrie SS, Buckton K, McIntyre MA, Adams DJ, Lewis AD, Scott AR, Smyth JF. (1987). Cellular heterogeneity and drug resistance in two ovarian adenocarcinoma cell lines derived from a single patient. Int J Cancer. 39:695-702.
32.Shang S, Yang J, Jazaeri AA, Duval AJ, Tufan T, Lopes Fischer N, Benamar M, Guessous F, Lee I, Campbell RM, Ebert PJ, Abbas T, Landen CN, Difeo A, Scacheri PC, Adli M. (2019). Chemotherapy-Induced Distal Enhancers Drive Transcriptional Programs to Maintain the Chemoresistant State in Ovarian Cancer. Cancer Res. 79:4599-611.
33.Johnson SW, Laub PB, Beesley JS, Ozols RF, Hamilton TC. (1997). Increased platinum-DNA damage tolerance is associated with cisplatin resistance and cross-resistance to various chemotherapeutic agents in unrelated human ovarian cancer cell lines. Cancer Res. 57:850-6.
34.Janas MM, Wang B, Harris AS, Aguiar M, Shaffer JM, Subrahmanyam YV, Behlke MA, Wucherpfennig KW, Gygi SP, Gagnon E, Novina CD. (2012). Alternative RISC assembly: binding and repression of microRNA-mRNA duplexes by human Ago proteins. RNA. 18:2041-55.
35.Flores O, Kennedy EM, Skalsky RL, Cullen BR. (2014). Differential RISC association of endogenous human microRNAs predicts their inhibitory potential. Nucleic Acids Res. 42:4629-39.
36.La Rocca G, Olejniczak SH, Gonzalez AJ, Briskin D, Vidigal JA, Spraggon L, DeMatteo RG, Radler MR, Lindsten T, Ventura A, Tuschl T, Leslie CS, Thompson CB. (2015). In vivo, Argonaute-bound microRNAs exist predominantly in a reservoir of low molecular weight complexes not associated with mRNA. Proc Natl Acad Sci U S A. 112:767-72.
37.Wu J, Zhang L, Wu S, Yi X, Liu Z. (2020). miR-194-5p inhibits SLC40A1 expression to induce cisplatin resistance in ovarian cancer. Pathol Res Pract. 216:152979.
38.Ameres SL, Horwich MD, Hung JH, Xu J, Ghildiyal M, Weng Z, Zamore PD. (2010). Target RNA-directed trimming and tailing of small silencing RNAs. Science. 328:1534-9.
39.Newman MA, Mani V, Hammond SM. (2011). Deep sequencing of microRNA precursors reveals extensive 3' end modification. RNA. 17:1795-803.
40.Javellana M, Hoppenot C, Lengyel E. (2019). The road to long-term survival: Surgical approach and longitudinal treatments of long-term survivors of advanced-stage serous ovarian cancer. Gynecol Oncol. 152:228-34.
41.Hoppenot C, Eckert MA, Tienda SM, Lengyel E. (2018). Who are the long-term survivors of high grade serous ovarian cancer? Gynecol Oncol. 148:204-12.
42.Patch AM, Christie EL, Etemadmoghadam D, Garsed DW, George J, Fereday S, Nones K, Cowin P, Alsop K, Bailey PJ, Kassahn KS, Newell F, Quinn MC, Kazakoff S, Quek K, Wilhelm-Benartzi C, Curry E, Leong HS, Hamilton A, Mileshkin L, Au-Yeung G, Kennedy C, Hung J, Chiew YE, Harnett P, Friedlander M, Quinn M, Pyman J, Cordner S, O'Brien P, Leditschke J, Young G, Strachan K, Waring P, Azar W, Mitchell C, Traficante N, Hendley J, Thorne H, Shackleton M, Miller DK, Arnau GM, Tothill RW, Holloway TP, Semple T, Harliwong I, Nourse C, Nourbakhsh E, Manning S, Idrisoglu S, Bruxner

TJ, Christ AN, Poudel B, Holmes O, Anderson M, Leonard C, Lonie A, Hall N, Wood S, Taylor DF, Xu Q, Fink JL, Waddell N, Drapkin R, Stronach E, Gabra H, Brown R, Jewell A, Nagaraj SH, Markham E, Wilson PJ, Ellul J, McNally O, Doyle MA, Vedururu R, Stewart C, Lengyel E, Pearson JV, deFazio A, Grimmond SM, Bowtell DD. (2015). Whole-genome characterization of chemoresistant ovarian cancer. Nature. 521:489-94.

43. Stadler B, Ivanovska I, Mehta K, Song S, Nelson A, Tan Y, Mathieu J, Darby C, Blau CA, Ware C, Peters G, Miller DG, Shen L, Cleary MA, Ruohola-Baker H. (2010). Characterization of microRNAs involved in embryonic stem cell states. Stem Cells Dev. 19:935-50.
44. Sastre D, Baiochi J, de Souza Lima IM, Canto de Souza F, Corveloni AC, Thome CH, Faca VM, Schiavinato J, Covas DT, Panepucci RA. (2019). Focused screening reveals functional effects of microRNAs differentially expressed in colorectal cancer. BMC Cancer. 19:1239.
45. Murmann AE, Gao QQ, Putzbach WT, Patel M, Bartom ET, Law CY, Bridgeman B, Chen S, McMahon KM, Thaxton CS, Peter ME. (2018). Small interfering RNAs based on huntingtin trinucleotide repeats are highly toxic to cancer cells. EMBO Rep. 19:e45336.
46. Smibert P, Yang JS, Azzam G, Liu JL, Lai EC. (2013). Homeostatic control of Argonaute stability by microRNA availability. Nat Struct Mol Biol. 20:789-95.
47. Martinez NJ, Gregory RI. (2013). Argonaute2 expression is post-transcriptionally coupled to microRNA abundance. RNA. 19:605-12.
48. Echevarría-Vargas IM, Valiyeva F, Vivas-Mejía PE. (2014). Upregulation of miR-21 in cisplatin resistant ovarian cancer via JNK-1/c-Jun pathway. PLoS One. 9:e97094.
49. Vandghanooni S, Eskandani M, Barar J, Omidi Y. (2018). AS1411 aptamer-decorated cisplatin-loaded poly(lactic-co-glycolic acid) nanoparticles for targeted therapy of miR-21-inhibited ovarian cancer cells. Nanomedicine. 13:2729-58.
50. Kong F, Sun C, Wang Z, Han L, Weng D, Lu Y, Chen G. (2011). miR-125b confers resistance of ovarian cancer cells to cisplatin by targeting pro-apoptotic Bcl-2 antagonist killer 1. J Huazhong Univ Sci Technolog Med Sci. 31:543.
51. Li N, Yang L, Wang H, Yi T, Jia X, Chen C, Xu P. (2015). MiR-130a and MiR-374a Function as Novel Regulators of Cisplatin Resistance in Human Ovarian Cancer A2780 Cells. PLoS One. 10:e0128886.
52. Xu M, Xiao J, Chen M, Yuan L, Li J, Shen H, Yao S. (2018). miR-149-5p promotes chemotherapeutic resistance in ovarian cancer via the inactivation of the Hippo signaling pathway. Int J Oncol. 52:815-27.
53. Zhang J, Liu J, Xu X, Li L. (2017). Curcumin suppresses cisplatin resistance development partly via modulating extracellular vesicle-mediated transfer of MEG3 and miR-214 in ovarian cancer. Cancer Chemother Pharmacol. 79:479-87.
54. Jin P, Liu Y, Wang R. (2018). STAT3 regulated miR-216a promotes ovarian cancer proliferation and cisplatin resistance. Biosci Rep. 38.
55. Wei Z, Liu Y, Wang Y, Zhang Y, Luo Q, Man X, Wei F, Yu X. (2016). Downregulation of Foxo3 and TRIM31 by miR-551b in side population promotes cell proliferation, invasion, and drug resistance of ovarian cancer. Med Oncol. 33:126.
56. Bogerd HP, Whisnant AW, Kennedy EM, Flores O, Cullen BR. (2014). Derivation and characterization of Dicer- and microRNA-deficient human cells. RNA. 20:923-37.
57. Eckenfelder A, Segeral E, Pinzon N, Ulveling D, Amadori C, Charpentier M, Nidelet S, Concordet JP, Zagury JF, Paillart JC, Berlioz-Torrent C, Seitz H, Emiliani S, Gallois-Montbrun S. (2017). Argonaute proteins regulate HIV-1 multiply spliced RNA and viral production in a Dicer independent manner. Nucleic Acids Res. 45:4158-73.
58. van Eijl R, van den Brand T, Nguyen LN, Mulder KW. (2017). Reactivity of human AGO2 monoclonal antibody 11A9 with the SWI/SNF complex: A case study for rigorously defining antibody selectivity. Sci Rep. 7:7278.
59. Putzbach W, Haluck-Kangas A, Gao QQ, Sarshad AA, Bartom ET, Stults A, Qadir AS, Hafner M, Peter ME. (2018). CD95/Fas ligand mRNA is toxic to cells. eLife. 7:e38621.
60. Wang Y, Zhao G, Condello S, Huang H, Cardenas H, Tanner EJ, Wei J, Ji Y, Li J, Tan Y, Davuluri RV, Peter ME, Cheng JX, Matei D. (2020). Frizzled-7 Identifies Platinum Tolerant Ovarian Cancer Cells Susceptible to Ferroptosis. Cancer Res.
61. Hauptmann J, Schraivogel D, Bruckmann A, Manickavel S, Jakob L, Eichner N, Pfaff J, Urban M, Sprunck S, Hafner M, Tuschl T, Deutzmann R, Meister G. (2015). Biochemical isolation of Argonaute protein complexes by Ago-APP. Proc Natl Acad Sci U S A. 112:11841-5.

62.Hafner M, Renwick N, Farazi TA, Mihailovic A, Pena JT, Tuschl T. (2012). Barcoded cDNA library preparation for small RNA profiling by next-generation sequencing. Methods. 58:164-70.

Figure 1

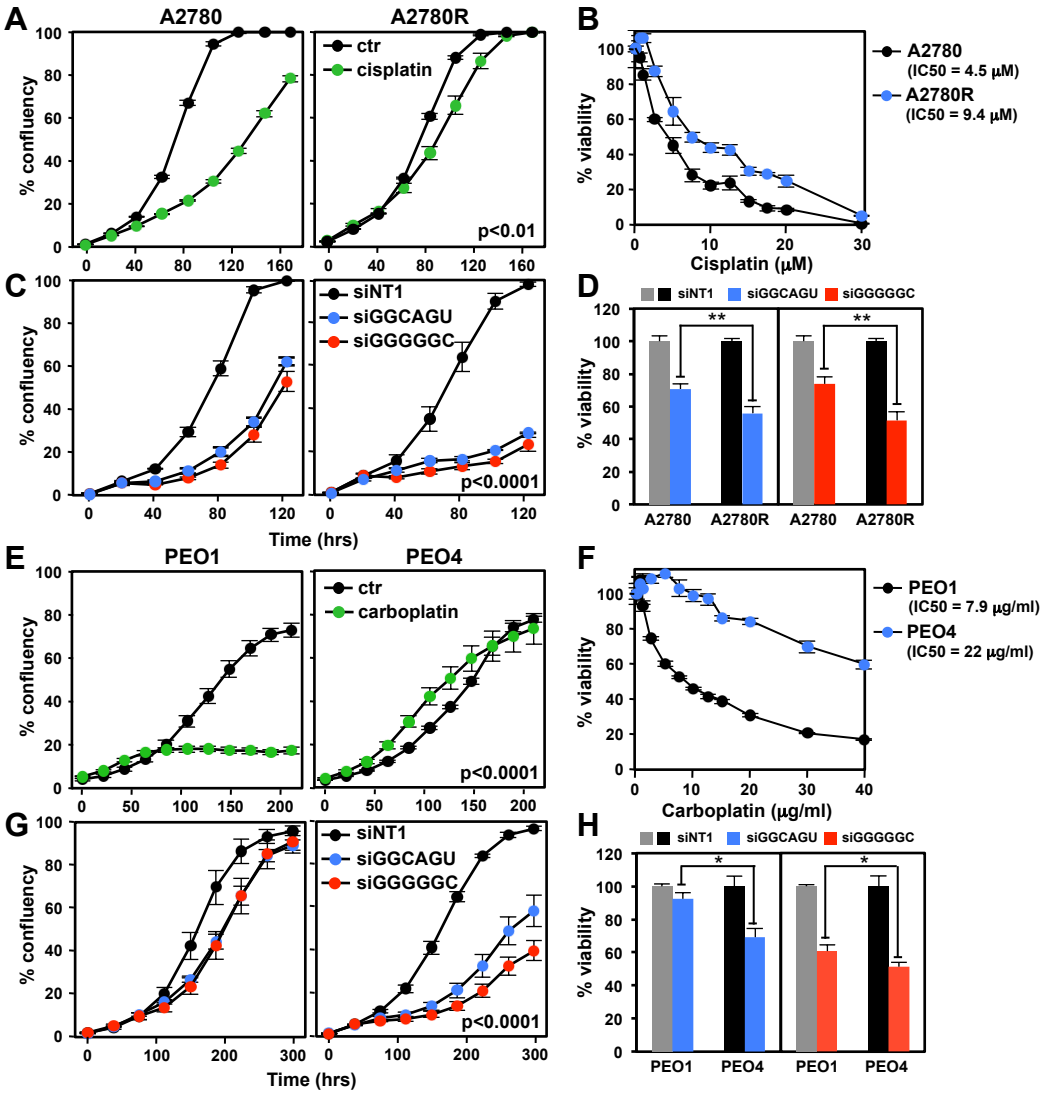
A
A2780
A2780R
ctr
cisplatin
% confluency
p<0.01
B
A2780
(IC50 = 4.5 μM)
A2780R
(IC50 = 9.4 μM)
% viability
Cisplatin (μM)
C
siNT1
siGGCAGU
siGGGGGC
p<0.0001
Time (hrs)
D
siNT1
siGGCAGU
siGGGGGC
**
A2780
A2780R
E
PEO1
PEO4
carboplatin
F
PEO1
(IC50 = 7.9 μg/ml)
PEO4
(IC50 = 22 μg/ml)
Carboplatin (μg/ml)
G
H
*
PEO1
PEO4

Figure 2

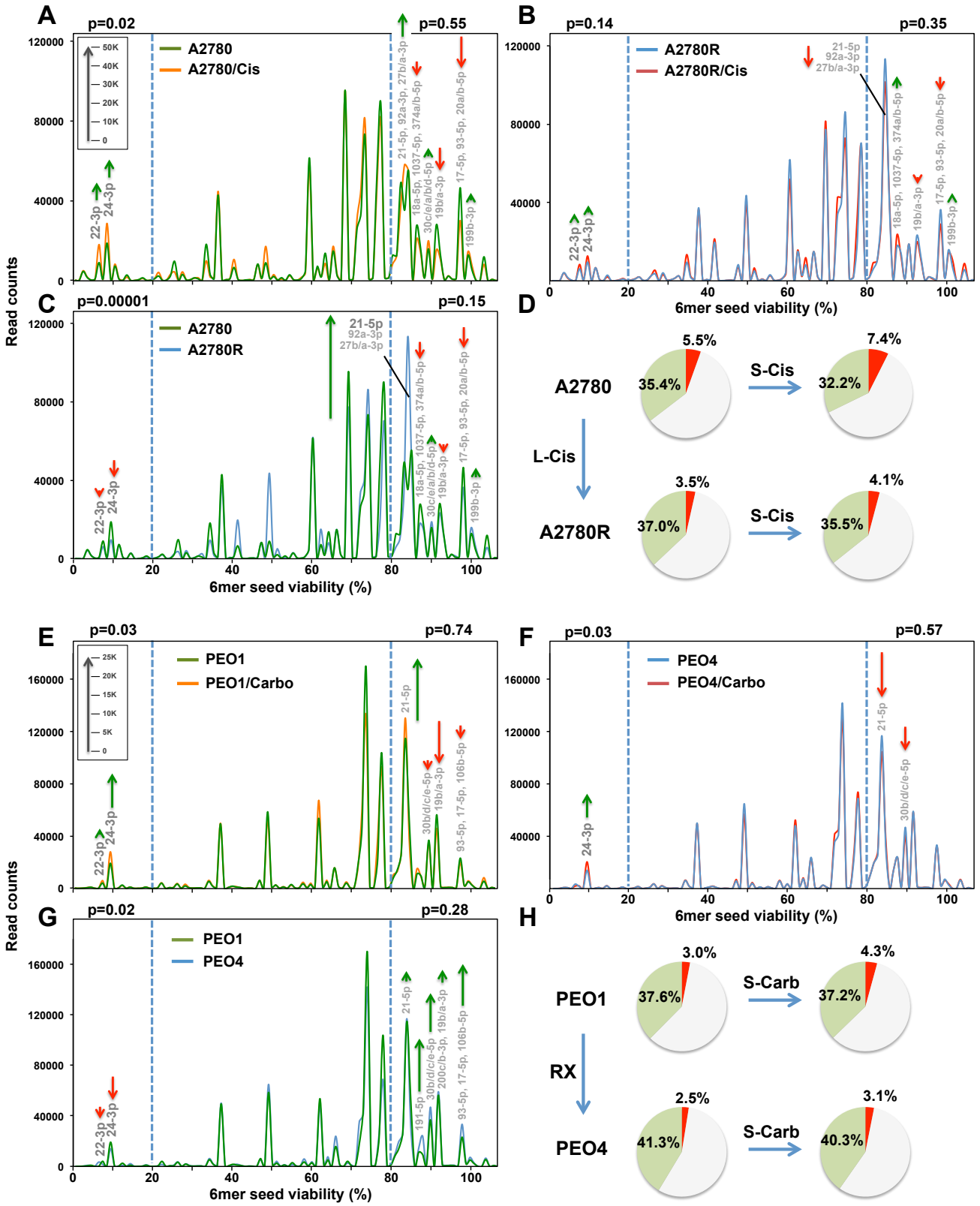
A
p=0.02
p=0.55
A2780
A2780/Cis
50K
40K
30K
20K
10K
0
22-3p
24-3p
21-5p, 92a-3p, 27b/a-3p
18a-5p, 1037-5p, 374a/b-5p
30c/e/a/b/d-5p
19b/a-3p
17-5p, 93-5p, 20a/b-5p
199b-3p
B
p=0.14
p=0.35
A2780R
A2780R/Cis
21-5p
92a-3p
27b/a-3p
18a-5p, 1037-5p, 374a/b-5p
19b/a-3p
17-5p, 93-5p, 20a/b-5p
199b-3p
22-3p
24-3p
C
p=0.00001
p=0.15
A2780
A2780R
21-5p
92a-3p
27b/a-3p
18a-5p, 1037-5p, 374a/b-5p
30c/e/a/b/d-5p
19b/a-3p
17-5p, 93-5p, 20a/b-5p
199b-3p
22-3p
24-3p
Read counts
6mer seed viability (%)
D
A2780
5.5%
35.4%
S-Cis
7.4%
32.2%
L-Cis
A2780R
3.5%
37.0%
S-Cis
4.1%
35.5%
E
p=0.03
p=0.74
PEO1
PEO1/Carbo
25K
20K
15K
10K
5K
0
21-5p
30b/d/c/e-5p
19b/a-3p
93-5p, 17-5p, 106b-5p
22-3p
24-3p
F
p=0.03
p=0.57
PEO4
PEO4/Carbo
21-5p
30b/d/c/e-5p
24-3p
G
p=0.02
p=0.28
PEO1
PEO4
21-5p
191-5p
30b/d/c/e-5p
200c/b-3p
19b/a-3p
93-5p, 17-5p, 106b-5p
22-3p
24-3p
H
PEO1
3.0%
37.6%
S-Carb
4.3%
37.2%
RX
PEO4
2.5%
41.3%
S-Carb
3.1%
40.3%

Figure 3

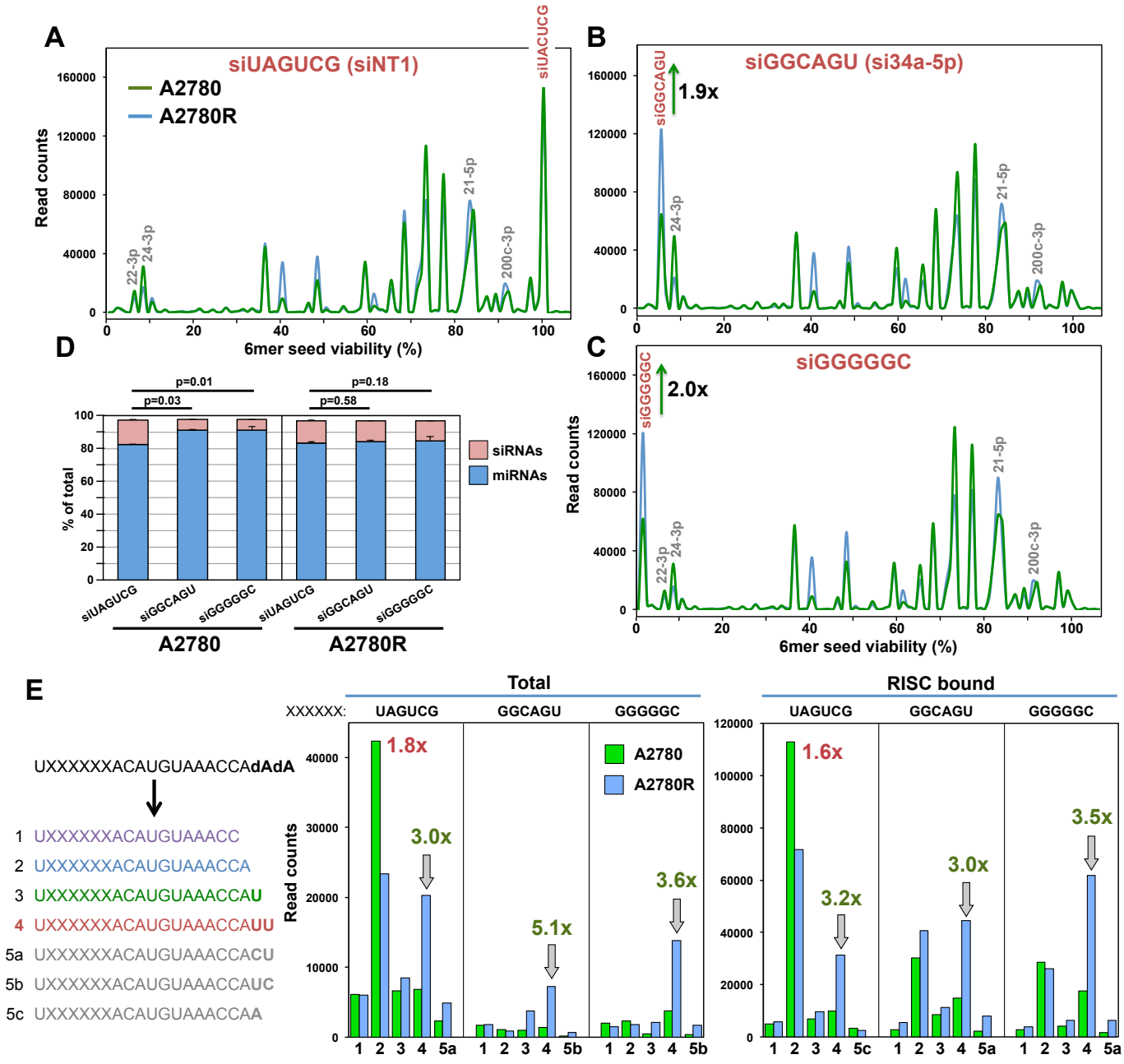
A
siUAGUCG (siNT1)
A2780
A2780R
Read counts
6mer seed viability (%)
22-3p
24-3p
21-5p
200c-3p
siUACUCG
B
siGGCAGU (si34a-5p)
siGGCAGU
1.9x
C
siGGGGGC
siGGGGGC
2.0x
D
p=0.01
p=0.03
p=0.18
p=0.58
% of total
siRNAs
miRNAs
siUAGUCG
siGGCAGU
siGGGGGC
A2780
A2780R
E
UXXXXXXACAUGUAAACCAdAdA
1 UXXXXXXACAUGUAAACC
2 UXXXXXXACAUGUAAACCA
3 UXXXXXXACAUGUAAACCAU
4 UXXXXXXACAUGUAAACCAUU
5a UXXXXXXACAUGUAAACCACU
5b UXXXXXXACAUGUAAACCAUC
5c UXXXXXXACAUGUAAACCAA
Total
RISC bound
XXXXXX:
UAGUCG
GGCAGU
GGGGGC
A2780
A2780R
Read counts
1.8x
3.0x
5.1x
3.6x
1.6x
3.2x
3.0x
3.5x

Figure 4

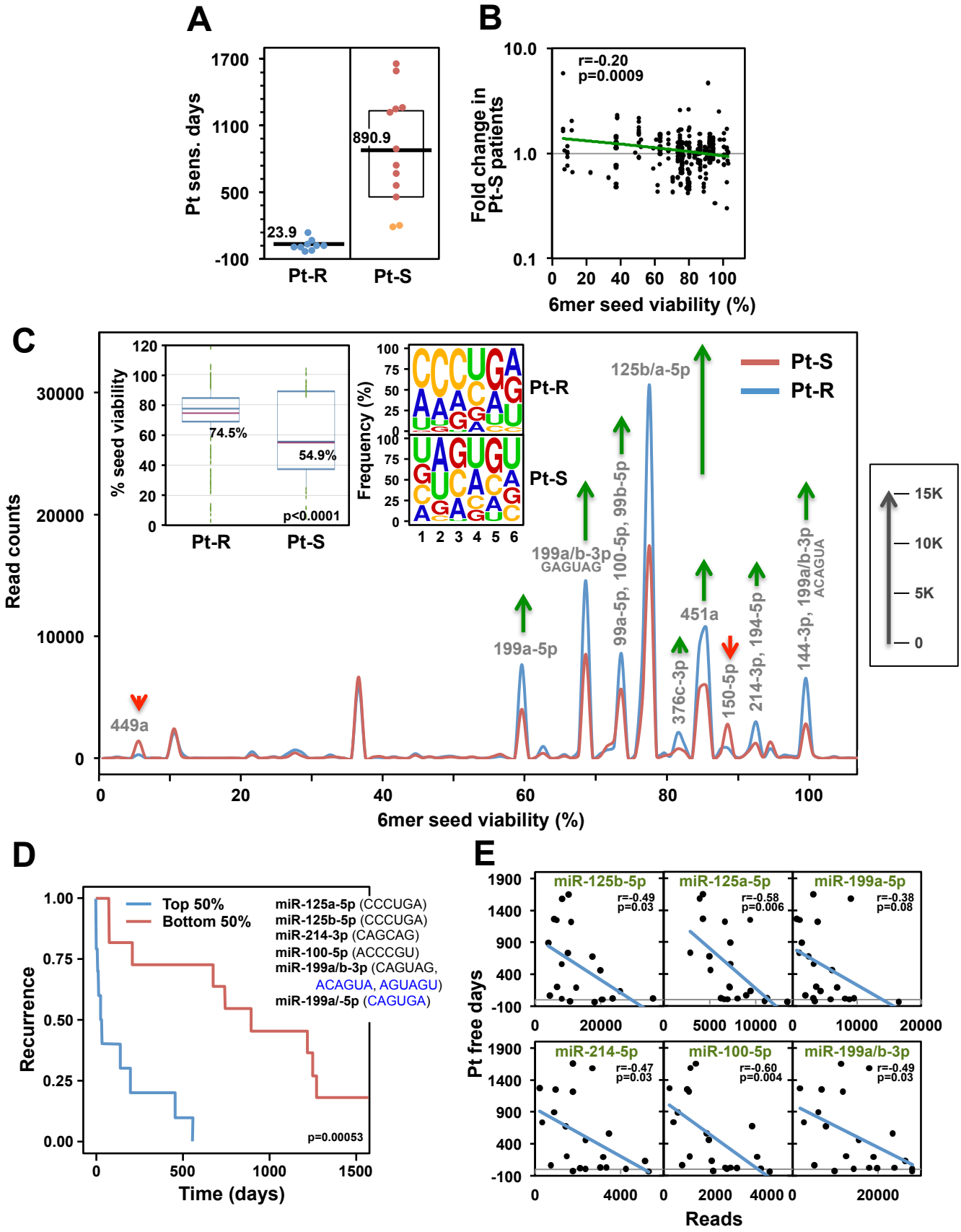
A
Pt sens. days
1700
1100
500
-100
23.9
890.9
Pt-R
Pt-S
B
Fold change in Pt-S patients
10.0
1.0
0.1
r=-0.20
p=0.0009
0 20 40 60 80 100
6mer seed viability (%)
C
Read counts
30000
20000
10000
0
% seed viability
74.5%
54.9%
p<0.0001
Pt-R
Pt-S
Frequency (%)
1 2 3 4 5 6
449a
199a-5p
199a/b-3p
GAGUAG
99a-5p, 100-5p, 99b-5p
125b/a-5p
376c-3p
451a
150-5p
214-3p, 194-5p
144-3p, 199a/b-3p
ACAGUA
15K
10K
5K
0
6mer seed viability (%)
D
Recurrence
1.00
0.75
0.50
0.25
0.00
Top 50%
Bottom 50%
miR-125a-5p (CCCUGA)
miR-125b-5p (CCCUGA)
miR-214-3p (CAGCAG)
miR-100-5p (ACCCGU)
miR-199a/b-3p (CAGUAG, ACAGUA, AGUAGU)
miR-199a/-5p (CAGUGA)
p=0.00053
0 500 1000 1500
Time (days)
E
Pt free days
miR-125b-5p
r=-0.49
p=0.03
miR-125a-5p
r=-0.58
p=0.006
miR-199a-5p
r=-0.38
p=0.08
miR-214-5p
r=-0.47
p=0.03
miR-100-5p
r=-0.60
p=0.004
miR-199a/b-3p
r=-0.49
p=0.03
Reads

Figure 5

A

Patient ID	Survival days	Pt sens. days	Age	Primary tumor site	Rec. 1	Rec. 2	Rec. 3
2490	897 (alive)	196	53	Ovary	on liver		
2068	1365 (alive)	71	71	Ovary	Soft tissue		
2065	1366 (alive)	306	42	Ovary	Inguinal LN		
1461	1996 (alive)	194	54	Ovary	on liver		
1441	2040 (alive)	545	55	Ovary	Brain mets		
828	3151 (alive)	395	74	Ovary	Pelvis		
598	3393	1123	80	Ovary	Bowel		
200	3943	1656	46	Peritoneum		on spleen	
290	4512 (alive)	1269	67	Ovary	on colon	on liver	Soft tissue
504	5178 (alive)	1130	50	Ovary		Other	

B

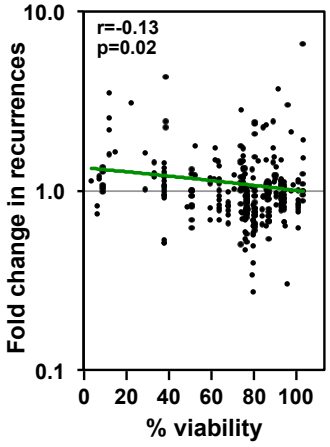

C

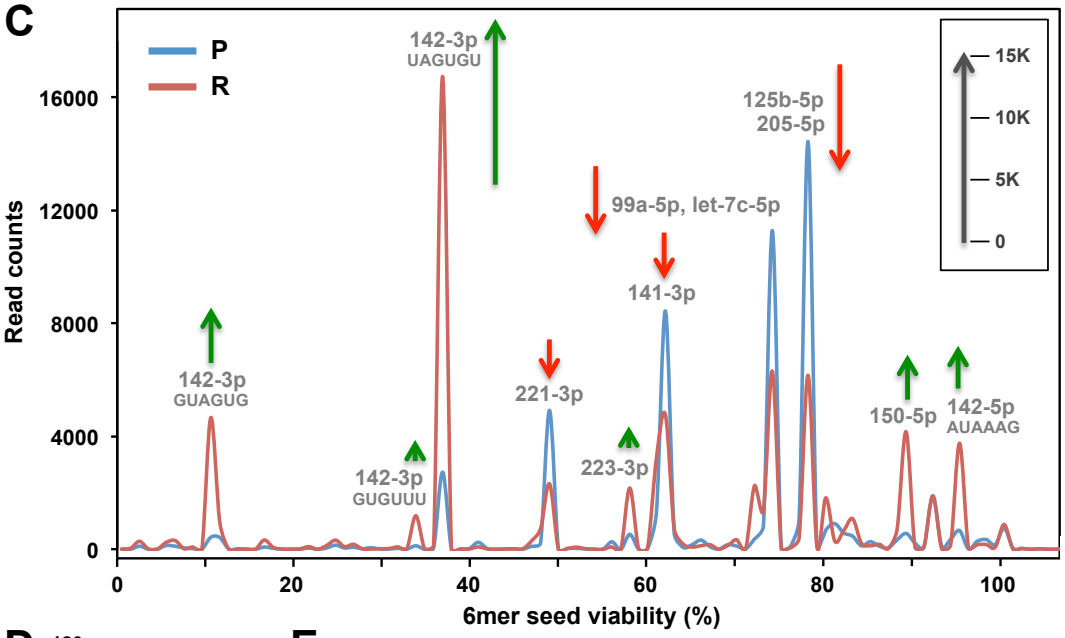

D

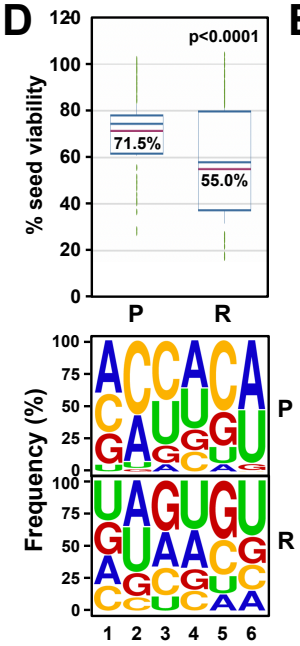

E

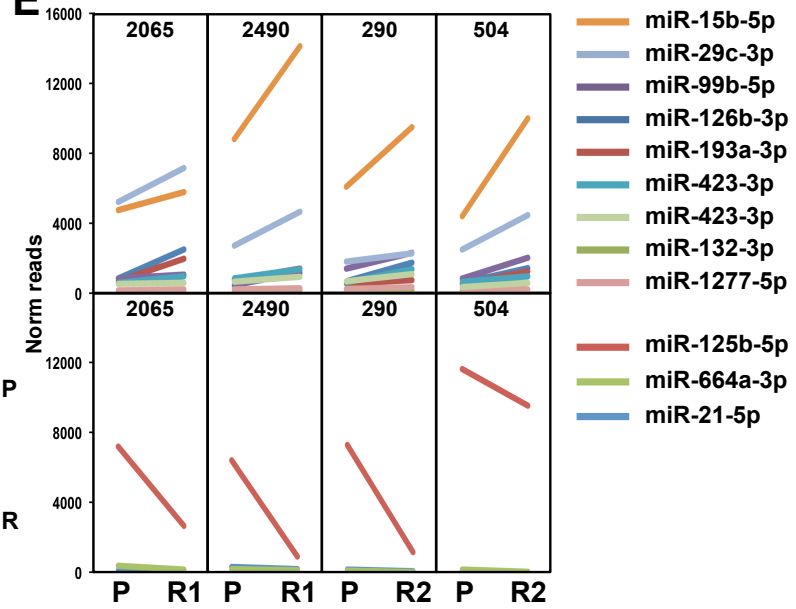

miRNA	Seed viab.	A2780R vs S	PEO4 vs PEO1	OVCAR5 + L-Carb	Corr. Pt-R vs Pt free days
21-5p	84.2%	**3.3**	1	1.1	0.49 (p=0.026)
125b-5p	77.5%	0.1	0.8	0.5	**-0.49 (p=0.026)**
130a-3p	81.6%	0.5	**2.6**	0.8	-0.11 (ns)
374a-5p	88.1%	1	1.1	1.2	0.07 (ns)
149-5p	63.9%	/	/	/	/
214-3p	78.1%	1	/	1.1	**-0.46 (p=0.034)**
216a-5p	64.9%	nd	nd	/	/
493-5p	75.6%	nd	nd	/	/
551b-3p	69.2%	/	/	/	/
194-5p	93.2%	/	/	**2.0**	/

Table 1: Different miRNAs are associated with Pt resistance in different models of OC and in OC patients. For each miRNA listed 6mer seed viability was determined in HeyA8 cells (6merdb.org). Only shown are miRNAs with average reads >1000 across all samples. Samples with average <1000 reads are labeled with /. nd, not detected = less than 10 reads across all samples. nd, not detected, less than 10 reads across all samples. In addition, miRNAs found to be enriched in Pt-R patients and to significantly correlate with Pt sensitive days are shown in the last column. Both Pearson coefficients and p-values are given. Only miRNAs are listed for which it has been demonstrated that overexpression of a miRNA mimic in Pt-S cells increases Pt resistance and inhibition of the same miRNA in isogenic Pt-R cells increases sensitivity. This was shown for miR-21 (48, 49), miR-125b (50), miR-130a and miR-374a (51), miR-149-5p (52), miR-214-3p (53), miR-216a-5p (54), miR-551b-3p (55), and miR-194-5p (37).

Supplemental Figures

6mer Seed Toxicity and Platinum Resistance in Ovarian Cancer

Monal Patel, Yinu Wang, Elizabeth T. Bartom, Rohin Dhir, Kenneth P. Nephew, Daniela Matei, Andrea E. Murmann, Ernst Lengyel, and Marcus E. Peter

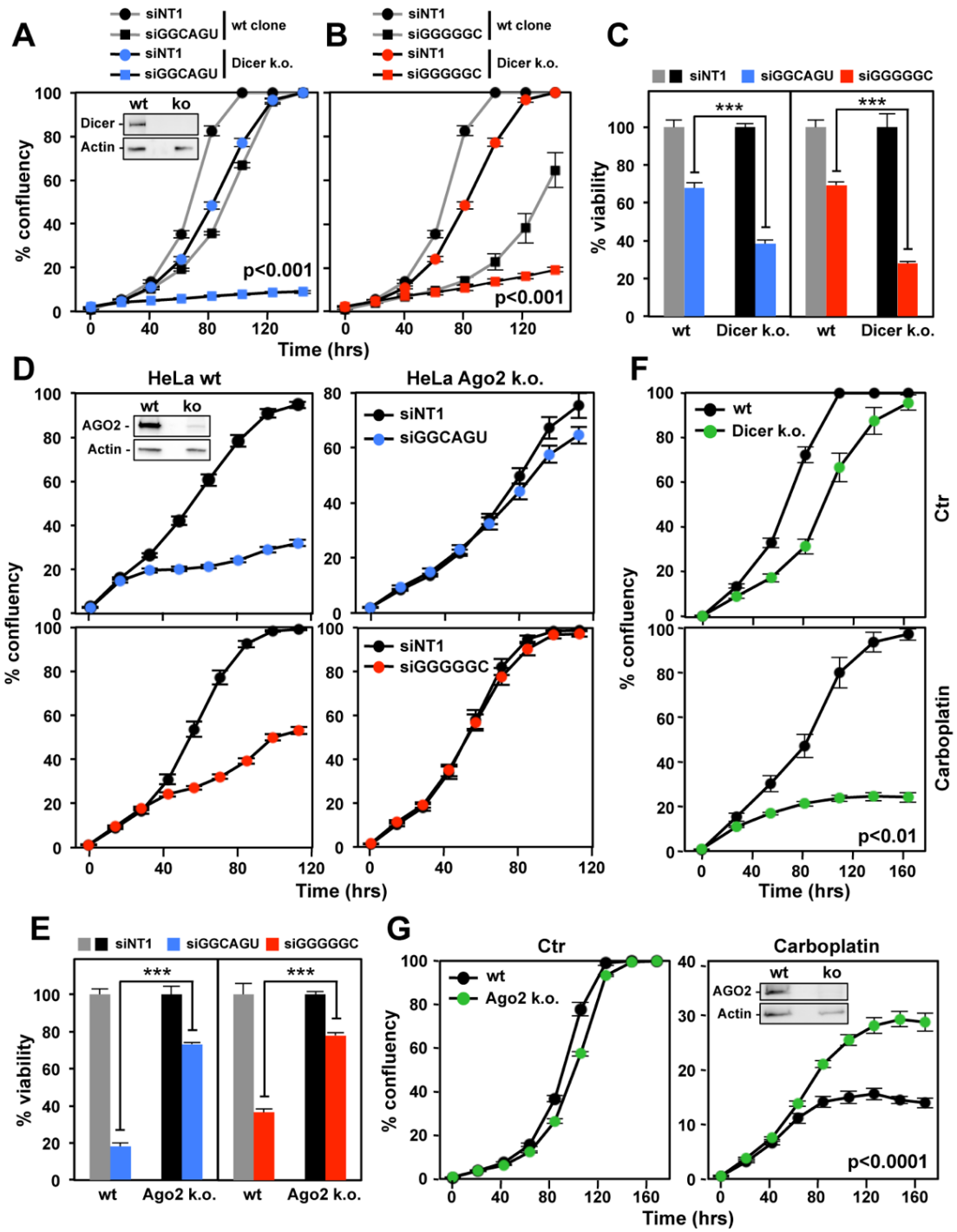

Supplemental Figure S1. Cell death induced by both toxic 6mer containing siRNAs and carboplatin involves RNAi. **A** and **B,** Confluency over time of 293T cells (wt or Dicer k.o.) transfected with 10 nM of siNT1, siGGCAGU or siGGGGGC. Insert: Western blot of Dicer in wt and k.o. cells. **C,** Viability of the cells in A and B 96 hrs after transfection with 10 nM of the siRNAs. **D,** Confluency over time of HeLa cells (wt or Ago2 k.o.) transfected with 10 nM of siNT1, siGGCAGU or siGGGGGC. Insert: Western blot of Ago2 in wt and k.o. cells. **E,** Viability of the 293T (wt or Ago2 k.o.) cells 96 hrs after transfection with 10 nM of the siRNAs. **F,** Confluency over time of 293T (wt or Dicer k.o.) treated with 3 μg/ml Carbo. **G,** Confluency over time of 293T (wt or Ago2 k.o.) treated with 10 μg/ml Carbo. Insert: Western blot of Ago2 in wt and k.o. cells. Each data point (A, B, D, F & G) represents mean ± SE of at least three replicates. Each bar (C, E) represents ± SD of three replicates. P-values were calculated using binomial distribution tests (A, B, F), ANOVA (G), or student's T-test (C, E). *** p<0.0001.

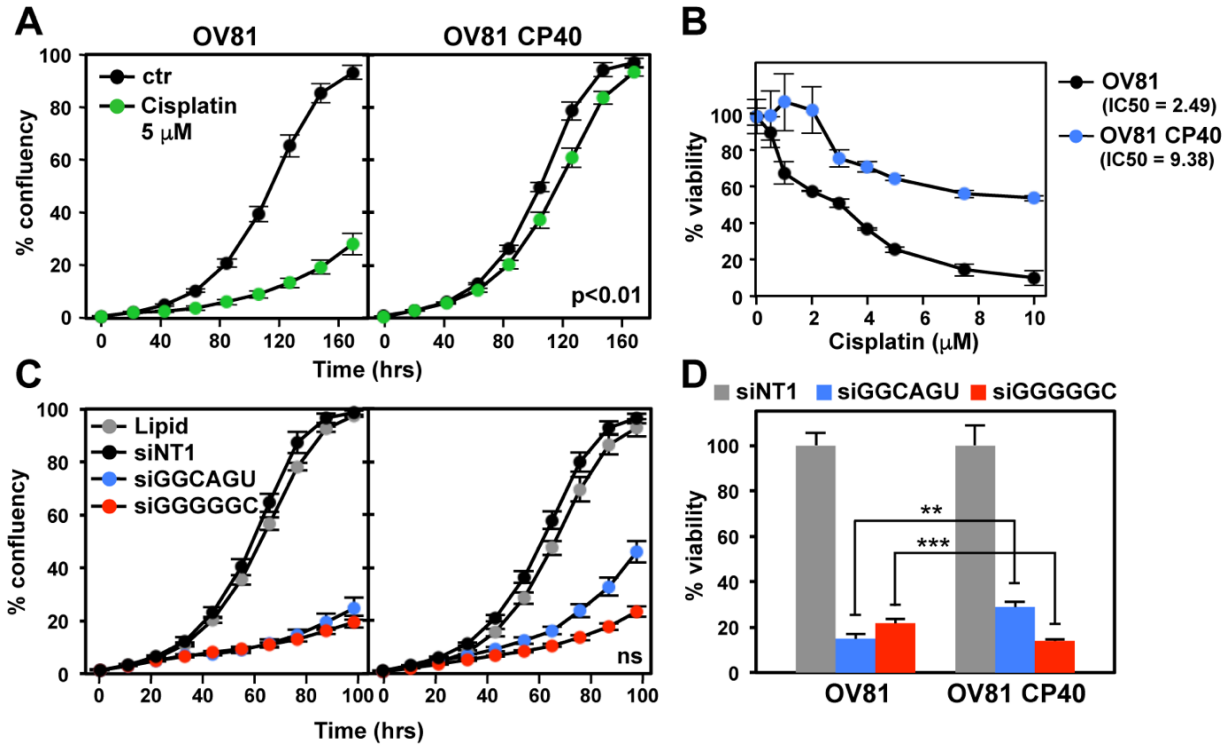

Supplemental Figure S2. OC cells resistant to platinum are still sensitive to 6mer Seed Tox. **A,** Change in confluency over time of OV81 cells and the Pt resistant counterpart OV81 CP40 treated with 5 μM Cis. **B,** Dose response curves (96 hrs ATP viability assay) of cells in A. **C,** Change in confluency over time of OV81 cells and OV81 CP40 treated with 10 nM of siRNAs. **D,** Viability assays 96 hrs after treatment with siRNAs (10 nM). Student's t-test p-values are shown, *** $p<0.0001$, ** $p<0.001$. P-values in A and C were calculated using binomial distribution tests. ns, not significant.

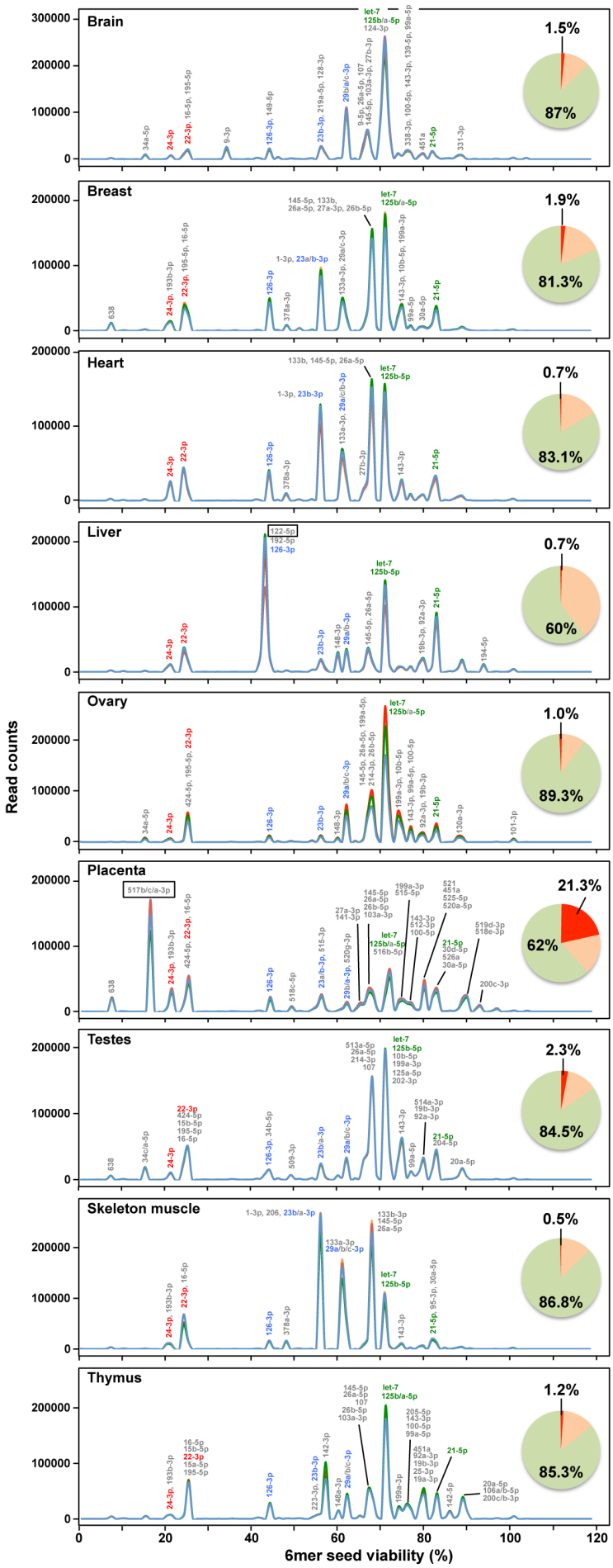
Brain
1.5%
87%
Breast
1.9%
81.3%
Heart
0.7%
83.1%
Liver
0.7%
60%
Ovary
1.0%
89.3%
Placenta
21.3%
62%
Testes
2.3%
84.5%
Skeleton muscle
0.5%
86.8%
Thymus
1.2%
85.3%
Read counts
6mer seed viability (%)

Supplemental Figure S3. Most tissues express predominantly nontoxic miRNAs**.** miRNA Seed Tox plots across 9 different tissues. In each case the cumulative read numbers are on the Y axis and the predicted toxicity on the X axis. Toxicity (shown as % viability) was the average of three human cell lines determined in a screen of all 4096 6mers in a neutral siRNA backbone [1]. miRNAs significantly expressed in all tissues are labeled in color (red = highly toxic, blue = intermediately toxic, and green = nontoxic). When a peak is labeled with multiple miRNAs, the most abundant one is listed first. Pie chart insert: Abundance of miRNAs with seeds of the following predicted viabilities: red: <20%; corral: >=20 <50%; green: >50%. Data were normalized to 1 million reads and all miRNAs were labeled that have more than 5000 normalized average reads across five (for brain, breast, heart, liver, ovary, placenta, and skeleton muscle) or four (for testes and thymus) individual samples, respectively. Some established tissue specific miRNAs are boxed. GSE11879 was the source of the smRNA Seq data analyzed.

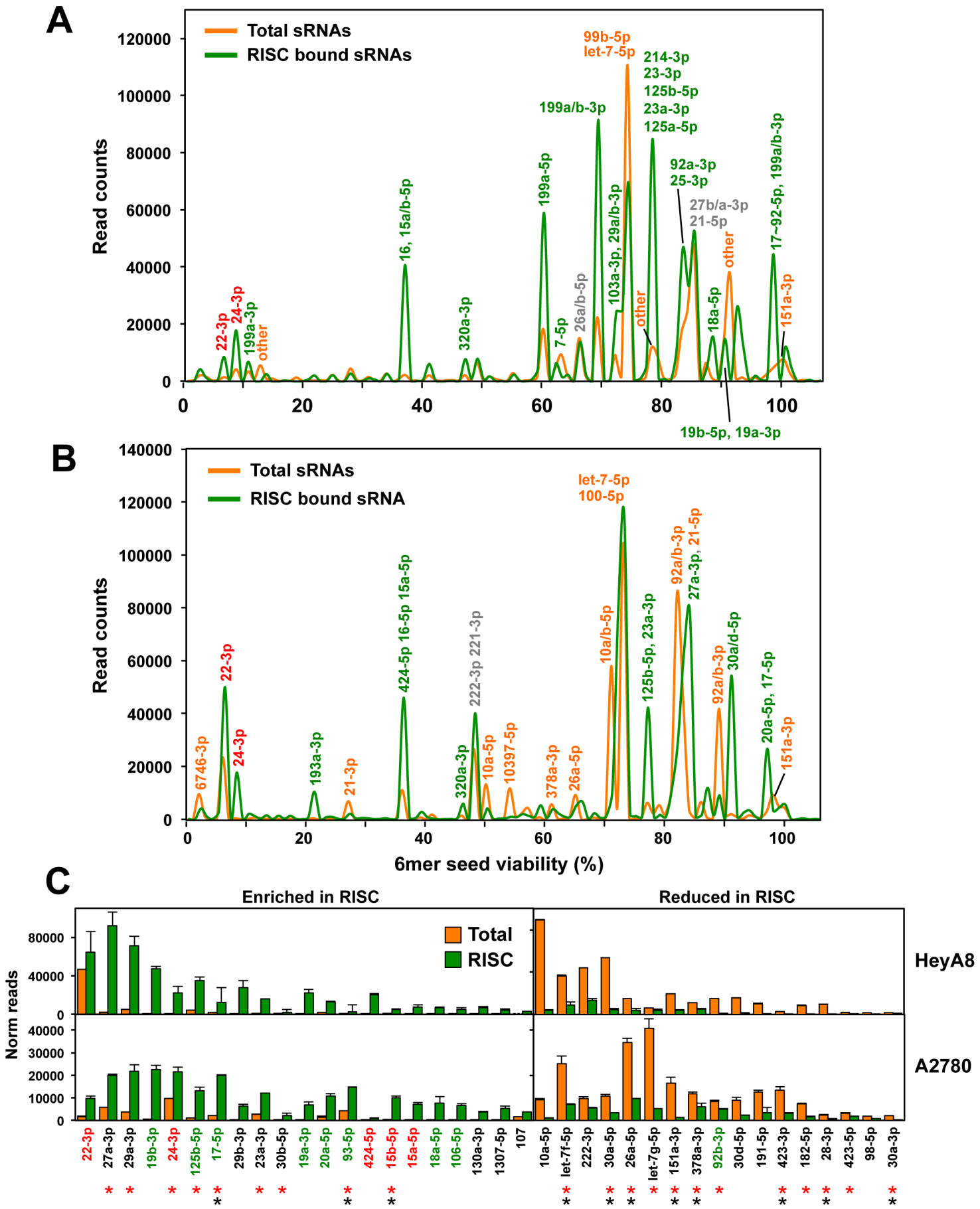
A
Total sRNAs
RISC bound sRNAs
Read counts
22-3p
24-3p
199a-3p
other
16, 15a/b-5p
320a-3p
199a-5p
7-5p
26a/b-5p
199a/b-3p
103a-3p, 29a/b-3p
99b-5p
let-7-5p
other
214-3p
23-3p
125b-5p
23a-3p
125a-5p
92a-3p
25-3p
27b/a-3p
21-5p
18a-5p
other
17~92-5p, 199a/b-3p
151a-3p
19b-5p, 19a-3p
B
Total sRNAs
RISC bound sRNA
Read counts
6746-3p
22-3p
24-3p
193a-3p
21-3p
424-5p 16-5p 15a-5p
320a-3p
222-3p 221-3p
10a-5p
10397-5p
378a-3p
26a-5p
10a/b-5p
let-7-5p
100-5p
125b-5p, 23a-3p
92a/b-3p
27a-3p, 21-5p
92a/b-3p
30a/d-5p
20a-5p, 17-5p
151a-3p
6mer seed viability (%)
C
Enriched in RISC
Reduced in RISC
Total
RISC
Norm reads
HeyA8
A2780
22-3p
27a-3p
29a-3p
19b-3p
24-3p
125b-5p
17-5p
29b-3p
23a-3p
30b-5p
19a-3p
20a-5p
93-5p
424-5p
15b-5p
15a-5p
18a-5p
106-5p
130a-3p
1307-5p
107
10a-5p
let-7f-5p
222-3p
30a-5p
26a-5p
let-7g-5p
151a-3p
378a-3p
92b-3p
30d-5p
191-5p
423-3p
182-5p
28-3p
423-5p
98-5p
30a-3p

Supplemental Figure S4. Selective uptake of miRNAs into the RISC of OC cells. **A** and **B,** miRNA Seed Tox plots of either RISC-bound or total miRNAs in A2780 (A) and HeyA8 (B) cells. miRNAs that contribute to peaks with >5000 reads are labeled. For each labeled peak miRNAs are listed in the order of abundance. The percentage of miRNAs bound to the RISC was higher than the percentage of miRNAs in the total short (s)RNA population (79%/88.2% total and 97.6%/96.3% RISC bound in A2780 and HeyA8 cells, respectively). The seed viability (X axis) for HeyA8 cells was used (6merdb.org). **C,** All miRNAs with an average read number of >1000 in either cell line and >1.5 fold enriched (left) or reduced (right) in the RISC ranked according to the combined read numbers (total and RISC). miRNAs with toxic seeds are shown in red and putative protective miRNAs with nontoxic seeds are shown in green. miRNAs that have been reported before to be enriched or depleted in the same way in either 293T (red asterisks) or A549 (black asterisks) [2] are labeled.

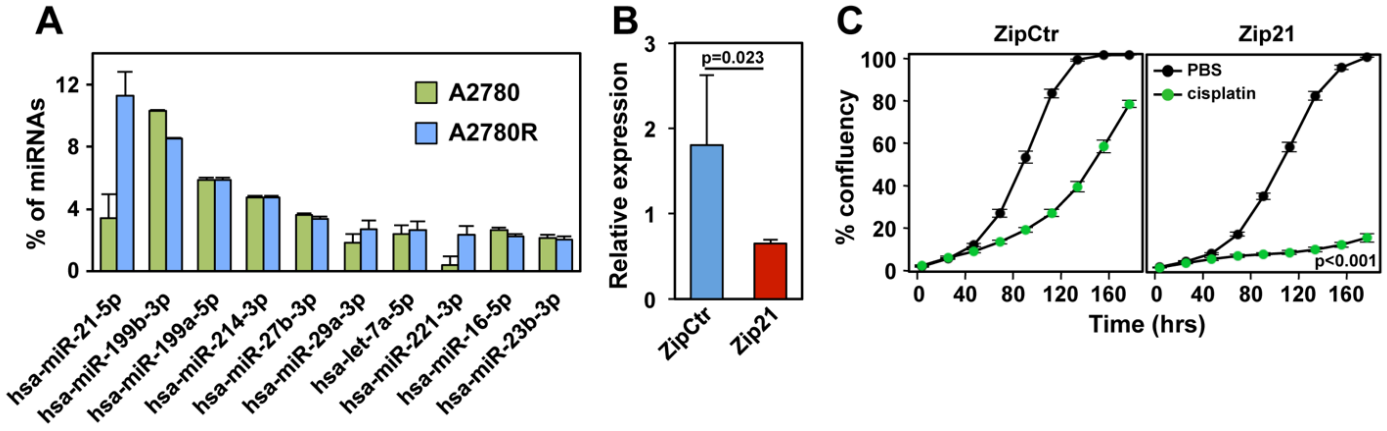

Supplemental Figure S5. miR-21-5p protects A2780R cells from platinum toxicity. **A,** Relative abundance (% of total reads) of the ten most highly expressed miRNAs in A2780 and A2780R cells (ranked according to highest expression in A2780R cells). Shown is the variance between duplicates. **B,** Real time PCR quantification of miR-21-5p in A2780R cells infected with control Zip vector or the miR-21 inhibitory lentivector Zip21. P-value from Student's T-test is shown. **C,** Confluency over time of ZipCtr or Zip21 expressing cells treated with either PBS or 5 μM Cis. P-value was calculated using a binomial distribution test. Experiments in B and C were done in triplicates.

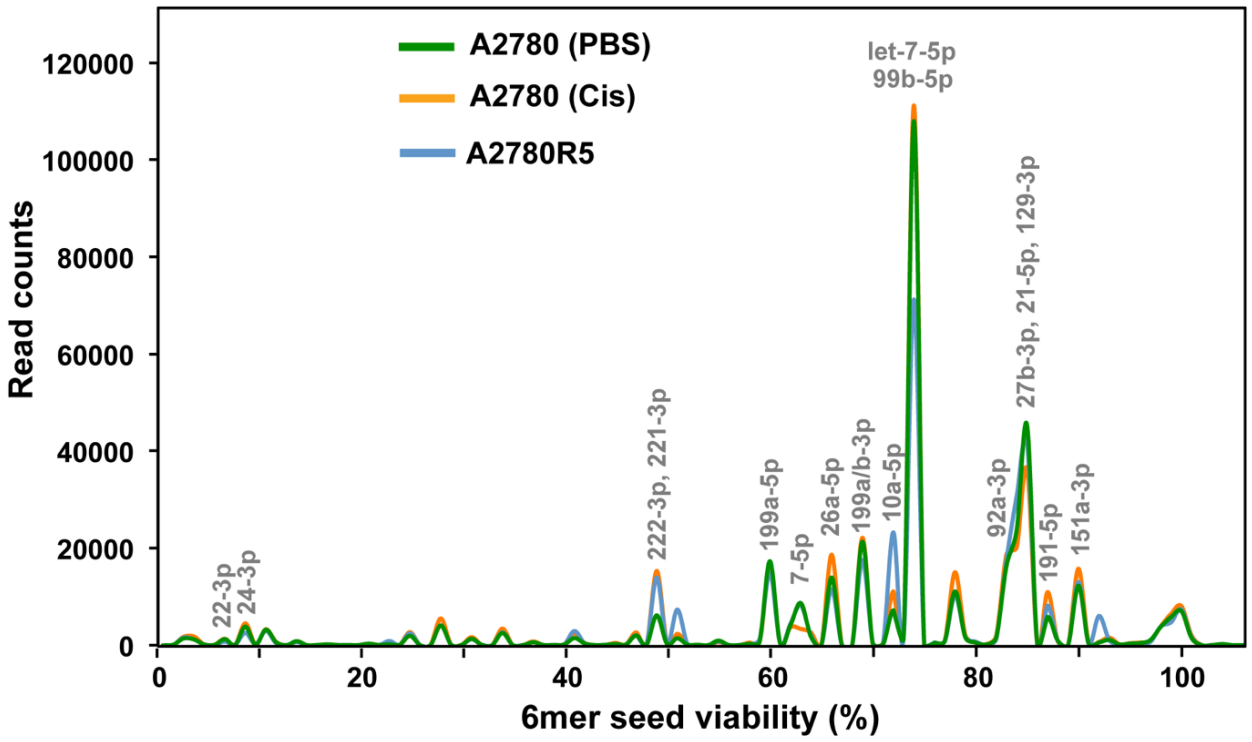

Supplemental Figure S6. Effect of cisplatin treatment on Seed Tox composition of the total miRNA fraction. Seed Tox plot of all miRNAs in A2780 cells treated with PBS or Cis and in A2780R cells. miRNAs that contribute to peaks with more than 5000 reads are labeled. For each labeled peak miRNAs are listed in the order of abundance.

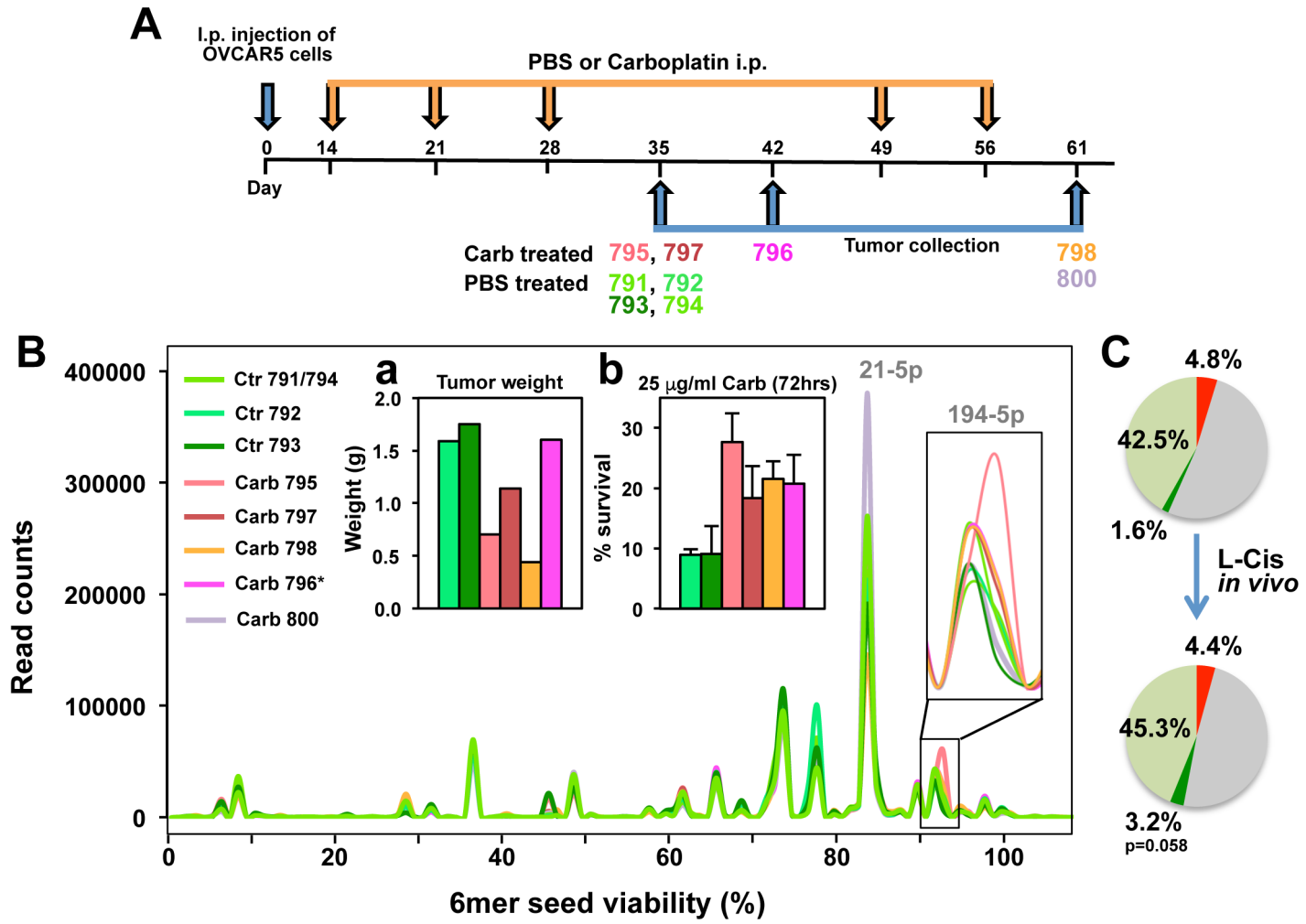

Supplemental Figure S7. Effect of long-term *in vivo* carboplatin treatment on Seed Tox of RISC-bound miRNAs in OVCAR5 cells. **A,** Treatment course. OVCAR5 (2 million) cells were injected i.p. into nude mice. Two weeks after inoculation, mice were grouped and treated i.p. with PBS (control, mice ID: 791, 792, 793, 794, n=4), or 25 mg/kg carboplatin (n = 5) as indicated: 3 doses of Carbo (n=2, mice ID: 795, 797); 3-weekly doses of Carbo + two-week recovery (n = 1, mice ID: 796); 3-weekly doses of Carbo, followed by 2-weeks recovery, followed by 2-weeks Carbo (n = 2, mice ID: 798, 800**). B,** Seed Tox plot of total RISC-bound miRNAs in OVCAR5 tumors isolated at different times after PBS or Carbo treatment as indicated in A. a, Total tumor weight; b, Viability assay of tumors 24 hours after isolated from mice treated as shown in A. ATP assay was performed 96 hrs after treatment. The area around the miR-194-5p peak is magnified. **C,** Pie charts: Average Seed Tox composition of RISC-bound miRNAs in mice treated with PBS (top) or with Carbo (bottom). miRNA reads with a predicted 6mer seed viability of <20% are shown in red, >80% in green and 20-80% in grey. Reads of miR-194-5p (part of the green section) are highlighted in darker green. miRNA content of this analysis was 96.1% (average of PBS treated) and 92.6% (Carbo treated).

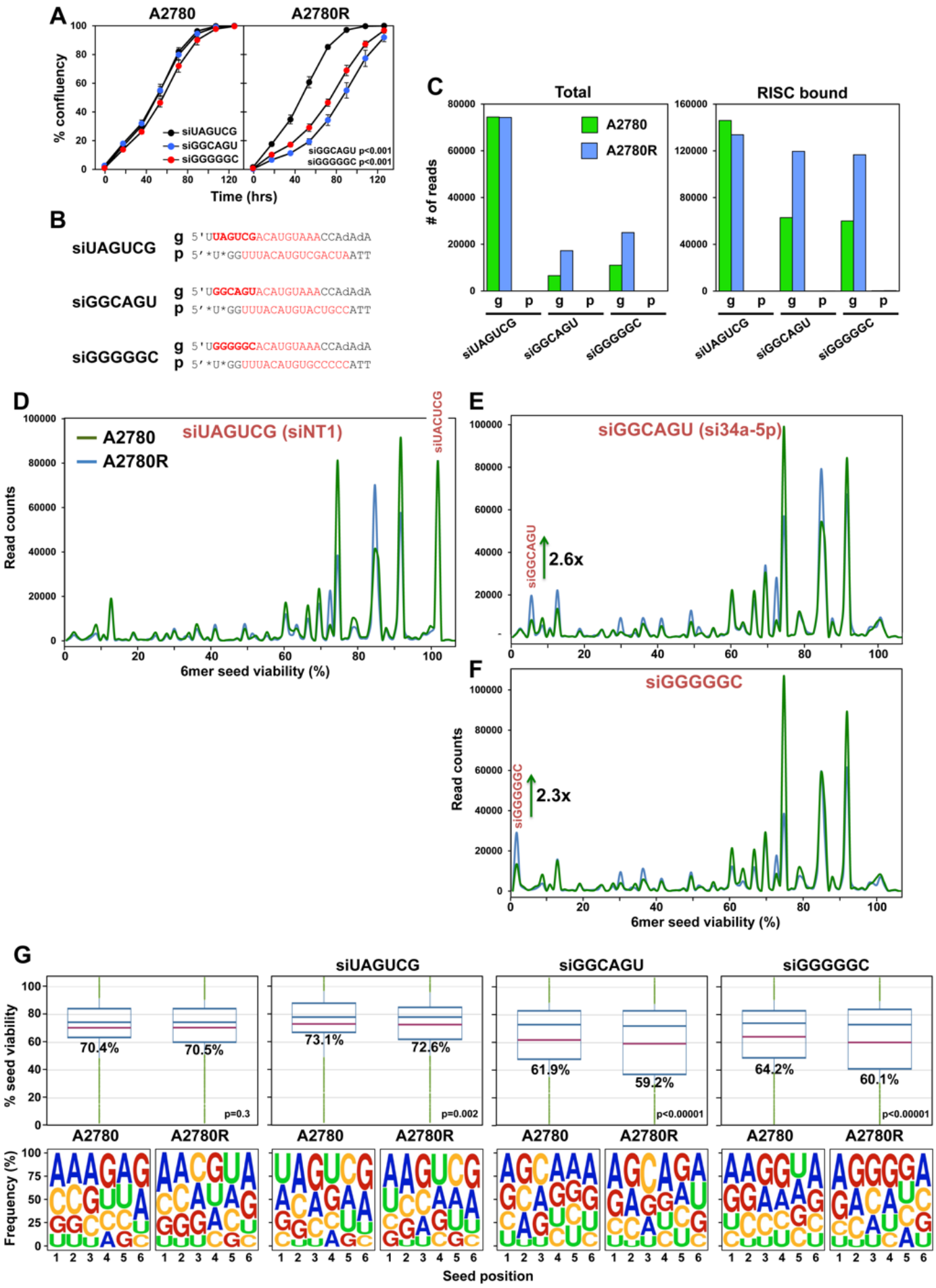
A
A2780
A2780R
% confluency
Time (hrs)
siUAGUCG
siGGCAGU
siGGGGGC
siGGCAGU p<0.001
siGGGGGC p<0.001
B
siUAGUCG
g 5'UUAGUCGACAUGUAAACCAdAdA
p 5'*U*GGUUUACAUGUCGACUAATT
siGGCAGU
g 5'UGGCAGUACAUGUAAACCAdAdA
p 5'*U*GGUUUACAUGUACUGCCATT
siGGGGGC
g 5'UGGGGGCACAUGUAAACCAdAdA
p 5'*U*GGUUUACAUGUGCCCCCATT
C
Total
RISC bound
# of reads
A2780
A2780R
siUAGUCG
siGGCAGU
siGGGGGC
D
siUAGUCG (siNT1)
siUACUCG
Read counts
6mer seed viability (%)
E
siGGCAGU (si34a-5p)
siGGCAGU
2.6x
F
siGGGGGC
siGGGGGC
2.3x
G
siUAGUCG
siGGCAGU
siGGGGGC
% seed viability
70.4%
70.5%
p=0.3
73.1%
72.6%
p=0.002
61.9%
59.2%
p<0.00001
64.2%
60.1%
p<0.00001
Frequency (%)
Seed position

Supplemental Figure S8. Preferential uptake of siRNAs with toxic seeds by Pt-R cells. **A,** Change in confluency of A2780/A2780R cells transfected with 1 nM of an siRNA backbone used in the 4096 siRNA screen containing three different 6mer seeds shown in B. P-values were calculated using ANOVA. **B,** Sequences of the three siRNAs differing in only the 6mer seed (6mers bolded). Both guide (g) and passenger (p) strands are shown 5' -> 3'. The sequences used to search the RNA Seq data (as DNA sequences) for presence of exogenous RNAs is shown in red. **C,** Total normalized numbers of sequences derived from the transfected siRNAs (either g or p) identified in the total or RISC-bound sRNA in cells transfected with the indicated siRNA. **D-F,** Seed Tox plot of miRNAs and exogenous siRNAs in total smRNA in A2780/A2780R cells 24 hrs after transfection with either siUAGUCG (siNT1), and the highly toxic siGGCAGU or siGGGGGC. **G,** Average Seed Tox (top) and seed composition (bottom) of all RISC-bound sRNAs in A2780/A2780R cells PBS treated or treated with the three siRNAs. P values at the top were calculated using a Wilcoxon rank test. The fraction of exogenous siRNAs and endogenous miRNAs was ~ 97% in all samples.

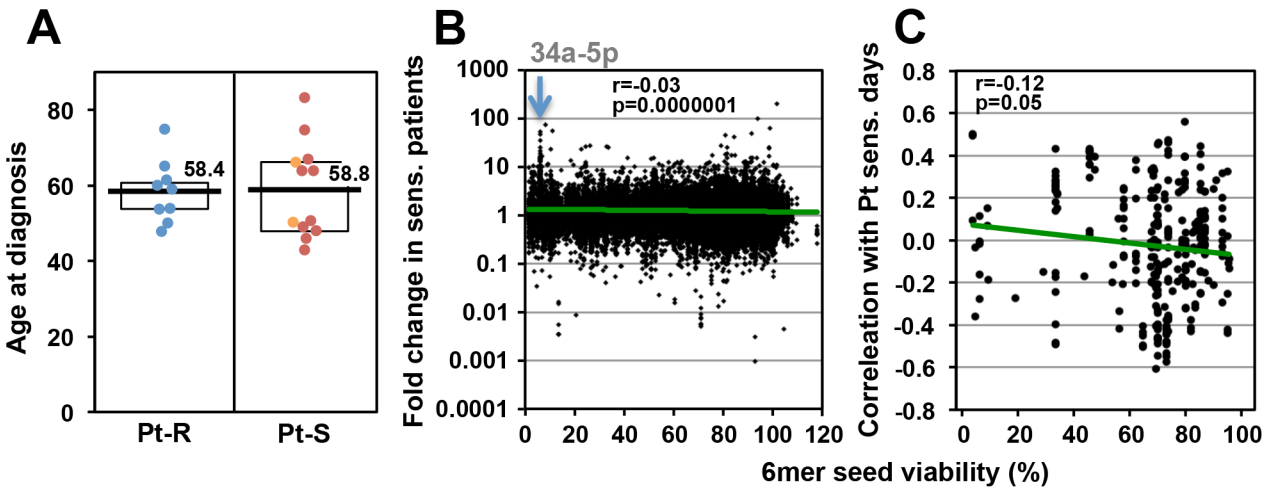

Supplemental Figure S9. Lower Seed Tox of RISC-bound sRNAs in OC tumors is associated with increased resistance to chemotherapy. **A,** Differences in age at diagnosis between the two groups in Fig. 4A. **B,** Pearson correlation between the fold change in Pt-S versus Pt-R patients and the 6mer Seed Tox (% viability in HeyA8 cells). Shown are all ~38,000 different reads across all samples. The position of a number of reads representing miR-34a-5p highly enriched in the Pt-S cells is indicated. Note, these reads while highly upregulated, did not reach statistical significance in the fold-change analyses. **C,** Pearson correlation between the correlation of the Pt sensitive days in all patients and the 6mer Seed Tox (% viability in HeyA8 cells). Shown are miRNAs with a sum of >10,000 across all samples.

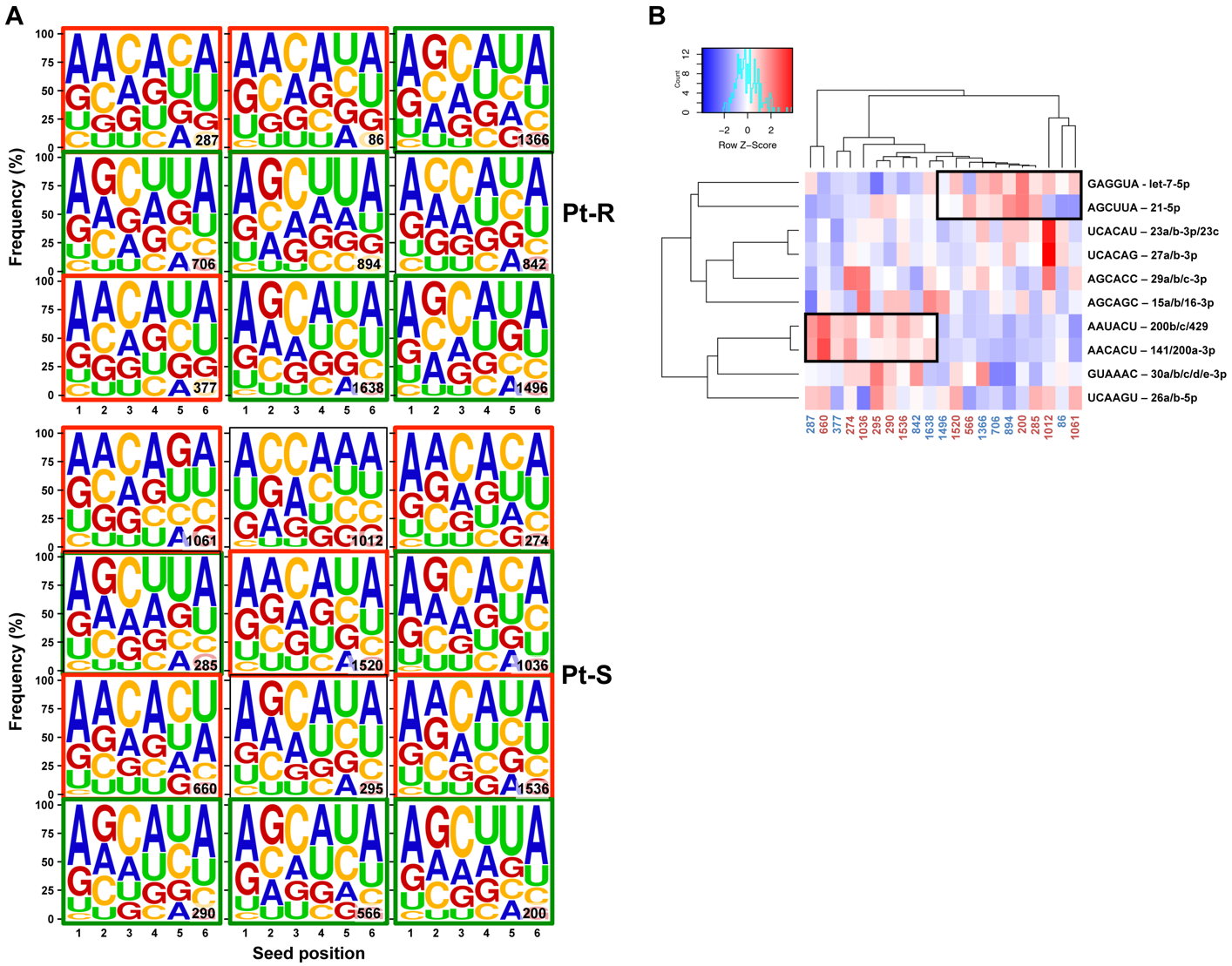

Supplemental Figure S10. OC patients can be divided into two subgroups. **A,** Seed composition plots of all RISC-bound sRNAs in all Pt-R and Pt-S tumors. Seeds that are dominated by AAC in the first three positions are boxed in red, the ones dominated by AGC are boxed in green. **B,** Heat map of an unsupervised hierarchical cluster analysis of the ten most abundant RISC-bound seeds in reads in tumors from Pt-S (labeled in blue) and Pt-R (labeled in red) patients. For each 6mer seed, the major miRNA or miRNA families they are part of, are shown. Two clusters of let-7-5p/21-5p and miR-200-5p members, respectively, are boxed.

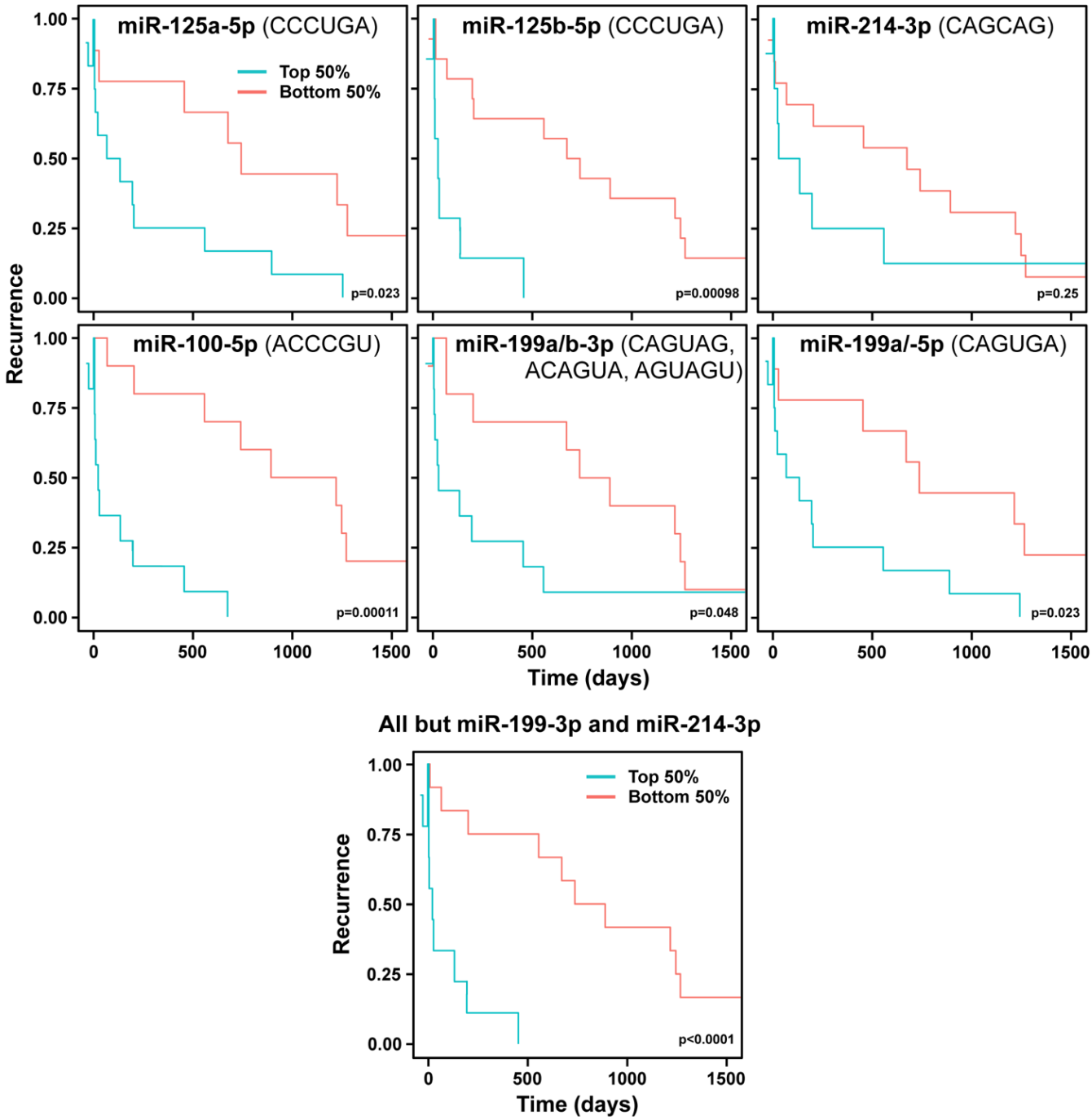

Supplemental Figure S11. Kaplan-Meier analyses of individual miRNAs. Kaplan-Meier analysis of patients with the top and bottom highest RISC content of the indicated miRNA. For miR-199-3p the average of all three isomiRs was used.

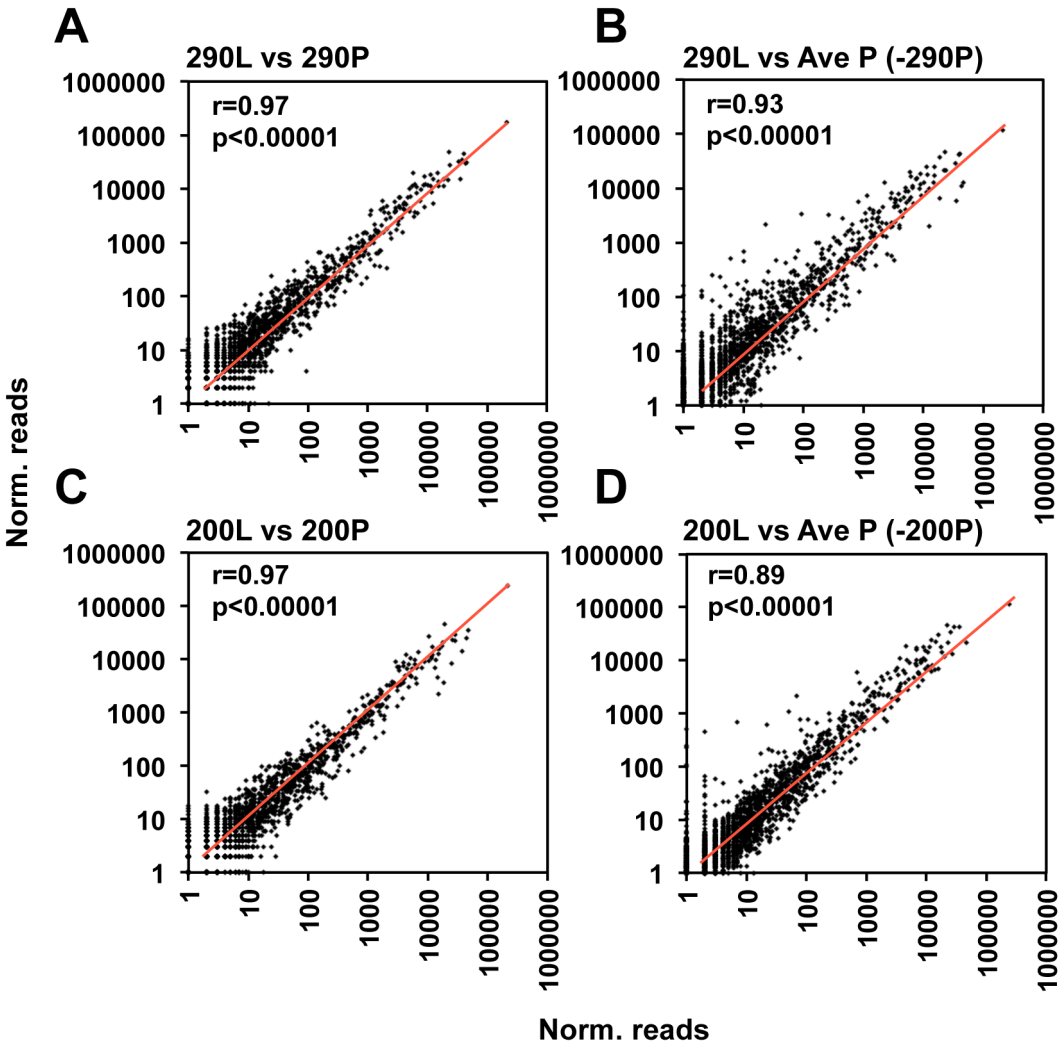

Supplemental Figure S12. Reproducibility of the Ago pull down/smRNA Seq analysis in two patients across the two analyses. **A,** Pearson correlation between reads from an Ago pull down analysis of the primary tumor from patient #290 in experiment #1 (short versus long-term survivors) and #2 (primary versus recurrence in long-term survivors). **B,** Pearson correlation between reads from an Ago pull down analysis of patient #290L in experiment #1 versus the average of all patients of experiment #2 minus patient #290P reads. **C,** Pearson correlation between reads from an Ago pull down analysis of the primary tumor from patient #200 in experiment #1 and #2**. D,** Pearson correlation between reads from an Ago pull down analysis of patient #200L in experiment #1 versus the average of all patients of experiment #2 minus patient #200P reads. In all cases all reads were analyzed but only the ones were plotted with an average minimum read count of 1 across all samples. Note, in both cases while the tumors analyzed were from the same patient, the analysis was performed with a different tumor from the same patient.

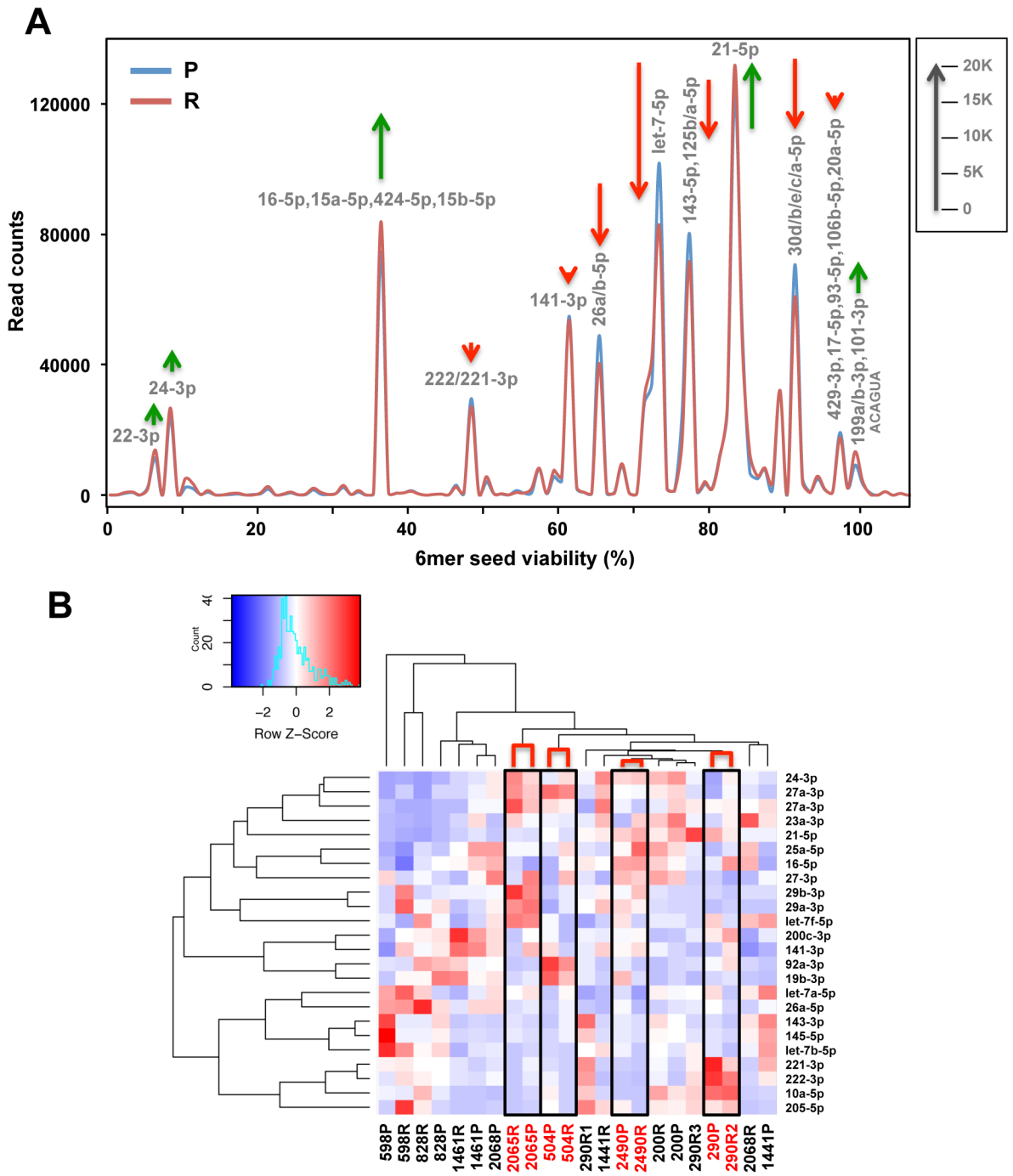

Figure S13. Analysis of primary tumors and matched recurrences. **A,** Seed Tox plot of all RISC-bound reads in primary tumors and matching recurrences. Green arrows, net increase, and red arrows, net decrease of >1000 reads in peak in recurrent tumors, respectively. **B,** Heat map of an unsupervised hierarchical cluster analysis of the most abundant miRNAs (read average across all samples >10,000) in primary tumors and matching recurrences from 10 patients. Primary tumor and matching recurrence that clustered directly together are boxed. Note, for patient #290 only recurrence R2 clustered together with the primary tumor and this pair was therefore used for further analysis. Patients in a subgroup of four highly related primary/recurrent tumor pairs are shown in red.

Supplemental References

1. Gao QQ, Putzbach W, Murmann AE, Chen S, Ambrosini G, Peter JM, Bartom E, Peter ME (2018) 6mer seed toxicity in tumor suppressive miRNAs. *Nature Comm* **9**: 4504
2. Flores O, Kennedy EM, Skalsky RL, Cullen BR (2014) Differential RISC association of endogenous human microRNAs predicts their inhibitory potential. *Nucleic Acids Res* **42**: 4629-39

Supplemental Tables

6mer Seed Toxicity and Platinum Resistance in Ovarian Cancer

Monal Patel, Yinu Wang, Elizabeth T. Bartom, Rohin Dhir, Kenneth P. Nephew,
Daniela Matei, Andrea E. Murmann, Ernst Lengyel, and Marcus E. Peter

Table S1: miRNAs involved in therapy resistance or associated with negative treatment outcome in OC

Main miRNA	Other miRNAs	Treatment	OvCa cell lines	Type of OvCa-patient sample	Clinical data/relevance	Identified miRNA target	Ref.
miR-17~92 cluster	-	Taxol	SKOV3 and Taxol-resistant SKOV3-TR30	-	-	BMI	1
miR-17-5p	-	Taxol	OVCAR3, SKOV3	-	-	PTEN	93
miR-21	-	Cisplatin	A2780R (Cis resistant)	-	-	-	2
miR-21-3p	>20 other miRNAs	Cisplatin	A2780, A2780-CP70, OVCAR5, OVCAR8 and IGROV1	Publically available datasets	Yes	NAV3	3
miR-21-5p	-	Taxol	A2780, PEA1, PEA2, ALST, OVCAR432, OVCAR433, HeyA8, HeyA8-MDR, SKOV3ip, SKOV3-TR, SKOV3, cancer asssociated fibroblasts and adipocytes	OvCa	Yes	APAF1	4
miR-21-5p	-	Cisplatin	A2780, A2780- Cp resistant, SKOV-3	Recurrent patients enrolled in TCGA	Yes	PDCD4	5
miR-21-5p	320 other miRNAs	Cisplatin	SKOV3ip1, HeyA8, A2780, A2780CP20	-	-	PDCD4	6
miR-27a	-	Taxol	A2780 and A2780/Taxol resistant cells	-	-	HIPK2	7
miR-31	-	Cisplatin	OVCAR5, A2780 and its cisplatin-resistant derivatives, MCP1, CP70	Publically available datasets	Yes	KCNMA1	8
miR-93-5p	7 other miRNAs	Cisplatin	OVCAR3, SKOV3, OVCAR3/CDDP, SKOV3/CDDP	OvCa	Yes	PTEN	94
miR-98-5p	let-7c-5p, let-7e-5p, let-7g-5p	Cisplatin	C13*, OV2008, A2780, HO8910, SKOV3, CaOV3, Hey, COV362,	Epithelial OvCa	Yes	Dicer1	9
miR-106a-5p	-	Cisplatin	OVCAR3, OVCAR3/CIS	-	-	PDCD4	95
miR-106a-5p	miR-96, miR-629	Taxol	SKOV3 and PTX resistant SKOV3 sublines	Ovarian serous tumors	Yes	BCL10, CASP-7	10
miR-125b-5p	-	Cisplatin	OV2008 and its resistant variant (C13*)	-	-	Bak1	11
miR-125b-2-3p	miR-126-5p	Cisplatin	A2780, A2780CIS, A2780TC1, A2780TC3	-	-	-	15
miR-129-5p	-	Taxol	SKOV3, SKOV3/PTX, HeyA8, HeyA8/PTX	-	-	ABCB	12
miR-130a	miR-374a, miR-146a, miR-182 and 32 others	Cisplatin	A2780, A2780/DDP	-	-	MDR-1/P-gp/PTEN	13
miR-130a	54 other miRNAs	Cisplatin	SKOV3, SKOV3/CIS	-	-	MDR1/P-gp	14
miR-130b	-	Cisplatin, Taxol	A2780, A2780/Taxol	-	-	-	96
miR-141-3p	5 other miRNAs	Cisplatin	A2780 and A2780 DDP, TOV112D, TOV21G, OV56, OAW42	Non-serous tumors	Yes	KEAP1	16
miR-149-5p	-	Cisplatin	TOV-21G, A2780, OVCAR-3, Caov-3, ES-2, HO-8910, SK-OV-3	Ovarian serous cystadenocarcinoma, benign ovarian lesions, TCGA dataset	Yes	Hippo signaling pathway	18
miR-197-3p	-	Taxol	A2780, SKOV3, A2780/Tax	-	-	NLK	20
miR-200c-with cytosolic HuR		Cisplatin, Taxol, Patupilone	-	OvCa patients	Yes	-	113
miR-214	miR-100, miR-199a-3p, miR-200a	Cisplatin	A2780S, A2780CP, OV119	Primary OvCa	Yes	PTEN	97
miR-214-3p	-	Cisplatin	A2780, A2780cp, OVCAR-3, SKOV3	-	-	MEG3	21
miR-216a-5p	-	Cisplatin	SKOV3, SKOV3 CR, OVCA433	-	-	PTEN	22
miR-224-5p	-	Cisplatin	A2780CP/A2780S, C13/OV2008	Ovarian papillary serous carcinoma	Yes	PRKCD	23
miR-363-3p	-	Taxol	SKOV3, KF, KF-TX, OVTOKO	OvCa	Yes	LATS2	24
miR-376c-3p	-	Cisplatin, Carboplatin	OV2008, A2780	Serous OvCa	Yes	ALK7	98
miR-433	-	Taxol	A2780, PEO1, PEO4	-	-	CDK6	25
miR-483-3p	-	Cisplatin, Oxiplatin	IGROV-1, IGROV-1/Pt1, IGROV-1/OHP, A2780, A2780/CP, OVCAR5, OVCAR5/Pt	GEO datasets	Yes	PRKCA	99
miR-490-3p	-	Taxol	A2780, A2780/Taxol	-	-	-	100
miR-493-3p	-	Taxol	CAOV- 3, OVCAR-8	High grade serous OvCa	Yes	Mad2	26
miR-493-5p	7 other miRNAs	PARPi, Platinum	BRCA2 mutant KURAMOCHI, OVSAHO, and VU423 cells	BrCa2 mutated OvCa, TCGA cohort	Yes	RNASEH2A, FEN1, SSRP1	27
miR-520g-3p	-	Cisplatin, Taxol	A2780, SKOV3, OVA433, ES-2, OV2008, CaOV-3, MCAS, OVK17	Epithelial OvCa	Yes	DAPK2	117
miR-551b-3p	-	Cisplatin	Side population from primary ascites-derived OvCA cells, SKOV3, 8910	OvCa	Yes	Foxo3, TRIM31	28
miR-622	-	Taxol, Carboplatin	-	High grade serous OvCa	Yes	-	89
miR-622	-	Cisplatin, Carboplatin, Olarparib, Veliparib	UWB1.289	OvCa datasets	Yes	Ku Complex	101
miR-630	-	Taxol	SKOV3 and SKOV3-TR	-	-	APAF-1	29
miR-1307	-	Cisplatin, Taxol	SKOV3 and SKOV3- TR30	Ovarian serous cystadenocarcinoma	Yes	DAPK3	32
miR-1307	-	Taxol	SKOV3 , A2780, A2780/Taxol	-	-	ING5	33
let-7e	-	Taxol	A2780, A2780TAX	-	-	-	15

Supplemental Table S1: List of miRNAs shown to be involved in therapy resistance or associated with negative treatment outcome in OC. Each row consists of a main miRNA and other miRNAs studied in a published article as well as other details from the study.

Table S2: miRNAs that can sensitize OvCa cells to therapy or are associated with positive treatment outcome in OC

Main miRNA	Other miRNAs	Treatment	OvCa cell lines	Type of OvCa-patient sample	Clinical data/relevance	Identified miRNA target	Ref.
miR-7-5p	-	Taxol	HO8910pm	-	-	EGFR, ERK pathway	43
miR-9	miR-145, miR-429, miR-26a	Cisplatin	Primary ovarian tumor cells	Serous epithelial OvCa	Yes	-	44
miR-9-5p	-	Cisplatin, PARP1 inhibitor	OV2008, C13*, SKOV3, A2780, CaOV3	Serous OvCa	Yes	BRCA1	45
miR-15a-5p, miR-16-5p	-	Cisplatin	A2780, A2780- CP20, OVSAHO, OVCAR4, OSE tsT/hTERT	High grade serous OvCa	Yes	BMI1	46
miR-18a-3p	miR-15a-5p, miR-25-3p	Docetaxel	SKOV3IP1, HeyA8, HeyA8-MDR, A2780, A2780CP20	High grade serous OvCa	Yes	K-RAS	42
miR-29	-	Cisplatin	CP-70, A2780, HeyAC2, SKOV-3	-	-	COL1A1	37
miR-29b	-	Taxol, Platinum, Cyclophosphamide	OVCAR3	High grade serous, clear cell, and mucinous ovarian adenocarcinomas	Yes	MAPK10, ATG9A	38
miR-29b	miR-7, miR-18a, miR-19a	Taxol	ES2, AMOC2	Epithelial OvCa	Yes	Mcl-1	39
miR-30a/c-5p	-	Cisplatin	A2780, A2780/CP70	-	-	DNMT1, Snail	103
miR-31	-	Taxol, Carboplatin	KFrHuman KF OvCa cells and KFr13 cisplatin-resistant KF13, SK-OV-3, OVCAR-3, TU-OM-144	Serous OvCa	Yes	MET	40
miR-34c-5p	-	Carboplatin, Docetaxel	OVS1, SKOV-I6	Ovarian serous cystadenocarcinoma	Yes	AREG	41
miR-100	-	Cisplatin	SKOV3, SKOV3/DDP	-	-	mTOR, PLK1	47
miR-101-3p	-	Cisplatin	A2780,A2780/DDP, SKOV3, SKOV3/DDP	Epithelial OvCa	Yes	EZH2	48
miR-106a-5p	-	Cisplatin	A2780,A2780/DDP	-	-	MCL1	49
miR-125b-2-3p	-	Taxol	A2780, A2780TAX	-	-	-	15
miR-128	-	Cisplatin	SKOV3, SKOV3/CP	-	-	ABCC5, BMI1	50
miR-130a-3p	-	Cisplatin	A2780, A2780/DDP	-	-	XIAP	104
miR-130a-3p	let-7e, miR-335	Cisplatin	A2780, A2780CIS, A2780TC1, A2780TC3	-	-	M-CSF	15
miR-130b-3p	-	Taxol, Cisplatin	A2780, A2780/CP, A2780/TAX, SKOV3, SKOV3/ TAX	Malignant and benign OvCa	Yes	CSF-1	51
miR-133b-3p	-	Taxol, Cisplatin	A2780, A2780/DDP, A2780/Taxol, OVCAR3	OvCa	Yes	GST-π, MDR1	52
miR-134 cluster	-	Taxol	SKOV3, Taxol-resistant SKOV3-TR30	-	-	c-Myc	1
miR-134-5p	-	Taxol	SKOV3, Taxol-resistant SKOV3-TR30	Serous epithelial OvCa	Yes	TAB1	53
miR-134-5p	-	Taxol	SKOV3, Taxol-resistant SKOV3-TR30	Serous epithelial OvCa	Yes	Pak2	54
miR-136-5p	-	Taxol	SKOV3 & its PTX-resistant sublines	High grade serous OvCa	Yes	Notch3	105
miR-136	-	Cisplatin	OV2008, C13	Epithelial OvCa	Yes	-	55
miR-137	-	Cisplatin	PEO1, PEO4 , IGROV1, OV90, IGROV1 CR, OV90 CR	OvCa	Yes	EZH2	56
miR-139-5p	-	Cisplatin	CAOV3, SNU119, CAOV3/cDDP, SNU119/cDDP	OvCa	Yes	ATP7A/B	57
miR-139-5p	-	Cisplatin	SKOV3, A2780, SKOV3-R, A2780-R	-	-	c-Jun	58
miR-141, miR-200a	-	Taxol	SKOV3	OvCa patient, publicly available datasets	Yes	-	116
miR-142-5p	-	Cisplatin	OVCAR3, SKOV3	Epithelial OvCa	Yes	XIAP1, BIRC3, BCL2, BCL2L2, MCL1	59
miR-145-5p	-	Taxol	A2780, SKOV3, A2780/PTX, SKOV3/PTX	Serous epithelial OvCa	Yes	Sp1, Cdk6 , P-gp, pRb	17
miR-146a-5p	-	Cisplatin	OVCAR3, SKOV3	Primary epithelialOvCa cells from freshly collected malignant ascites	Yes	XIAP, BCL2L2 and BIRC5	60
miR-146b-5p	-	Taxol, Cisplatin	SKOV3, HO8910, A2780, OVCAR-3	Epithelial OvCa	Yes	FBXL10	61
miR-149-5p	-	Taxol	A2780	-	-	MyD88	19
miR-152 -3p	-	Cisplatin	C13*, OV2008, A2780, HO8910, SKOV3, CaOV3, Hey, COV362,	Epithelial OvCa	Yes	-	9
miR-152-3p, miR-185-5p	-	Cisplatin	SKOV3, A2780, A2780/DDP, SKOV3/DDP	-	-	DNMT1	62
miR-155-5p	-	Cisplatin	SKOV3, A2780	Primary epithelial OvCa cells from freshly collected malignant ascites	Yes	XIAP	63
miR-182	-	Platinum	-	High grade serous OvCa	Yes		64
miR-186-5p	-	Cisplatin	A2780, OV2008, OVCAR3, SKOV3, CAOV3, the related cDDP-resistant cell lines (ACRP, C13* and OVCAR3/ DDP)	Serous OvCa	Yes	Twist1	65
miR-186-5p	-	Taxol, Cisplatin	OVCAR3, A2780, A2780/DDP, A2780/Taxol	-	-	ABCB1	66

Table S2, cont.: miRNAs that can sensitize OvCa cells to therapy or are associated with positive treatment outcome in OC

Main miRNA	Other miRNAs	Treatment	OvCa cell lines	Type of OvCa-patient sample	Clinical data/relevance	Identified miRNA target	Ref.
miR-199a	-	Taxol, Cisplatin, Adriamycin	CD44+/CD117+ ovarian tumor cells from inpatient clinic patients	Epithelial OvCa	Yes	CD44	67
miR-199a-3p	-	Cisplatin	SKOV3 , SKOV3-CDDP	OvCa	Yes	ITGB8	68
miR-199-3p	-	Cisplatin, 5Aza-dC	SKOV3, HO-8910, IOSE386 (immortalized ovarian epithelial cell line)	Epithelial OvCa	Yes	DDR1	106
miR-199b-5p	-	Cisplatin	A2780s, A2780cp, OV2008, C13*, SKOV3, OVCA433, ES-2	Epithelial OvCa	Yes	JAG1	69
miR-200 family	-	Taxol	-	OvCa	Yes	β-tubulin III	114
miR-200a	-	Taxol	OVCAR3	-	-	-	115
miR-200b, miR-200c	-	Cisplatin	HIOSE-80, MCC-3, SKOV3, A2780CP, A2780, OV119	Primary ovarian tumor	Yes	DNMTs	70
miR-200c	-	Taxol	HEY, SKOV3, OVCA 420, OV 1847, OVCA 433	Serous OvCa	Yes	TUBB3	71
miR-200c-3p	-	Cisplatin, Olaparib	UWB1.289, UWB1.289-BRCA and SKOV3	Serous and mucinous carcinomas	Yes	Neuropilin 1	72
miR-200c-3p	-	Cisplatin, Taxol, Doxorubicin, Mitomycin C, Vincristine, Epothilone	2008, Hey, SKOV3, OVCA 420, OVCA 433	-	-	TUBB3	107
miR-200c-with nuclear HuR		Cisplatin, Taxol, Patupilone	-	OvCa patients	Yes	-	113
miR-204-5p	-	Cisplatin	A2780, SKOV3, OVCAR3, OV2008, C13*	Epithelial OvCa	Yes	IL-6R	73
miR-215	-	Taxol	OVCAR3, CAOV3, SKOV3, HEY	Epithelial OvCa	Yes	XIAP	74
miR-216b-5p		Cisplatin	SKOV3, SKOV3/CDDP	OvCa	Yes	PARP1	75
miR-335	-	-	-	Epithelial OvCa	Yes	-	108
miR-335-5p	8 other miRNAs	Cisplatin	A2780, A2780/DDP, OV90, OVCAR-3,	-	-	BCL2L2	76
miR-338-3p	-	Cisplatin	A2780, A2780/DDP, SKOV3, SKOV3/CDDP	PrimaryOvCa	Yes	WNT2B	77
miR-363-3p	-	Cisplatin	OV2008, A2780, C13, A2780cp	OvCa	Yes	Snail	78
miR-370-3p	-	Cisplatin	SKOV3, UWB1.289, HEY, OV2008, IGROV1, TOV112D, ES-2, TOV21G	Endometriod OvCa	Yes	ENG	109
miR-378a-3p	-	Cisplatin	OVCAR3, SKOV3	OvCa	Yes	MAPK1, GRB2	79
miR-383-5p	-	Taxol	SKOV3, A2780, OVCAR-3, Caov-3	OvCa	Yes	TRIM27	80
miR-411-5p	-	Cisplatin, Taxol	SKOV3, OVCAR3	Primary OvCa	Yes	ABCG2	81
miR-429	-	Cisplatin	OVCAR3 & Hey	-	-	-	112
miR-449a	-	Cisplatin	A2780, A2780/CDDP, SKOV3, SKOV3/CDDP	-	-	NOTCH1	110
miR-489-3p	-	Cisplatin	SKOV3, OVCAR3, SKOV3/CDDP, OVCAR3/CDDP	-	-	Akt3	82
miR-490-3p	-	Cisplatin	SKOV3, OVCAR3, SKOV3/CDDP, OVCAR3/CDDP	OvCa	Yes	ABCC2	83
miR-497-5p	9 other miRNAs	Cisplatin	A2780, A2780/ CP, SKOV3, SKOV3/CP	OvCa	Yes	mTOR, P70S6K1	84
miR-503	-	Cisplatin	SKOV3, SKOV3/DDP	-	-	PI3K p85	85
miR-503-5p	-	Taxol	CaOV3, SKOV3, OVCAR3, OV90, CaOV3/PTX-R, SKOV3/PTX-R	-	-	CD97	86
miR-506-3p	-	Cisplatin, Olaparib	HeyA8, OVCA433, SKOV3	Serous OvCa	Yes	RAD-51	111
miR-509-3p	-	Cisplatin	SKOV3	OvCa tissue	Yes	GOLPH3, WLS	87
miR-514-5p	-	Cisplatin	SKOV3, OVCA433	NCBI's GEO datasets	Yes	ATP binding cassette subfamily	88
miR-591	miR-106a-5p	Taxol	SKOV3 and PTX resistant SKOV3 sublines	Epithelial OvCa	Yes	ZEB1	10
miR-708-5p	-	Cisplatin	A2780, A2780/DDP, SKOV3, SKOV3/CDDP	-		IGF2BP1	90
miR-770-5p	-	Cisplatin	OV2008, A2780, C13, A2780cp	Epithelial OvCa	Yes	ERCC2	91
miR-873	-	Cisplatin, Taxol	A2780, A2780/DDP, A2780/Taxol, OVCAR3	-	-	ABCB1	30
miR-874-5p, miR-874-3p	-	Taxol	Caov3, SKOV3	Epithelial OvCa	Yes	SIK2	92
miR-1294	-	Cisplatin	SKOV3	Advanced stage OvCa	Yes	IGF1R	31
let-7d-3p	let-7a	Taxol, Carboplatin	SKOV-3	High grade serous, endometrioid, mucinous, serous papillary low grade or clear cell OvCa	Yes	-	34
let-7e-5p	-	Cisplatin	A2780, HO8910, ES2, CAOV3, SKOV3	Serous epithelial OvCa	Yes	BRCA1, Rad51	35
let-7e	-	Cisplatin	A2780, ES2, SKOV3, A2780/CP	-	-	-	102
let-7g	let-7d	Taxol, Carboplatin, Vinblastine	ADR-RES, OVCAR-8, T47D, IGROV1	Epithelial OvCa	Yes	MDR1, IMP-1	36

Supplemental Table S2: List of miRNAs shown to either sensitize OC to therapy or associated with positive treatment outcome in OC. Each row consists of a main miRNA and other miRNAs studied in a published article as well as other details from the study.

Supplemental Table S3: Patient tumor samples used in analysis #1 (long-term vs. short-term survivors) and analysis #2 (primary vs. recurrent tumors).

Supplemental Table S4: Identification of the most abundant miRNAs enriched in Pt-R patients. Tab "All": A list of all reads collapsed into miRNAs according to their 6mer seeds in analysis #1 (comparison of short term and long term Pt sensitive patients). S, short-term sensitive; I, intermediate sensitive; L, long-term sensitive. Tab "Top abundant miRNAs". miRNA read numbers were correlated using Pearson correlations with the Pt sensitive days. All miRNAs as shown that had a correlation p value of <0.05 an average read number of >1000 and a downregulation of >1.5 fold between the Pt-S and Pt-R groups.

References Supplemental Table S1 and S2

1.Zhu H, Yang SY, Wang J, Wang L, Han SY. (2016). Evidence for miR-17-92 and miR-134 gene cluster regulation of ovarian cancer drug resistance. Eur Rev Med Pharmacol Sci. 20:2526-31.
2.Vandghanooni S, Eskandani M, Barar J, Omidi Y. (2018). AS1411 aptamer-decorated cisplatin-loaded poly(lactic-co-glycolic acid) nanoparticles for targeted therapy of miR-21-inhibited ovarian cancer cells. Nanomedicine. 13:2729-58.
3.Pink RC, Samuel P, Massa D, Caley DP, Brooks SA, Carter DR. (2015). The passenger strand, miR-21-3p, plays a role in mediating cisplatin resistance in ovarian cancer cells. Gynecol Oncol. 137:143-51.
4.Au Yeung CL, Co NN, Tsuruga T, Yeung TL, Kwan SY, Leung CS, Li Y, Lu ES, Kwan K, Wong KK, Schmandt R, Lu KH, Mok SC. (2016). Exosomal transfer of stroma-derived miR21 confers paclitaxel resistance in ovarian cancer cells through targeting APAF1. Nat Commun. 7:11150.
5.Chan JK, Blansit K, Kiet T, Sherman A, Wong G, Earle C, Bourguignon LY. (2014). The inhibition of miR-21 promotes apoptosis and chemosensitivity in ovarian cancer. Gynecol Oncol. 132:739-44.
6.Echevarría-Vargas IM, Valiyeva F, Vivas-Mejía PE. (2014). Upregulation of miR-21 in cisplatin resistant ovarian cancer via JNK-1/c-Jun pathway. PLoS One. 9:e97094.
7.Li Z, Hu S, Wang J, Cai J, Xiao L, Yu L, Wang Z. (2010). MiR-27a modulates MDR1/P-glycoprotein expression by targeting HIPK2 in human ovarian cancer cells. Gynecol Oncol. 119:125-30.
8.Samuel P, Pink RC, Caley DP, Currie JM, Brooks SA, Carter DR. (2016). Over-expression of miR-31 or loss of KCNMA1 leads to increased cisplatin resistance in ovarian cancer cells. Tumour Biol. 37:2565-73.
9.Wang Y, Bao W, Liu Y, Wang S, Xu S, Li X, Li Y, Wu S. (2018). miR-98-5p contributes to cisplatin resistance in epithelial ovarian cancer by suppressing miR-152 biogenesis via targeting Dicer1. Cell Death Dis. 9:447.
10.Huh JH, Kim TH, Kim K, Song JA, Jung YJ, Jeong JY, Lee MJ, Kim YK, Lee DH, An HJ. (2013). Dysregulation of miR-106a and miR-591 confers paclitaxel resistance to ovarian cancer. Br J Cancer. 109:452-61.
11.Kong F, Sun C, Wang Z, Han L, Weng D, Lu Y, Chen G. (2011). miR-125b confers resistance of ovarian cancer cells to cisplatin by targeting pro-apoptotic Bcl-2 antagonist killer 1. Journal of Huazhong University of Science and Technology Medical sciences = Hua zhong ke ji da xue xue bao Yi xue Ying De wen ban = Huazhong keji daxue xuebao Yixue Yingdewen ban. 31:543.
12.Wang J, Ye C, Liu J, Hu Y. (2018). UCA1 confers paclitaxel resistance to ovarian cancer through miR-129/ABCB1 axis. Biochem Biophys Res Commun. 501:1034-40.
13.Li N, Yang L, Wang H, Yi T, Jia X, Chen C, Xu P. (2015). MiR-130a and MiR-374a Function as Novel Regulators of Cisplatin Resistance in Human Ovarian Cancer A2780 Cells. PLoS One. 10:e0128886.
14.Yang L, Li N, Wang H, Jia X, Wang X, Luo J. (2012). Altered microRNA expression in cisplatin-resistant ovarian cancer cells and upregulation of miR-130a associated with MDR1/P-glycoprotein-mediated drug resistance. Oncol Rep. 28:592-600.
15.Sorrentino A, Liu CG, Addario A, Peschle C, Scambia G, Ferlini C. (2008). Role of microRNAs in drug-resistant ovarian cancer cells. Gynecol Oncol. 111:478-86.
16.van Jaarsveld MT, Helleman J, Boersma AW, van Kuijk PF, van Ijcken WF, Despierre E, Vergote I, Mathijssen RH, Berns EM, Verweij J, Pothof J, Wiemer EA. (2013). miR-141 regulates KEAP1 and modulates cisplatin sensitivity in ovarian cancer cells. Oncogene. 32:4284-93.
17.Zhu X, Li Y, Xie C, Yin X, Liu Y, Cao Y, Fang Y, Lin X, Xu Y, Xu W, Shen H, Wen J. (2014). miR-145 sensitizes ovarian cancer cells to paclitaxel by targeting Sp1 and Cdk6. Int J Cancer. 135:1286-96.
18.Xu M, Xiao J, Chen M, Yuan L, Li J, Shen H, Yao S. (2018). miR-149-5p promotes chemotherapeutic resistance in ovarian cancer via the inactivation of the Hippo signaling pathway. Int J Oncol. 52:815-27.

19.Zhan Y, Xiang F, Wu R, Xu J, Ni Z, Jiang J, Kang X. (2015). MiRNA-149 modulates chemosensitivity of ovarian cancer A2780 cells to paclitaxel by targeting MyD88. J Ovarian Res. 8:48.
20.Zou D, Wang D, Li R, Tang Y, Yuan L, Long X, Zhou Q. (2015). MiR-197 induces Taxol resistance in human ovarian cancer cells by regulating NLK. Tumour Biol. 36:6725-32.
21.Zhang J, Liu J, Xu X, Li L. (2017). Curcumin suppresses cisplatin resistance development partly via modulating extracellular vesicle-mediated transfer of MEG3 and miR-214 in ovarian cancer. Cancer Chemother Pharmacol. 79:479-87.
22.Jin P, Liu Y, Wang R. (2018). STAT3 regulated miR-216a promotes ovarian cancer proliferation and cisplatin resistance. Biosci Rep. 38.
23.Zhao H, Bi T, Qu Z, Jiang J, Cui S, Wang Y. (2014). Expression of miR-224-5p is associated with the original cisplatin resistance of ovarian papillary serous carcinoma. Oncol Rep. 32:1003-12.
24.Mohamed Z, Hassan MK, Okasha S, Mitamura T, Keshk S, Konno Y, Kato T, El-Khamisy SF, Ohba Y, Watari H. (2018). miR-363 confers taxane resistance in ovarian cancer by targeting the Hippo pathway member, LATS2. Oncotarget. 9:30053-65.
25.Weiner-Gorzel K, Dempsey E, Milewska M, McGoldrick A, Toh V, Walsh A, Lindsay S, Gubbins L, Cannon A, Sharpe D, O'Sullivan J, Murphy M, Madden SF, Kell M, McCann A, Furlong F. (2015). Overexpression of the microRNA miR-433 promotes resistance to paclitaxel through the induction of cellular senescence in ovarian cancer cells. Cancer Med. 4:745-58.
26.Tambe M, Pruikkonen S, Mäki-Jouppila J, Chen P, Elgaaen BV, Straume AH, Huhtinen K, Cárpen O, Lønning PE, Davidson B, Hautaniemi S, Kallio MJ. (2016). Novel Mad2-targeting miR-493-3p controls mitotic fidelity and cancer cells' sensitivity to paclitaxel. Oncotarget. 7:12267-85.
27.Meghani K, Fuchs W, Detappe A, Drané P, Gogola E, Rottenberg S, Jonkers J, Matulonis U, Swisher EM, Konstantinopoulos PA, Chowdhury D. (2018). Multifaceted Impact of MicroRNA 493-5p on Genome-Stabilizing Pathways Induces Platinum and PARP Inhibitor Resistance in BRCA2-Mutated Carcinomas. Cell Rep. 23:100-11.
28.Wei Z, Liu Y, Wang Y, Zhang Y, Luo Q, Man X, Wei F, Yu X. (2016). Downregulation of Foxo3 and TRIM31 by miR-551b in side population promotes cell proliferation, invasion, and drug resistance of ovarian cancer. Med Oncol. 33:126.
29.Eoh KJ, Lee SH, Kim HJ, Lee JY, Kim S, Kim SW, Kim YT, Nam EJ. (2018). MicroRNA-630 inhibitor sensitizes chemoresistant ovarian cancer to chemotherapy by enhancing apoptosis. Biochem Biophys Res Commun. 497:513-20.
30.Wu DD, Li XS, Meng XN, Yan J, Zong ZH. (2016). MicroRNA-873 mediates multidrug resistance in ovarian cancer cells by targeting ABCB1. Tumour Biol. 37:10499-506.
31.Zhang Y, Huang S, Guo Y, Li L. (2018). MiR-1294 confers cisplatin resistance in ovarian Cancer cells by targeting IGF1R. Biomed Pharmacother. 106:1357-63.
32.Zhou Y, Wang M, Wu J, Jie Z, Chang S, Shuang T. (2015). The clinicopathological significance of miR-1307 in chemotherapy resistant epithelial ovarian cancer. J Ovarian Res. 8:23.
33.Chen WT, Yang YJ, Zhang ZD, An Q, Li N, Liu W, Yang B. (2017). MiR-1307 promotes ovarian cancer cell chemoresistance by targeting the ING5 expression. J Ovarian Res. 10:1.
34.García-Vázquez R, Gallardo Rincón D, Ruiz-García E, Meneses García A, Hernández De La Cruz ON, Astudillo-De La Vega H, Isla-Ortiz D, Marchat LA, Salinas-Vera YM, Carlos-Reyes Á, López-González S, Ramos-Payan R, López-Camarillo C. (2018). let-7d-3p is associated with apoptosis and response to neoadjuvant chemotherapy in ovarian cancer. Oncol Rep. 39:3086-94.
35.Xiao M, Cai J, Cai L, Jia J, Xie L, Zhu Y, Huang B, Jin D, Wang Z. (2017). Let-7e sensitizes epithelial ovarian cancer to cisplatin through repressing DNA double strand break repair. J Ovarian Res. 10:24.
36.Boyerinas B, Park SM, Murmann AE, Gwin K, Montag AG, Zillhardt M, Hua YJ, Lengyel E, Peter ME. (2012). Let-7 modulates acquired resistance of ovarian cancer to Taxanes via IMP-1-mediated stabilization of multidrug resistance 1. Int J Cancer. 130:1787-97.
37.Yu PN, Yan MD, Lai HC, Huang RL, Chou YC, Lin WC, Yeh LT, Lin YW. (2014). Downregulation of miR-29 contributes to cisplatin resistance of ovarian cancer cells. Int J Cancer. 134:542-51.

38.Dai F, Zhang Y, Chen Y. (2014). Involvement of miR-29b signaling in the sensitivity to chemotherapy in patients with ovarian carcinoma. Hum Pathol. 45:1285-93.
39.Sugio A, Iwasaki M, Habata S, Mariya T, Suzuki M, Osogami H, Tamate M, Tanaka R, Saito T. (2014). BAG3 upregulates Mcl-1 through downregulation of miR-29b to induce anticancer drug resistance in ovarian cancer. Gynecol Oncol. 134:615-23.
40.Mitamura T, Watari H, Wang L, Kanno H, Hassan MK, Miyazaki M, Katoh Y, Kimura T, Tanino M, Nishihara H, Tanaka S, Sakuragi N. (2013). Downregulation of miRNA-31 induces taxane resistance in ovarian cancer cells through increase of receptor tyrosine kinase MET. Oncogenesis. 2:e40.
41.Tung SL, Huang WC, Hsu FC, Yang ZP, Jang TH, Chang JW, Chuang CM, Lai CR, Wang LH. (2017). miRNA-34c-5p inhibits amphiregulin-induced ovarian cancer stemness and drug resistance via downregulation of the AREG-EGFR-ERK pathway. Oncogenesis. 6:e326.
42.Rodriguez-Aguayo C, Monroig PDC, Redis RS, Bayraktar E, Almeida MI, Ivan C, Fuentes-Mattei E, Rashed MH, Chavez-Reyes A, Ozpolat B, Mitra R, Sood AK, Calin GA, Lopez-Berestein G. (2017). Regulation of hnRNPA1 by microRNAs controls the miR-18a-K-RAS axis in chemotherapy-resistant ovarian cancer. Cell Discov. 3:17029.
43.Cui X, Sun Y, Shen M, Song K, Yin X, Di W, Duan Y. (2018). Enhanced Chemotherapeutic Efficacy of Paclitaxel Nanoparticles Co-delivered with MicroRNA-7 by Inhibiting Paclitaxel-Induced EGFR/ERK pathway Activation for Ovarian Cancer Therapy. ACS Appl Mater Interfaces. 10:7821-31.
44.Zhao HM, Wei W, Sun YH, Gao JH, Wang Q, Zheng JH. (2015). MicroRNA-9 promotes tumorigenesis and mediates sensitivity to cisplatin in primary epithelial ovarian cancer cells. Tumour Biol. 36:6867-73.
45.Sun C, Li N, Yang Z, Zhou B, He Y, Weng D, Fang Y, Wu P, Chen P, Yang X, Ma D, Zhou J, Chen G. (2013). miR-9 regulation of BRCA1 and ovarian cancer sensitivity to cisplatin and PARP inhibition. J Natl Cancer Inst. 105:1750-8.
46.Dwivedi SK, Mustafi SB, Mangala LS, Jiang D, Pradeep S, Rodriguez-Aguayo C, Ling H, Ivan C, Mukherjee P, Calin GA, Lopez-Berestein G, Sood AK, Bhattacharya R. (2016). Therapeutic evaluation of microRNA-15a and microRNA-16 in ovarian cancer. Oncotarget. 7:15093-104.
47.Guo P, Xiong X, Zhang S, Peng D. (2016). miR-100 resensitizes resistant epithelial ovarian cancer to cisplatin. Oncol Rep. 36:3552-8.
48.Liu L, Guo J, Yu L, Cai J, Gui T, Tang H, Song L, Wang J, Han F, Yang C, Chen C, Marks A, Wang Z. (2014). miR-101 regulates expression of EZH2 and contributes to progression of and cisplatin resistance in epithelial ovarian cancer. Tumour Biol. 35:12619-26.
49.Rao YM, Shi HR, Ji M, Chen CH. (2013). MiR-106a targets Mcl-1 to suppress cisplatin resistance of ovarian cancer A2780 cells. J Huazhong Univ Sci Technolog Med Sci. 33:567-72.
50.Li B, Chen H, Wu N, Zhang WJ, Shang LX. (2014). Deregulation of miR-128 in ovarian cancer promotes cisplatin resistance. Int J Gynecol Cancer. 24:1381-8.
51.Yang C, Cai J, Wang Q, Tang H, Cao J, Wu L, Wang Z. (2012). Epigenetic silencing of miR-130b in ovarian cancer promotes the development of multidrug resistance by targeting colony-stimulating factor 1. Gynecol Oncol. 124:325-34.
52.Chen S, Jiao JW, Sun KX, Zong ZH, Zhao Y. (2015). MicroRNA-133b targets glutathione S-transferase π expression to increase ovarian cancer cell sensitivity to chemotherapy drugs. Drug Des Devel Ther. 9:5225-35.
53.Shuang T, Wang M, Zhou Y, Shi C, Wang D. (2017). NF-κB1, c-Rel, and ELK1 inhibit miR-134 expression leading to TAB1 upregulation in paclitaxel-resistant human ovarian cancer. Oncotarget. 8:24853-68.
54.Shuang T, Wang M, Shi C, Zhou Y, Wang D. (2015). Down-regulated expression of miR-134 contributes to paclitaxel resistance in human ovarian cancer cells. FEBS Lett. 589:3154-64.
55.Zhao H, Liu S, Wang G, Wu X, Ding Y, Guo G, Jiang J, Cui S. (2015). Expression of miR-136 is associated with the primary cisplatin resistance of human epithelial ovarian cancer. Oncol Rep. 33:591-8.
56.Sun J, Cai X, Yung MM, Zhou W, Li J, Zhang Y, Li Z, Liu SS, Cheung ANY, Ngan HYS, Li Y, Dai Z, Kai Y, Tzatsos A, Peng W, Chan DW, Zhu W. (2019). miR-137 mediates the functional link between c-Myc and EZH2 that regulates cisplatin resistance in ovarian cancer. Oncogene. 38:564-80.

57.Xiao F, Li Y, Wan Y, Xue M. (2018). MircroRNA-139 sensitizes ovarian cancer cell to cisplatin-based chemotherapy through regulation of ATP7A/B. Cancer Chemother Pharmacol. 81:935-47.
58.Jiang Y, Jiang J, Jia H, Qiao Z, Zhang J. (2018). Recovery of miR-139-5p in Ovarian Cancer Reverses Cisplatin Resistance by Targeting C-Jun. Cell Physiol Biochem. 51:129-41.
59.Li X, Chen W, Jin Y, Xue R, Su J, Mu Z, Li J, Jiang S. (2019). miR-142-5p enhances cisplatin-induced apoptosis in ovarian cancer cells by targeting multiple anti-apoptotic genes. Biochem Pharmacol. 161:98-112.
60.Li X, Jin Y, Mu Z, Chen W, Jiang S. (2017). MicroRNA-146a-5p enhances cisplatin-induced apoptosis in ovarian cancer cells by targeting multiple anti-apoptotic genes. Int J Oncol. 51:327-35.
61.Yan M, Yang X, Shen R, Wu C, Wang H, Ye Q, Yang P, Zhang L, Chen M, Wan B, Zhang Q, Xia S, Lu X, Shao G, Zhou X, Yu J, Shao Q. (2018). miR-146b promotes cell proliferation and increases chemosensitivity, but attenuates cell migration and invasion via FBXL10 in ovarian cancer. Cell Death Dis. 9:1123.
62.Xiang Y, Ma N, Wang D, Zhang Y, Zhou J, Wu G, Zhao R, Huang H, Wang X, Qiao Y, Li F, Han D, Wang L, Zhang G, Gao X. (2014). MiR-152 and miR-185 co-contribute to ovarian cancer cells cisplatin sensitivity by targeting DNMT1 directly: a novel epigenetic therapy independent of decitabine. Oncogene. 33:378-86.
63.Chen W, Huang L, Hao C, Zeng W, Luo X, Li X, Zhou L, Jiang S, Chen Z, He Y. (2016). MicroRNA-155 promotes apoptosis in SKOV3, A2780, and primary cultured ovarian cancer cells. Tumour Biol. 37:9289-99.
64.Ramalho S, Andrade LAA, Filho CC, Natal RA, Pavanello M, Ferracini AC, Sallum LF, Sarian LO, Derchain S. (2019). Role of discoidin domain receptor 2 (DDR2) and microRNA-182 in survival of women with high-grade serous ovarian cancer. Tumour Biol. 41:1010428318823988.
65.Zhu X, Shen H, Yin X, Long L, Xie C, Liu Y, Hui L, Lin X, Fang Y, Cao Y, Xu Y, Li M, Xu W, Li Y. (2016). miR-186 regulation of Twist1 and ovarian cancer sensitivity to cisplatin. Oncogene. 35:323-32.
66.Sun KX, Jiao JW, Chen S, Liu BL, Zhao Y. (2015). MicroRNA-186 induces sensitivity of ovarian cancer cells to paclitaxel and cisplatin by targeting ABCB1. J Ovarian Res. 8:80.
67.Cheng W, Liu T, Wan X, Gao Y, Wang H. (2012). MicroRNA-199a targets CD44 to suppress the tumorigenicity and multidrug resistance of ovarian cancer-initiating cells. Febs j. 279:2047-59.
68.Cui Y, Wu F, Tian D, Wang T, Lu T, Huang X, Zhang P, Qin L. (2018). miR-199a-3p enhances cisplatin sensitivity of ovarian cancer cells by targeting ITGB8. Oncol Rep. 39:1649-57.
69.Liu MX, Siu MK, Liu SS, Yam JW, Ngan HY, Chan DW. (2014). Epigenetic silencing of microRNA-199b-5p is associated with acquired chemoresistance via activation of JAG1-Notch1 signaling in ovarian cancer. Oncotarget. 5:944-58.
70.Liu J, Zhang X, Huang Y, Zhang Q, Zhou J, Zhang X, Wang X. (2019). miR-200b and miR-200c co-contribute to the cisplatin sensitivity of ovarian cancer cells by targeting DNA methyltransferases. Oncol Lett. 17:1453-60.
71.Cittelly DM, Dimitrova I, Howe EN, Cochrane DR, Jean A, Spoelstra NS, Post MD, Lu X, Broaddus RR, Spillman MA, Richer JK. (2012). Restoration of miR-200c to ovarian cancer reduces tumor burden and increases sensitivity to paclitaxel. Mol Cancer Ther. 11:2556-65.
72.Vescarelli E, Gerini G, Megiorni F, Anastasiadou E, Pontecorvi P, Solito L, De Vitis C, Camero S, Marchetti C, Mancini R, Benedetti Panici P, Dominici C, Romano F, Angeloni A, Marchese C, Ceccarelli S. (2020). MiR-200c sensitizes Olaparib-resistant ovarian cancer cells by targeting Neuropilin 1. J Exp Clin Cancer Res. 39:3.
73.Zhu X, Shen H, Yin X, Long L, Chen X, Feng F, Liu Y, Zhao P, Xu Y, Li M, Xu W, Li Y. (2017). IL-6R/STAT3/miR-204 feedback loop contributes to cisplatin resistance of epithelial ovarian cancer cells. Oncotarget. 8:39154-66.
74.Ge G, Zhang W, Niu L, Yan Y, Ren Y, Zou Y. (2016). miR-215 functions as a tumor suppressor in epithelial ovarian cancer through regulation of the X-chromosome-linked inhibitor of apoptosis. Oncol Rep. 35:1816-22.
75.Liu Y, Niu Z, Lin X, Tian Y. (2017). MiR-216b increases cisplatin sensitivity in ovarian cancer cells by targeting PARP1. Cancer Gene Ther. 24:208-14.

76.Liu R, Guo H, Lu S. (2018). MiR-335-5p restores cisplatin sensitivity in ovarian cancer cells through targeting BCL2L2. Cancer Med. 7:4598-609.
77.Niu Q, Liu Z, Gao J, Wang Q. (2019). MiR-338-3p Enhances Ovarian Cancer Cell Sensitivity to Cisplatin by Downregulating WNT2B. Yonsei Med J. 60:1146-56.
78.Cao L, Wan Q, Li F, Tang CE. (2018). MiR-363 inhibits cisplatin chemoresistance of epithelial ovarian cancer by regulating snail-induced epithelial-mesenchymal transition. BMB Rep. 51:456-61.
79.Xu ZH, Yao TZ, Liu W. (2018). miR-378a-3p sensitizes ovarian cancer cells to cisplatin through targeting MAPK1/GRB2. Biomed Pharmacother. 107:1410-7.
80.Jiang J, Xie C, Liu Y, Shi Q, Chen Y. (2019). Up-regulation of miR-383-5p suppresses proliferation and enhances chemosensitivity in ovarian cancer cells by targeting TRIM27. Biomed Pharmacother. 109:595-601.
81.Chen FD, Chen HH, Ke SC, Zheng LR, Zheng XY. (2018). SLC27A2 regulates miR-411 to affect chemo-resistance in ovarian cancer. Neoplasma. 65:915-24.
82.Wu H, Xiao Z, Zhang H, Wang K, Liu W, Hao Q. (2014). MiR-489 modulates cisplatin resistance in human ovarian cancer cells by targeting Akt3. Anticancer Drugs. 25:799-809.
83.Tian J, Xu YY, Li L, Hao Q. (2017). MiR-490-3p sensitizes ovarian cancer cells to cisplatin by directly targeting ABCC2. American journal of translational research. 9:1127-38.
84.Xu S, Fu GB, Tao Z, OuYang J, Kong F, Jiang BH, Wan X, Chen K. (2015). MiR-497 decreases cisplatin resistance in ovarian cancer cells by targeting mTOR/P70S6K1. Oncotarget. 6:26457-71.
85.Wu D, Lu P, Mi X, Miao J. (2018). Downregulation of miR-503 contributes to the development of drug resistance in ovarian cancer by targeting PI3K p85. Arch Gynecol Obstet. 297:699-707.
86.Park GB, Kim D. (2019). MicroRNA-503-5p Inhibits the CD97-Mediated JAK2/STAT3 Pathway in Metastatic or Paclitaxel-Resistant Ovarian Cancer Cells. Neoplasia. 21:206-15.
87.Niu L, Ni H, Hou Y, Du Q, Li H. (2019). miR-509-3p enhances platinum drug sensitivity in ovarian cancer. Gene. 686:63-7.
88.Xiao S, Zhang M, Liu C, Wang D. (2018). MiR-514 attenuates proliferation and increases chemoresistance by targeting ATP binding cassette subfamily in ovarian cancer. Mol Genet Genomics. 293:1159-67.
89.Vigneron N, Vernon M, Meryet-Figuière M, Lambert B, Briand M, Louis MH, Krieger S, Joly F, Lheureux S, Blanc-Fournier C, Gauduchon P, Poulain L, Denoyelle C. (2020). Predictive Relevance of Circulating miR-622 in Patients with Newly Diagnosed and Recurrent High-Grade Serous Ovarian Carcinoma. Clin Chem. 66:352-62.
90.Qin X, Sun L, Wang J. (2017). Restoration of microRNA-708 sensitizes ovarian cancer cells to cisplatin via IGF2BP1/Akt pathway. Cell Biol Int. 41:1110-8.
91.Zhao H, Yu X, Ding Y, Zhao J, Wang G, Wu X, Jiang J, Peng C, Guo GZ, Cui S. (2016). MiR-770-5p inhibits cisplatin chemoresistance in human ovarian cancer by targeting ERCC2. Oncotarget. 7:53254-68.
92.Xia B, Lin M, Dong W, Chen H, Li B, Zhang X, Hou Y, Lou G. (2018). Upregulation of miR-874-3p and miR-874-5p inhibits epithelial ovarian cancer malignancy via SIK2. J Biochem Mol Toxicol. 32:e22168.
93.Fang Y, Xu C, Fu Y. (2015). MicroRNA-17-5p induces drug resistance and invasion of ovarian carcinoma cells by targeting PTEN signaling. J Biol Res (Thessalon). 22:12.
94.Fu X, Tian J, Zhang L, Chen Y, Hao Q. (2012). Involvement of microRNA-93, a new regulator of PTEN/Akt signaling pathway, in regulation of chemotherapeutic drug cisplatin chemosensitivity in ovarian cancer cells. FEBS Lett. 586:1279-86.
95.Li H, Xu H, Shen H, Li H. (2014). microRNA-106a modulates cisplatin sensitivity by targeting PDCD4 in human ovarian cancer cells. Oncol Lett. 7:183-8.
96.Zong C, Wang J, Shi TM. (2014). MicroRNA 130b enhances drug resistance in human ovarian cancer cells. Tumour Biol. 35:12151-6.

97.Yang H, Kong W, He L, Zhao JJ, O'Donnell JD, Wang J, Wenham RM, Coppola D, Kruk PA, Nicosia SV, Cheng JQ. (2008). MicroRNA expression profiling in human ovarian cancer: miR-214 induces cell survival and cisplatin resistance by targeting PTEN. Cancer Res. 68:425-33.
98.Ye G, Fu G, Cui S, Zhao S, Bernaudo S, Bai Y, Ding Y, Zhang Y, Yang BB, Peng C. (2011). MicroRNA 376c enhances ovarian cancer cell survival by targeting activin receptor-like kinase 7: implications for chemoresistance. J Cell Sci. 124:359-68.
99.Arrighetti N, Cossa G, De Cecco L, Stucchi S, Carenini N, Corna E, Gandellini P, Zaffaroni N, Perego P, Gatti L. (2016). PKC-alpha modulation by miR-483-3p in platinum-resistant ovarian carcinoma cells. Toxicol Appl Pharmacol. 310:9-19.
100.Chen S, Chen X, Xiu YL, Sun KX, Zong ZH, Zhao Y. (2014). microRNA 490-3P enhances the drug-resistance of human ovarian cancer cells. J Ovarian Res. 7:84.
101.Choi YE, Meghani K, Brault ME, Leclerc L, He YJ, Day TA, Elias KM, Drapkin R, Weinstock DM, Dao F, Shih KK, Matulonis U, Levine DA, Konstantinopoulos PA, Chowdhury D. (2016). Platinum and PARP Inhibitor Resistance Due to Overexpression of MicroRNA-622 in BRCA1-Mutant Ovarian Cancer. Cell Rep. 14:429-39.
102.Cai J, Yang C, Yang Q, Ding H, Jia J, Guo J, Wang J, Wang Z. (2013). Deregulation of let-7e in epithelial ovarian cancer promotes the development of resistance to cisplatin. Oncogenesis. 2:e75.
103.Han X, Zhen S, Ye Z, Lu J, Wang L, Li P, Li J, Zheng X, Li H, Chen W, Li X, Zhao L. (2017). A Feedback Loop Between miR-30a/c-5p and DNMT1 Mediates Cisplatin Resistance in Ovarian Cancer Cells. Cell Physiol Biochem. 41:973-86.
104.Zhang X, Huang L, Zhao Y, Tan W. (2013). Downregulation of miR-130a contributes to cisplatin resistance in ovarian cancer cells by targeting X-linked inhibitor of apoptosis (XIAP) directly. Acta Biochim Biophys Sin (Shanghai). 45:995-1001.
105.Jeong JY, Kang H, Kim TH, Kim G, Heo JH, Kwon AY, Kim S, Jung SG, An HJ. (2017). MicroRNA-136 inhibits cancer stem cell activity and enhances the anti-tumor effect of paclitaxel against chemoresistant ovarian cancer cells by targeting Notch3. Cancer Lett. 386:168-78.
106.Deng Y, Zhao F, Hui L, Li X, Zhang D, Lin W, Chen Z, Ning Y. (2017). Suppressing miR-199a-3p by promoter methylation contributes to tumor aggressiveness and cisplatin resistance of ovarian cancer through promoting DDR1 expression. J Ovarian Res. 10:50.
107.Cochrane DR, Spoelstra NS, Howe EN, Nordeen SK, Richer JK. (2009). MicroRNA-200c mitigates invasiveness and restores sensitivity to microtubule-targeting chemotherapeutic agents. Mol Cancer Ther. 8:1055-66.
108.Cao J, Cai J, Huang D, Han Q, Chen Y, Yang Q, Yang C, Kuang Y, Li D, Wang Z. (2014). miR-335 represents an independent prognostic marker in epithelial ovarian cancer. Am J Clin Pathol. 141:437-42.
109.Chen XP, Chen YG, Lan JY, Shen ZJ. (2014). MicroRNA-370 suppresses proliferation and promotes endometrioid ovarian cancer chemosensitivity to cDDP by negatively regulating ENG. Cancer Lett. 353:201-10.
110.Zhou Y, Chen Q, Qin R, Zhang K, Li H. (2014). MicroRNA-449a reduces cell survival and enhances cisplatin-induced cytotoxicity via downregulation of NOTCH1 in ovarian cancer cells. Tumour Biol. 35:12369-78.
111.Liu G, Yang D, Rupaimoole R, Pecot CV, Sun Y, Mangala LS, Li X, Ji P, Cogdell D, Hu L, Wang Y, Rodriguez-Aguayo C, Lopez-Berestein G, Shmulevich I, De Cecco L, Chen K, Mezzanzanica D, Xue F, Sood AK, Zhang W. (2015). Augmentation of response to chemotherapy by microRNA-506 through regulation of RAD51 in serous ovarian cancers. J Natl Cancer Inst. 107.
112.Wang L, Mezencev R, Švajdler M, Benigno BB, McDonald JF. (2014). Ectopic over-expression of miR-429 induces mesenchymal-to-epithelial transition (MET) and increased drug sensitivity in metastasizing ovarian cancer cells. Gynecol Oncol. 134:96-103.
113.Prislei S, Martinelli E, Mariani M, Raspaglio G, Sieber S, Ferrandina G, Shahabi S, Scambia G, Ferlini C. (2013). MiR-200c and HuR in ovarian cancer. BMC Cancer. 13:72.
114.Leskelä S, Leandro-García LJ, Mendiola M, Barriuso J, Inglada-Pérez L, Muñoz I, Martínez-Delgado B, Redondo A, de Santiago J, Robledo M, Hardisson D, Rodríguez-Antona C. (2011). The miR-200 family controls beta-tubulin III expression and is associated with paclitaxel-based treatment response and progression-free survival in ovarian cancer patients. Endocr Relat Cancer. 18:85-95.

115.Liu N, Zhong L, Zeng J, Zhang X, Yang Q, Liao D, Wang Y, Chen G, Wang Y. (2015). Upregulation of microRNA-200a associates with tumor proliferation, CSCs phenotype and chemosensitivity in ovarian cancer. Neoplasma. 62:550-9.
116.Mateescu B, Batista L, Cardon M, Gruosso T, de Feraudy Y, Mariani O, Nicolas A, Meyniel JP, Cottu P, Sastre-Garau X, Mechta-Grigoriou F. (2011). miR-141 and miR-200a act on ovarian tumorigenesis by controlling oxidative stress response. Nat Med. 17:1627-35.
117.Zhang J, Liu L, Sun Y, Xiang J, Zhou D, Wang L, Xu H, Yang X, Du N, Zhang M, Yan Q, Xi X. (2016). MicroRNA-520g promotes epithelial ovarian cancer progression and chemoresistance via DAPK2 repression. Oncotarget. 7:26516-34.